THE ROLE OF THE INTEGRATED STRESS RESPONSE TRANSCRIPTION FACTOR ATF4 IN MYC INDUCED TUMORIGENESIS

Feven Tameire

A DISSERTATION

in

Cell and Molecular Biology

Presented to the Faculties of the University of Pennsylvania

in

Partial Fulfillment of the Requirements for the

Degree of Doctor of Philosophy

2018

Supervisor of Dissertation	Graduate Group Chairperson
_____	_____
Constantinos Koumenis, PhD	Daniel S. Kessler, PhD
Richard H. Chamberlain Professor of Research Oncology	Associate Professor of Cell and
Vice Chair and Research Division Director of	Developmental Biology
Department of Radiation Oncology	

Dissertation Committee

David M. Feldser, PhD	Assistant Professor of Cancer Biology
Serge Fuchs, MD, PhD	Professor of Cell Biology,
	Director, Mari Lowe Center for Comparative Oncology
Craig Bassing, PhD	Associate Professor of Pathology and Laboratory Medicine
J. Alan Diehl, PhD	Professor of Biochemistry and Molecular Biology
	Endowed Professor of Lipidomics and Pathobiology

THE ROLE OF THE INTEGRATED STRESS RESPONSE TRANSCRIPTION FACTOR ATF4 IN MYC INDUCED TUMORIGENESIS

ACKNOWLEDGMENTS

First and foremost I would like to thank God who gave me the opportunity to undertake this research and for always supporting me, I could not have accomplished this without Him.

My research journey could not have been possible without my dedicated mentor Costas Koumenis. Thank you for all your support and guidance throughout my graduate years. You have inspired me to be passionate about science and pushed me to undertake challenging but rewarding projects. Thank you for always having my back and encouraging me to aim high. You have been very instrumental for my growth as an independent scientist. I also appreciate the opportunity to attend many scientific conferences which has helped me get to know great scientists in the cancer field. Ευχαριστώ!

I would like to specially thank my thesis committee members, David Feldser, Alan Diehl, Serge Fuchs and Craig Bassing for their valuable time, guidance and great scientific advice throughout my graduate years. I would especially like to thank David Feldser for chairing my thesis committee and always taking his time to provide constructive advice both for my scientific and professional growth.

To past and present Koumenis lab crew – Steve Tuttle, Ioannis Verginadis, Nektaria Leli, Frank Chinga, Carlo Salas, Giovanna Sena, Harris Avgousti, Victoria Wu, Armaun Rouhi, Lori Hart, Stacey Lehman, Carly Sayers, Natalie Daurio, David Guttman, Lauren Brady, Souvik Dey, Alexandra Monroy, Yue Bi, Vladimir Popov and George Cerniglia (Maity lab) thank you for helping me with my experiments and making our lab a fun place to work in. I will always cherish your support and friendship!

I would also like to acknowledge my undergraduate mentor Dr. Keith Kozminski for steering me towards research and supporting me in applying to graduate schools. I ended up at Penn because of your encouragement and for that I am truly grateful. I would also like to thank Dr. Joyce Hamlin, my previous PI at UVA. Your passion for science is still inspiring to me.

To my dear parents- thank you for always believing in me and encouraging me to pursue my dream. I am forever grateful for your continued love and support throughout my life. This process hasn't been easy but I am grateful to have you by my side through all the ups and downs. Thank you for being a constant source of joy, strength and sound advice. I would like to thank my brothers, my sister- in -law and all our extended family here and in Ethiopia as well as Hiwotsha, my best friend, for always being there for me, supporting my endeavors and for all the laughs and great memories. I would also like to thank my friends and second family at EECP church for their encouragement and support- you have truly been a source of strength. To my niece and nephews- I love you and I hope my accomplishment of this work inspires you to pursue your dreams in the future. There are many more people who are not mentioned here but who have helped me throughout my life and graduate years, thank you all for making this possible.

ABSTRACT

THE ROLE OF THE INTEGRATED STRESS RESPONSE TRANSCRIPTION FACTOR ATF4 IN MYC INDUCED TUMORIGENESIS

Feven Tameire

Constantinos Koumenis

The ability of cancer cells to adapt to non-cell autonomous (extrinsic) and cell autonomous (intrinsic) stresses is critical for maintaining cell viability and therapy resistance. The Integrated Stress Response (ISR) transcription factor ATF4 is essential in helping cancer cells cope with extrinsic stresses such as deficits in oxygen and nutrients. ATF4 deficient cells exhibit decreased viability and survival when subjected to hypoxia or nutrient deprivation stresses. However the role of ATF4 in oncogene-induced intrinsic stress remains unclear. Dysregulation of the proto-oncogene c-*Myc* (MYC henceforward) drives malignant progression, but also induces robust anabolic and proliferative programs leading to intrinsic stress. The mechanisms enabling adaptation to MYC-induced stress are not fully understood. This work shows that MYC induces ATF4 expression through activation of the ISR kinases PERK and GCN2. Using a tRNA microarray we discovered that MYC activates GCN2 through accumulation of uncharged tRNAs. Functionally, loss of ATF4 enhanced apoptosis and decreased survival during MYC activation. Genome-wide ChIP-seq analysis revealed that ATF4 co-occupies promoter regions of over 30 MYC target genes, including those regulating amino acid biosynthesis/transport and protein synthesis. ATF4 is essential for MYC-induced upregulation of the negative translational regulator and mTORC1 target 4E-BP1 and genetic or pharmacological inhibition of mTORC1 signaling rescues ATF4 deficient cells from MYC-induced stress. To test the role of ATF4 in MYC induced tumorigenesis we employed the Eμ-Myc mouse model of MYC-induced spontaneous lymphoma. Acute deletion of ATF4 significantly delays MYC-driven tumor progression and increases survival in lymphoma and colon cancer xenograft models. Collectively, our results demonstrate ATF4

exerts pro-survival activities during MYC induced intrinsic stress and identifies ATF4 as a potential therapeutic target in MYC driven cancers.

TABLE OF CONTENTS

LIST OF TABLES

LIST OF FIGURES

CHAPTER 1: GENERAL INTRODUCTION

A portion of this Chapter includes work that was previously published in Seminars in Cancer Biology.

Reprinted with permission from Elsevier

Tameire, F., Verginadis, II & Koumenis, C. Cell intrinsic and extrinsic activators of the unfolded protein response in cancer: Mechanisms and targets for therapy. *Semin Cancer Biol* (2015).

Cancer cells experience numerous insults in the microenvironment they reside in, including low availability of oxygen and nutrients. In addition to the extrinsic stresses present in the tumor microenvironment, cancer cells are also subject to intrinsic stresses due to activation of oncogenes or loss of tumor suppressors. The ability to adapt to such stresses becomes critical for malignancy and therapy resistance. In order to sense and respond to stress, cancer cells rely on coordinated pathways such as the Unfolded Protein Response (UPR) and the Integrated Stress Response pathway (ISR). The UPR and ISR elicit translational and transcriptional responses to achieve homeostasis and adaptation to stress. Activating transcription factor 4 (ATF4) is downstream of both pathways. This work herein investigates the different components of ISR and UPR and their impact on MYC-induced intrinsic stress and tumorigenesis with a special focus on ATF4.

The Unfolded Protein Response (UPR)

The endoplasmic reticulum (ER) is an extensive membranous network found in all eukaryotic cells. The ER regulates calcium (Ca^{2+}) homeostasis, lipid biogenesis and folding of secretory and membrane bound proteins. The complexity of the ER depends on the predominant functions of the cell type. For example, highly secretory cells, such as pancreatic islets, immune B cells and endothelial cells demand a well-developed ER to perform their functions. Proper protein folding and post-translational modifications (glycosylation and lipidation) require both an oxidizing and a Ca^{2+}-rich environment, which is accompanied by high concentrations of ER chaperone proteins, such as the glucose-regulated protein 78 (GRP78, also known as BiP), calnexin, calreticulin and protein disulfide isomerases (PDI). Many of these chaperones are Ca^{2+} dependent, underscoring the significance of maintaining the ER Ca^{2+} concentrations at optimal levels[1, 2]. Depletion of Ca^{2+} levels, oxidative stress caused by reactive oxygen species (ROS), low oxygen (hypoxia), glucose deprivation and acidosis encountered in pathological conditions (cancer, neurodegenerative diseases, viral infections), affect ER homeostasis, leading to the accumulation of unfolded/misfolded proteins, known as "ER stress"[3]. Additionally, enhanced

protein synthesis can overcrowd the ER and activate the UPR. To overcome these perturbations, a set of signal transduction pathways are activated, which are collectively referred to as the UPR[4] (Figure. 1.1).

In mammalian cells, there are three major ER stress sensors, pancreatic ER kinase (PKR)-like ER kinase (PERK), inositol-requiring enzyme 1 (IRE1) and activating transcription factor-6 (ATF6), whose main role is to convey the signal from the ER lumen to cytoplasm and nucleus in order to initiate mechanisms to alleviate ER stress[4]. Primarily, the UPR aims to restore ER homeostasis by increasing ER capacity, reducing the load of newly synthesized proteins in the ER lumen through inhibition of global protein synthesis and by enhancing ER associated degradation of misfolded proteins (ERAD)[5,6]. However, if the ER stress persists or ER homeostasis cannot be restored, the role of the UPR tilts towards cell death primarily by initiating apoptosis[7,8]. Interestingly, the UPR is often co-opted by cancer cells to promote growth and survival in unfavorable conditions.

Evidence of UPR involvement in cancer

Activation of all arms of the UPR has been widely reported in a variety of human tumors including glioblastoma, lymphoma, myeloma and carcinoma of the cervix and breast[9-12]. Tumor cells are often characterized by increased rates of protein synthesis and also face conditions of glucose and oxygen deprivation in the tumor microenvironment[13,14]. Adaptation to such adverse conditions requires an ER with enhanced folding capacity achieved by chaperones and folding enzymes. Indeed, elevated levels of ER chaperones such as GRP78 (also known as BiP) and GRP94 have been widely reported in tumors and associate with poor outcome and recurrence[15]. Historically, the glucose-regulated proteins were found to be induced during glucose starvation and subsequently their expression was shown to also be increased during ER stress[16, 17]. GRP78 was shown to promote tumorigenesis through the regulation of proliferation, invasion, metastasis, angiogenesis as well as therapy resistance through extensive studies in cell culture and transgenic mouse models of cancer[18-21].

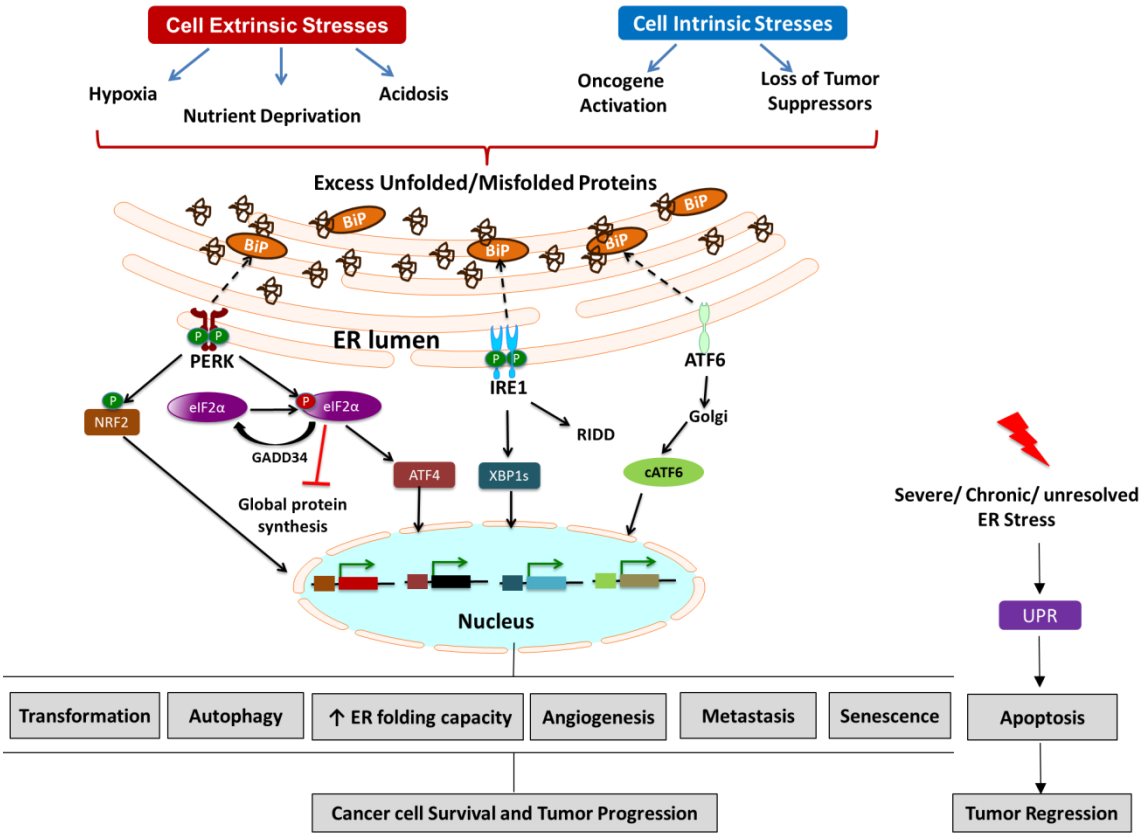

Figure 1.1 The Unfolded Protein Response. Cell extrinsic stresses such as hypoxia, nutrient deprivation and acidosis as well as cell intrinsic stresses that result from oncogene activation and loss of tumor suppressors lead to accumulation of unfolded/misfolded proteins in the ER creating an imbalance between nascent polypeptides and chaperones. Upon ER stress, GRP78 (BiP) is titrated away from ER resident transmembrane proteins to help fold nascent polypeptides and misfolded proteins. Activation of PERK, IRE1 and ATF6 is often seen in tumors and found to be important in regulating processes such as transformation, autophagy, ER folding capacity, angiogenesis, metastasis and senescence, thus promoting tumor initiation and progression. However during chronic or severe ER stress that cannot be mitigated, the UPR can also elicit apoptosis which promotes tumor regression. Thus, the UPR can be a double-edged sword during tumorigenesis.

GRP78 has been firmly established as a major regulator of the ER stress sensors PERK, IRE1 and ATF6[22]. According to the current models, in non-stressed conditions, GRP78 associates with PERK, IRE1 and ATF6 keeping them in an inactive state. During ER stress, GRP78 dissociates from the ER stress sensors to aid in the folding of nascent polypeptides, resulting in activation of the UPR transducers[23]. An alternative mechanism of activation for IRE1

and PERK has been recently described where unfolded proteins directly bind and activate IRE1 and PERK[24, 25]. This model provides an insight of how the UPR kinases are able to sense a slight perturbation of ER folding status in a timely manner even though BiP is present at much elevated levels compared to the kinases.

ATF6

Activation of ATF6 during ER stress involves dissociation of GRP78 from the luminal domain and translocation to the Golgi apparatus where it is cleaved by two resident proteases, S1P and S2P[26]. This process releases the ATF6 domain, which serves as a potent transcription factor, targeting a set of genes encoding ER chaperones, proteins involved in quality control and ER associated degradation (ERAD)[27]. Although the role of ATF6 in tumorigenesis has not been studied as extensively as other arms of the UPR, elevated expression of active ATF6 is seen in patient tissues of hepatocellular carcinoma (HCC) as well as Hodgkin lymphoma[28, 29].

IRE1

IRE1 is the only branch of the UPR that is conserved in all eukaryotic cells. Activation of IRE1 during ER stress depends on dissociation of GRP78[23]. IRE1 uses its kinase domain for auto-transactivation and its RNase domain to specifically remove an intron from XBP1 mRNA, which is ligated by a tRNA ligase to form spliced XBP1 (XBP1s)[30]. The RNase domain also leads to decay of other mRNAs, which further contributes to decreased protein synthesis during ER stress[31]. XBP1s is a potent transcription factor responsible for the activation of genes that regulate ER quality control, chaperones and degradation of misfolded proteins[32]. High levels of XBP1s is observed in breast cancer, hepatocellular carcinoma, lymphoma and multiple myeloma (MM)[28, 33, 34]. In pre-clinical studies, preventing XBP1 splicing by small molecules that inhibit the endoribonuclease domain of IRE1, are cytotoxic in several xenograft tumor models strongly implicating IRE pathway as a treatment modality in multiple tumor types[35-37].

PERK

PERK is activated through oligomerization and trans-autophosphorylation Upon GRP78 dissociation[38]. Active PERK transiently inhibits global translation, reducing the influx of nascent polypeptides to the ER through phosphorylation of the alpha subunit of eukaryotic initiation factor (eIF2α) at serine 51[39]. Concomitant with suppression of translation, phosphorylation of eIF2α enhances the preferential translation of select mRNAs such as the transcription factor ATF4. ATF4 induces the transcription of chaperones, antioxidants and autophagy promoting genes[40, 41]. Moreover, ATF4 relieves translation inhibition by indirectly upregulating growth arrest and DNA damage gene 34 (GADD34), a protein phosphatase 1 (PP1) cofactor, responsible for eIF2α dephosphorylation, completing a negative feedback loop[42]. In addition to eIF2α, PERK phosphorylates the transcription factor NF-E2-related factor-2 (NRF2), which promotes redox homeostasis during ER stress[43] (Figure 1.1).

The PERK arm of the UPR has been implicated in tumor initiation and progression [9, 11, 44]. PERK knockout RAS^{V12}-transformed mouse embryonic fibroblasts (MEFs) grow slowly compared to their WT counterparts when injected into flanks of nude mice[9]. PERK has been shown to regulate proliferation, growth, vascularity and antioxidant response in transgenic mouse models of insulinoma and breast cancer[45, 46]. Furthermore, the PERK/ATF4 axis is important in the metastatic process through regulation of antioxidant response as well as autophagy and prevents apoptosis of cells undergoing extracellular matrix detachment, a process tightly linked to metastasis[47, 48].

Additionally, PERK regulates survival and protein synthesis through regulation of a microRNA, mir-211[49]. PERK/eIF2α/ATF4-mediated expression of miR-211 promotes survival during ER stress by repressing pro-apoptotic CHOP (C/EBP homologous protein) expression[49]. Additionally, PERK mediated induction of mir-211 also impacts the circadian clock which regulates expression of metabolic genes in periodic manner following dark/light cycles. In this context, mir-211 represses the core circadian regulators Bmal and Clock during ER stress resulting in a phase-shift in circadian oscillations. Suppression of Bmal expression during stress

is important for reducing protein synthesis, which promotes survival and tumor growth[44]. In addition to PERK other kinases also phosphorylate eIF2α as part of a coordinated signaling pathway known as the Integrated Stress Response.

The Integrated Stress Response (ISR)

The ISR senses a wide array of stresses to achieve homeostasis by coupling translational and transcriptional response tailored towards each stress. The ISR is mediated by a family of four serine/therionine kinases, PERK, general control non-derepressible 2 (GCN2), RNA-dependent protein kinase (PKR) and heme regulated inhibitor (HRI)[50]. Each kinase senses distinct perturbations experienced by cells (Figure 1.2). For example, PERK senses accumulation of misfolded proteins in the endoplasmic reticulum (ER), GCN2 senses amino acid deprivation, PKR senses double stranded RNA and HRI senses heme deprivation. Once activated, the four kinases catalyze phosphorylation of their common target, eIF2α at serine 51.

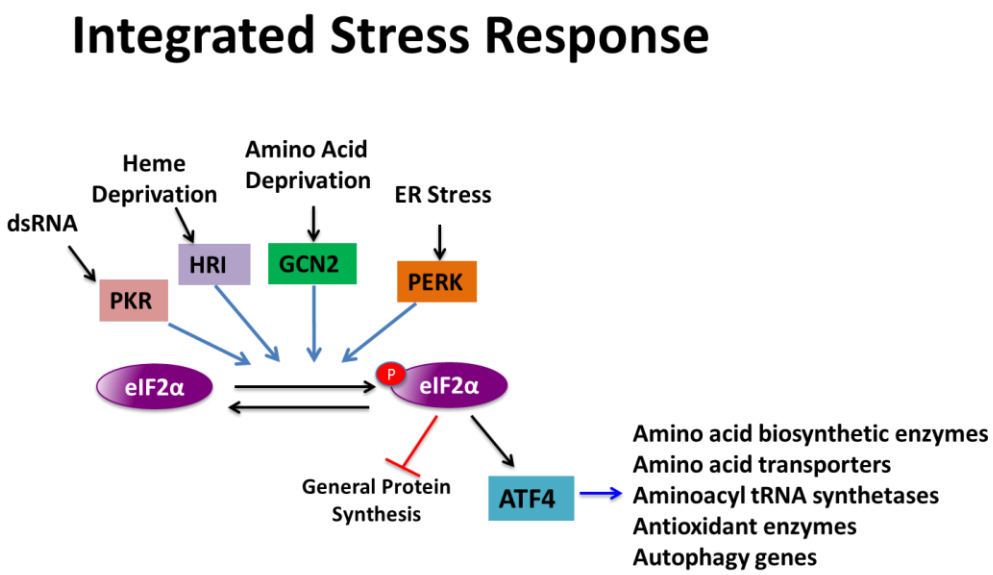

Figure 1.2. The Integrated Stress Response pathway. ISR is mediated by four kinases, PKR, HRI, GCN2 and PERK which respond to their own respective stress. Activation of the kinases leads to phosphorylation of eIF2α which inhibits general protein synthesis while promotes preferential translation of select mRNAs such as the transcription factor ATF4. ATF4 is critical in inducing expression of genes that promote adaptation of stress.

Consequences of eIF2α phosphorylation

Broadly, phosphorylation of eIF2α (P-eIF2α) by any of the four ISR kinases results in two types of responses (Figure 1.2). First, P-eIF2α leads to transient inhibition of protein synthesis which serves to conserve adenosine 5'-triphosphate (ATP) and amino acids during unfavorable conditions[50]. Translation initiation requires eIF2α bound to GTP that associates with initiator methionyl-tRNA (Met-tRNA$_i^{Met}$) to form the ternary complex (TC). The TC along with other initiation factors and the 40S ribosome forms the pre-initiation complex (PIC) which is recruited to the 5' of 7-methylguanosine capped mRNA to begin processively scanning from 5' to 3' direction until the start codon is recognized and bound by the Met-tRNA$_i^{Met}$ [51]. This step initiates the hydrolysis of GTP on eIF2α and dissociation of eIF2α-GDP facilitating loading of the 60S large ribosomal subunit to form the 80S ribosome which carries out elongation step of protein synthesis. eIF2B, a guanine nucleotide exchange factor (GEF), catalyzes the recycling of eIF2α-GDP to eIF2α-GTP for the next round of translation. Under stressed conditions, phosphorylated eIF2α sequesters eIF2B inhibiting its GEF activity. This leads to decreased eIF2α-GTP levels and inhibition of global protein synthesis[52]. The second response mediated by P-eIF2α involves the preferential translation of select mRNAs containing short upstream open reading frame (uORF) in their 5' untranslated region (UTR). One of the well-studied effectors of ISR whose translation is enhanced in this process is ATF4.

ATF4: structure and regulation

ATF4 is a basic leucine-zipper (bZIP) transcription factor and a member of the cAMP responsive element binding protein (CREB/ ATF) family of proteins that is ubiquitously expressed but whose translation is rapidly increased during phosphorylation of eIF2α[53]. ATF4 protein contains a strong transcriptional activator domain located at the N-terminus[54] and a basic domain for DNA binding at the C-terminus (Figure 1.3). ATF4 mediates expression of target genes by

binding to CCAAT-enhancer binding protein-activating transcription factor (C/EBP-ATF) response elements (CARE)[55]. As an important effector of UPR and ISR pathway, ATF4 forms a homodimer or heterodimerizes with other transcription factors to activate or repress expression of target genes[56]. ATF4 interacting partners determine transcriptional selectivity and influence activation of target genes. Hence, interaction with different partners allows ATF4 to respond to various stresses by regulating expression of target genes tailored towards each stress in a context and cell type dependent manner[57]. ATF4 itself is regulated at the transcriptional, translational and post-translational level as described below.

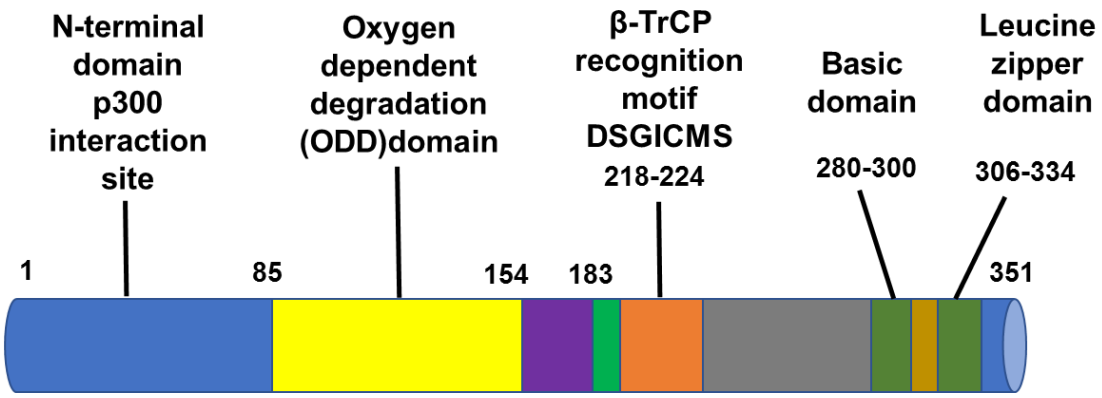

Figure 1.3. Functional domains in ATF4 protein. ATF4 protein contains an N-terminus domain for interaction with p300, an oxygen dependent degradation domain that regulates its stability by binding to PHD3, a β-TrCP recognition motif in which phosphorylation at S219 targets it for proteasomal degradation, a basic domain for DNA binding and a leucine zipper domain for protein-protein interaction. (Adapted from Pakos-Zebrucka et. al)

Transcriptional regulation of ATF4

Although ATF4 is primarily regulated at the translational level, its transcription has been shown to be induced during various stresses by different transcription factors. ATF4 mRNA expression is enhanced during amino acid and glucose deprivation conditions[58]. Furthermore, ER stress and oxidative stress also upregulate ATF4 transcription[59, 60]. Transcription factors that have been shown to positively regulate ATF4 include MYC, NRF2, CLOCK and PDX1[61-65]. Regulation of ATF4 mRNA levels is context dependent. For example, ATF4 mRNA is induced during ER stress but repressed under UV radiation even though these stresses activate PERK and GCN2 respectively. Repression of ATF4 during UV stress provides survival advantage due to decreased expression of the ATF4 target CHOP which promotes apoptosis[66]. Therefore, transcriptional repression can inhibit ATF4 expression during certain stresses providing another node of regulation besides translation.

Translational regulation of ATF4

The main mechanism of regulation of ATF4 expression is at the translational level during stress conditions that promote phosphorylation of eIF2α. This is mediated by uORFs present at the 5' UTR of *ATF4* [67, 68]. Murine *ATF4* contains two uORFs where as human *ATF4* contains three uORFs which regulate preferential translation of ATF4 (Figure 1.3). Translation initiation begins when the PIC containing eIF2α-GTP binds to the 5'-cap and encounters the start codon of uORF1. After translation of uORF1, the large ribosome dissociates but the small ribosome keeps scanning and associates with eIF2α-GTP TC to reinitiate translation at uORF2. Translation of uORF2 terminates within ATF4 ORF and is out of frame with ATF4 transcript preventing ATF4 translation. However, during stress conditions, enhanced phosphorylation of eIF2α decreases eIF2α-GTP levels. As a result, the small ribosome is delayed to initiate translation at uORF2 but reinitiates translation at ATF4 start codon. This delayed translation allows preferential translation of ATF4 mRNA which then activates genes that ameliorate stress. Other mRNAs that are

translated in a similar mechanism include GADD34 [69], activating transcription factor 5 [70] (ATF5) and p21[Cip1] [71].

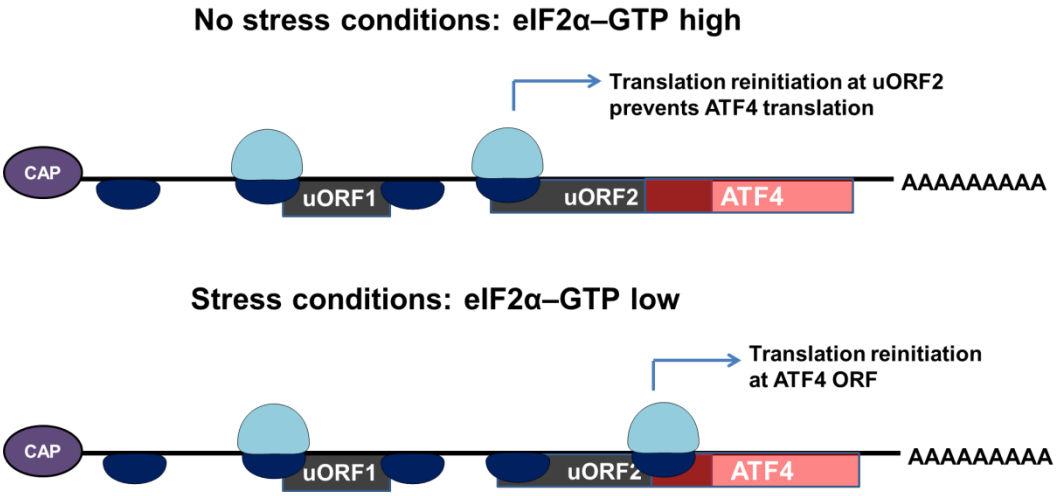

Fig 1.3 Translational regulation of murine ATF4 mRNA. In unstressed cells, where eIF2α-GTP is abundant, scanning ribosomes translate uORF1 and rapidly reinitiate translation at uORF2. uORF2 overlaps with ATF4 ORF and is out-of-frame with ATF4 coding sequence preventing ATF4 translation. Under stress conditions, phosphorylation of eIF2α leads to lower levels of eIF2α-GTP, delaying the scanning ribosome to engage with a functional eIF2α-GTP required for translation at uORF2. Instead, translation initiation occurs at ATF4 start codon leading to preferential translation of ATF4 under stress conditions.

Post-translational regulation of ATF4

ATF4 protein is subject to post-translational modifications such as phosphorylation, ubiquitination, and acetylation which are known to affect its transcriptional activity and stability[72]. Transcriptional activity of ATF4 has been shown to be enhanced during bone formation and osteogenesis through phosphorylation at S245 and S254 by Ribosomal S6 Kinase α-2 (RSK2) and protein kinase A (PKA) respectively. Phosphorylation of ATF4 at S219 enhances its interaction with the receptor of Skp, Cullin, F-box containing (SCF) E3 ubiquitin ligase complex known as beta transducin repeat containing ubiquitin protein ligase (β-TrCP) which targets ATF4 for proteasomal degradation.[73]. The oxygen-dependent degradation (ODD) domain on ATF4 also

regulates its stability by regulating its interaction with the oxygen sensor prolyl-4-hydroxylase domain 3 (PHD3)[74].

Physiological function of ATF4

ATF4 plays a vital role in hematopoiesis, bone and eye development as well as long term memory [75-77]. Accordingly, ATF4 knockout embryos suffer from fetal anemia, which is resolved in adults [78]. ATF4 regulates fetal liver hematopoietic stem cell expansion and migration partially through production of cytokines such as angiopoietin-like protein 3 (Angptl3) in the supporting stroma[76]. Whole body knockout of ATF4 results in 30% perinatal lethality and the mice that survive are infertile, runted and have defective eye morphology[75]. ATF4 knockout mice exhibit microphthalmia due to severe p53 mediated apoptosis in the developing lens which can be partially rescued by deletion of p53[79]. Furthermore, ATF4 regulates fat mass, as a result ATF4 knockout mice are small, lean and resistant to high fat diet induced obesity[72, 80].

ATF4 is implicated in synaptic plasticity and long-term memory although current studies indicate both positive and negative role of ATF4[77, 81, 82]. Some studies that target ATF4 indirectly either by inhibition of C/EBP family of proteins or by reducing phosphorylation of eIF2α have shown enhanced learning, long term memory and plasticity in mice[81, 82]. However, short hairpin mediated knockdown of ATF4 in hippocampal neurons of mice led to deficits in long term spatial memory and memory flexibility[77].

ATF4 expression and function in tumors

Several experiments have highlighted the tumorigenic role of ATF4[48, 83-86]. ATF4 expression is elevated and tends to localize at hypoxic regions in patient tumor samples of glioblastoma, melanoma, breast and cervical cancer relative to surrounding normal tissue, suggesting its involvement in tumor progression[9]. High ATF4 expression in triple negative breast cancer (TNBC) patients associates with poor survival and relapse free survival. Importantly, silencing ATF4 reduces migration, invasiveness, proliferation and mammosphere forming efficiency in TNBC cell lines and also results in reduced tumor growth in TNBC patient derived

xenograft models[87]. Similarly, enhanced expression of ATF4 is observed in glioma patients and correlates with poor survival[88].

Role of ATF4 in tumor extrinsic stress responses

Hypoxia

Inadequate oxygen availability is a common feature of tumors as cancer cells outgrow their blood supply due to accelerated proliferation and is associated with a more aggressive phenotype and therapy resistance[89]. Oxygen levels in tumors tend to have a very heterogeneous distribution, ranging from moderate to severe hypoxia followed by intermittent re-oxygenation. Clinically, hypoxia compromises the effect of ionizing radiation due to incomplete fixation of DNA damage[90]. Hypoxic stress elicits response pathways that enable adaptation, thus promoting survival of cancer cells. The most studied pathway involves stabilization of the oxygen sensitive hypoxia-inducible factors, HIF1α and HIF2α. The HIFα form a heterodimer with the constitutively expressed HIF1β to induce expression of a wide range of genes that support adaptation, metabolism and migration of tumor cells enabling escape to a secondary site[91].

Several reports also show that severe hypoxia results in ER stress triggering the UPR[92, 93]. Protein synthesis is an energy demanding process and during hypoxia, when cellular energy is limiting, pathways that inhibit protein synthesis become critical for survival. The HIFs inhibit mTORC1 which decreases cap-dependent protein synthesis, whereas PERK exerts an inhibitory effect on protein synthesis via phosphorylation of eIF2α[93, 94]. As a result, cells with a compromised PERK/eIF2α arm of the UPR fail to block protein synthesis and exhibit reduced survival during hypoxia[9, 92, 95]. PERK-mediated protection of tumors from apoptosis during hypoxia is also observed in xenograft models. Apoptotic cells colocalize in hypoxic areas of the tumor, in PERK-/- but not in PERK +/+ tumors, suggesting that PERK promotes survival of tumor cells experiencing hypoxia[9].

PERK promotes translation of ATF4 following severe hypoxia in a P-eIF2α dependent manner[96]. ATF4 deficient cells undergo apoptosis in hypoxic conditions compared to their

wildtype counterparts[9]. Furthermore, ATF4 colocalizes with hypoxic regions of tumors from cervical patients suggesting its clinical relevance in tumor progression. ATF4 enhances tolerance to severe hypoxia by activating cytoprotective autophagy through upregulation of several autophagy genes[97, 98]. Autophagy can degrade accumulated unfolded proteins and also recycle essential amino acids, thus providing nutrients until a new blood supply is obtained by the tumor. ATF4 also promotes invasion, migration and metastasis of hypoxic breast cancer cells through activation of lysosomal-associated membrane protein 3 (LAMP3)[99].

Nutrient Deprivation

In addition to hypoxia, nutrient deprivation is a common feature of tumors attributed to abnormal vasculature and poor perfusion. Eukaryotic cells adapt to nutrient starvation conditions by activating GCN2, which phosphorylates eIF2α and subsequently increases ATF4 translation. GCN2 senses amino acid deprivation in cells by directly binding to uncharged tRNAs through its histidyl-tRNA synthetase-like (HisRS-like) domain[100]. Binding to uncharged tRNAs leads to a conformational change in an autoinhibitory loop promoting autophosphorylation and activation of GCN2[101]. Glucose deprivation has also been shown to activate GCN2, possibly due to enhanced amino acid consumption as an alternate source of energy which in turn increases accumulation of uncharged tRNAs[83].

ATF4 regulates adaptation to amino acid deprivation by augmenting amino acid metabolism through transcription of amino acid transporters (SLC1A5, SLC3A2, SLC7A5 and GLYT1) and enzymes that regulate synthesis of amino acids, such as asparagine synthase (ASNS). Activation of ATF4 is also vital for suppressing oxidative stress through induction of glutathione biosynthesis. Therefore, ATF4 deficient MEFs require supplementation of non-essential amino acids and antioxidants for growth *in vitro* and fail to form tumors *in vivo*[40, 102].

The GCN2/eIF2α/ATF4 signaling is elevated in primary human liver, breast, lung and head and neck tumors[83, 84]. GCN2 is required for cancer cell survival during both amino acid and glucose deprivation conditions[83]. Tumor cells require ATF4 for proliferation and growth *in vitro*. This defect can be partially rescued by expression of ASNS, an enzyme that is involved in the

synthesis of asparagine[83]. GCN2-ATF4 pathway also regulates angiogenesis *in vivo*. Impairing GCN2 expression in human head and neck squamous cell carcinoma cells resulted in decreased expression of ATF4 and VEGF and reduced blood vessel density[84]. Importantly, ATF4 promotes transcription of several pro-angiogenic factors such as VEGF, FGF-2 and IL-6 in response to glucose deprivation to support survival and maturation of blood vessels that aid tumor growth[103].

Cell Intrinsic Stresses

The path to becoming a cancer cell is a multistep process that involves stages such as neoplastic transformation, aberrant proliferation, cell growth and eventually metastasis. Importantly, to form a tumor, cancer cells have to override multiple "check points" including apoptotic pathways that block aberrant growth and be able to sustain the energy to meet the demands of rapid proliferation. The transformation stage involves mutations that result in oncogene activation and loss of tumor suppressors. A previous study showed that loss of the tuberous sclerosis complex (*TSC1* and *TSC2*) tumor suppressor genes activates the UPR in a cell autonomous manner[104]. Oncogene activation induces replicative and metabolic stresses in cells[105, 106]. Thus, oncogene activation is a type of intrinsic stress because of the increased burden placed on cells to augment biosynthetic pathways and rewire metabolism to meet the demand of rapid proliferation.

The proto-oncogene MYC and cancer

The proto-oncogene *c-MYC* (hereafter referred to as *MYC*) belongs to a family of genes (*MYC, MYCN, MYCL*) and regulates important biological processes such as proliferation, metabolism, protein synthesis, cell growth and apoptosis[107]. Given its pleiotropic functions that are vital for cancer cell growth and survival, it is not surprising that it is one of the highly deregulated genes in human tumors[108, 109]. MYC deregulation associates with poor patient survival in many cancers including diffused large B cell lymphoma, breast cancer as well as colon cancer[110-112]. MYC is tightly regulated in non-transformed cells and is constantly subject to

proteasome dependent degradation. Its expression in non-transformed cells is dependent on growth factor signaling and nutrient availability[107].

MYC is a basic helix-loop-helix zipper protein (bHLH-ZIP) transcription factor and dimerizes with its partner MAX, also in the same family, to bind to consensus DNA sites known as E-box sequences with higher affinity as well as non-consensus sites with lower affinity[113, 114]. Several studies have focused on identifying genes regulated by MYC and have demonstrated that MYC activates the transcription of several genes involved in proliferation, cell cycle progression, metabolism, apoptosis, migration, protein synthesis and cell growth[115, 116].

A growing body of research has demonstrated the oncogenic potential of MYC. Overexpression of MYC in various murine tissues leads to development of aggressive tumors[117-119]. Continued expression of MYC seems to be required for tumors as silencing it leads to tumor regression in mouse tumor models[120]. These studies highlight that tumors become addicted to MYC driven pathways for growth and survival. Even though MYC promotes tumorigenesis, it does not act alone. MYC requires cooperation with other oncogenes or non-oncogenes in inducing and maintaining tumorigenesis. While MYC is a potent activator of proliferation, it can also induce apoptosis via transcription of p53 and other apoptotic genes such as BIM[121]. However, MYC driven cancer cells evade oncogene-induced apoptosis through inactivation of pro-apoptotic genes such as p53, and by overexpression of anti-apoptotic genes, such as Bcl-2 and oncogenic RAS[122, 123].

MYC is rather unique as an oncogene, as its activation dramatically enhances protein synthesis via transcriptional upregulation of the translational machinery, including ribosomal proteins, initiation factors as well as elongation factors[13]. The ability of MYC to upregulate protein synthesis was observed previously in a transgenic mouse model of lymphoma, Eμ-Myc, which overexpress MYC in the B cell lineage[116, 124]. These mice develop pre-B and B cell lymphoma that is pathologically similar to human non-Hodgkin's lymphoma. Many groups have focused on targeting the translation machinery to test whether it is required for MYC induced lymphomagenesis in the Eμ-Myc mouse[125-127]. Indeed, targeting initiation factors significantly

delays lymphomagenesis and enhances survival of lymphoma bearing mice. Furthermore, genetically restoring protein synthesis in Eμ-Myc mice to normal levels also significantly reduces lymphomagenesis through enhanced apoptosis of lymphoma cells[126]. Collectively, these studies demonstrate that the oncogenic potential of MYC requires enhanced protein synthesis during tumorigenesis which can be therapeutically targeted in MYC-driven cancers.

We previously demonstrated that the ability of MYC to increase rate of protein synthesis in cells activates the PERK arm of UPR, which is required for supporting MYC induced transformation and survival[11]. Although MYC is a potent activator of proliferation, it also induces apoptosis, preventing transformation and tumor initiation. Hence, suppression of apoptosis through cooperation with other oncogenes and pathways are reported to promote MYC induced transformation[107]. PERK activation was required for suppression of MYC induced apoptosis. Ablation of PERK in hematopoietic progenitor cells significantly reduced transformation by MYC and dominant negative p53 as a result of increased apoptosis. PERK was required for counteracting MYC induced apoptosis by activating cytoprotective autophagy and attenuating Ca+ release from the ER[11]. Importantly, enhanced activation of the PERK/eIF2α pathway was observed in B cells isolated from lymphoma patients compared to healthy donors suggesting that MYC can activate stress response pathways such as the UPR that sustain its tumorigenic property and further promote survival.

Another study in *Drosophila melanogaster* has corroborated these findings. Overexpression of MYC in Drosophila fat cells results in PERK-mediated autophagy induction. Interestingly, PERK and autophagy were both dispensable for physiological growth of fat cells but required for MYC induced cell growth as inhibition of PERK or autophagy suppressed MYC induced cell growth[128]. Therefore, through its direct effect on eIF2α, PERK appears to act as a "brake" to fine-tune protein synthesis as well as activate cytoprotective autophagy. Although the molecular mechanisms of survival that are mediated by autophagy to counteract apoptosis in these conditions remain to be elucidated, an attractive hypothesis is that autophagy prevents protein toxicity through degradation of excess unfolded proteins. Thus, the PERK axis of UPR is

one such pathway activated to support MYC induced transformation and cell growth, making it an attractive therapeutic target in MYC driven cancers. However, whether or how ATF4 elicits a cytoprotective response to relieve cells from MYC induced intrinsic stress was not known.

Gaps in knowledge prior to this work and overall hypothesis

ATF4 appears to have dual roles in MYCN driven cancer cells, as it has been reported to induce apoptosis in response to glutamine deprivation but also required for glutamine metabolism. Qing and colleagues reported that ATF4 mediates apoptosis upon glutamine deprivation in human neuroblastoma cells with amplified *MYCN* through the transcription of pro-apoptotic NOXA, PUMA and TRIB3. Silencing ATF4 partially rescued viability during glutamine starvation[129]. Interestingly, in another study ATF4 was shown to regulate glutamine metabolism in neuroblastoma cells through cooperative transcriptional induction of a glutamine transporter, ASCT2, with MYCN. The same study showed that relative expression of MYCN, ATF4 and ASCT2 was significantly elevated in human neuroblastomas with amplified MYCN[130]. These studies indicate the complex role of ATF4 in MYC overexpressing cells and calls for further examination of the role of ATF4 at different stages of tumor initiation and progression as well as correlation with its levels induced by physiological stress versus pharmaceutical intervention.

A previous report suggested that ATF4 can contribute to HRAS and SV40-mediated transformation through suppression of INK4a/ARF cell senescence factors[102]. However, the underlying mechanisms of ATF4 regulation in the context of other cellular oncogenes remain to be elucidated. Deregulated MYC increases biomass production in the form of nucleotides, proteins and amino acids which is necessary to support cell growth and proliferation. Biomass accumulation comes with a cost of having higher nutrient import as well as heightened expression of enzymes involved in anabolic growth. Besides the energy cost associated with biomass production, enhanced metabolism and protein synthesis creates a bioenergetics stress that must be carefully regulated. Thus, activation of adaptive pathways that support metabolism and

prevent proteotoxicity become vital for MYC overexpressing cancer cells. While we have observed upregulation of ATF4 in extrinsic stress conditions, the specific responses that ATF4 elicits during MYC induced stress need to be studied in order to therapeutically target the ISR in MYC driven tumors.

Based on these published studies, I formulated the following hypothesis: **The pro-tumorigenic properties of MYC can be shifted to anti tumorigenic state by targeting the Integrated Stress Response (GCN2/PERK/eIF2α/ATF4), which promotes survival and fuels growth in MYC induced tumorigenesis.** I set out to test this hypothesis by addressing the following aims.

Project aims

Aim 1: First, we sought to investigate whether the ISR effector ATF4 becomes upregulated in response to MYC induced intrinsic stress. Towards this end we demonstrated that ATF4 is activated by MYC in multiple cell lines and is required for survival during MYC activation. Furthermore, genome wide ChIP-seq analysis revealed that both ATF4 and MYC share target genes such as amino acid transporters, tRNA synthetases and translation regulators. Importantly, we identified the translation regulator 4E-BP1 is a target of both ATF4 and MYC. Inhibition of mTORC1 during MYC activation was able to rescue ATF4 deficient cells from apoptosis.

Aim 2: Second, we aimed to understand the functional role of PERK/GCN2/eIF2α/ATF4 pathway in determining cell fate decisions in MYC induced tumorigenesis. To address this, we employed the Eμ-Myc mouse, a transgenic mouse model of MYC induced spontaneous lymphoma. We demonstrated that combined inhibition of PERK and GCN2 suppresses phosphorylation of eIF2α and promotes survival of lymphoma bearing mice. Interestingly, inhibition of both kinases did not affect ATF4 levels suggesting the critical role ATF4 plays in tumorigenesis. However, conditionally deleting ATF4 showed a potent delay in lymphomagenesis and promoted overall survival. We also identified that ATF4 gene signature strongly correlates with expression of 4E-

BP1 in sarcoma, diffused large B cell lymphoma, colon and breast cancer highlighting the clinical relevance. High 4E-BP1 expression correlated with poor progression free as well as overall survival in diffused large B cell lymphoma. Overall, this work illustrates the important pro-survival role the ISR, particularly ATF4 plays in MYC induced intrinsic stress.

CHAPTER 2: ATF4 COUPLES MYC-DEPENDENT TRANSLATIONAL ACTIVITY TO BIOENERGETIC DEMANDS DURING TUMOR PROGRESSION

This chapter contributes to a manuscript submitted to Nature Cell Biology with the same title and is currently under revisions.

Introduction

Cells utilize distinct and divergent stress response pathways to overcome environmental and physiological stresses. The Integrated Stress Response (ISR) pathway promotes cellular adaptation to various stresses such as viral infection, heme deprivation, hypoxia, nutrient deprivation and acidosis[57]. The ISR kinases, PKR-like ER kinase (PERK), general control non-derepressible 2 (GCN2), double-stranded RNA-dependent protein kinase (PKR) and heme-regulated eIF2α kinase (HRI), sense distinct stresses and catalyze phosphorylation of the α subunit of the eukaryotic initiation factor (eIF2α)[50]. Phosphorylation of eIF2α at serine 51 attenuates general protein synthesis while enhancing the translation of select transcripts containing distinct regulatory sequences in their 5' UTR[50, 131]. An important example of these transcripts is the activating transcription factor 4 (ATF4), which is highly translated during phosphorylation of eIF2α and serves as a key effector of the ISR pathway. Once translated, ATF4 translocates to the nucleus where it binds to and drives the transcription of genes involved in antioxidant response, autophagy, amino acid biosynthesis and transport[40, 48].

The ability of cancer cells to adapt to non-cell autonomous (extrinsic) and cell autonomous (intrinsic) stresses is critical for maintaining cell viability and growth. We and others previously showed that the ISR is essential in adaptation to extrinsic stresses present in the tumor microenvironment such as hypoxia and nutrient deprivation[9, 83, 95, 132]. In addition to extrinsic stress, cancer cells also experience intrinsic stress due to activation of oncogenes that increase bioenergetic processes[11, 104, 133]. In this context, amplification of the MYC oncogene, a frequent event in multiple human cancer types[109] results in intrinsic stress due to enhanced protein synthesis and rewired metabolic pathways to meet the demands of rapid cell growth and proliferation[116, 134]. MYC upregulates protein synthesis by transactivating components of the translational machinery including several initiation factors, ribosomal proteins and tRNAs[134]. The enhanced protein synthesis driven by MYC is critical for its oncogenic properties as targeting the translation machinery has proven to be effective in MYC driven cancers[125, 126].

Regulation of protein synthesis is critical for survival of cancer cells during tumor development. For example, increased protein synthesis has to be accompanied by a concomitant increase in ER folding capacity and size. The initial response triggered by ISR through eIF2α phosphorylation is a transient reduction of protein synthesis rates which reduces ER load and also conserves energy. Cells deficient in PERK, eIF2α or ATF4 fail to buffer augmented translation rates, as a result are defective in upregulating chaperones and ER expansion. These cells are therefore highly sensitive to ER stress inducers, in a process termed "proteotoxicity" [39].

Although ATF4 has been implicated in supporting survival of cancer cells experiencing the deficit of oxygen and nutrients, the role of ATF4 in oncogene-induced stress has not been well characterized. Moreover, whether or how ATF4 elicits a cytoprotective response to relieve cells from oncogene-induced stress remains unclear. Here, we show that optimal ATF4 expression upon MYC dysregulation requires both the PERK and GCN2 kinases, the latter being activated by excess uncharged amino acids produced by increased MYC activity. Induced ATF4 cooperatively co-regulates a number of gene products along with MYC, including the transcription of 4E-BP1 to fine-tune mRNA translation induced by MYC. Furthermore, our results demonstrate the critical role of ISR signaling-induced ATF4 in supporting cell adaptation and survival during MYC-dependent tumor growth and progression.

Results

ATF4 is induced by MYC and promotes survival. We previously reported that activation of MYC leads to phosphorylation of PERK and eIF2α[11]. To test whether MYC activation also induces ATF4, we first measured expression of ATF4 following MYC induction in DLD-1, human colon adenocarcinoma cells and mouse embryonic fibroblasts (MEFs) stably expressing a tamoxifen inducible MYC chimera, MycER. Treatment with 4-hydroxy-tamoxifen (4-OHT) led to accumulation of MYC in the nucleus and expression of ATF4 protein in both cell lines (Figure. 2.1A). Similarly, in the human Burkitt's lymphoma cell line P493-6, in which expression of MYC is turned off by administration of tetracycline, suppression of MYC, resulted in a concomitant

decrease of ATF4. Upon restoration of MYC levels, ATF4 protein levels also recovered (Figure. 2.1B). These data indicate that elevated MYC induces ATF4 expression.

Notably, ablation of ATF4 in MEFs significantly enhanced MYC-induced cell death, which was evident by levels of the apoptosis markers cleaved Poly-ADP ribose polymerase, cl-PARP, and cleaved caspase 3 (Figure. 2.1C) as well as by significantly reduced clonogenic survival (Figure. 2.1D). Similarly, knockdown of ATF4 in DLD-1 cells also markedly enhanced apoptosis following MYC activation (Figure. 2.1E). Collectively, these results highlight a significant role for ATF4 in promoting survival of transformed cells upon MYC activation.

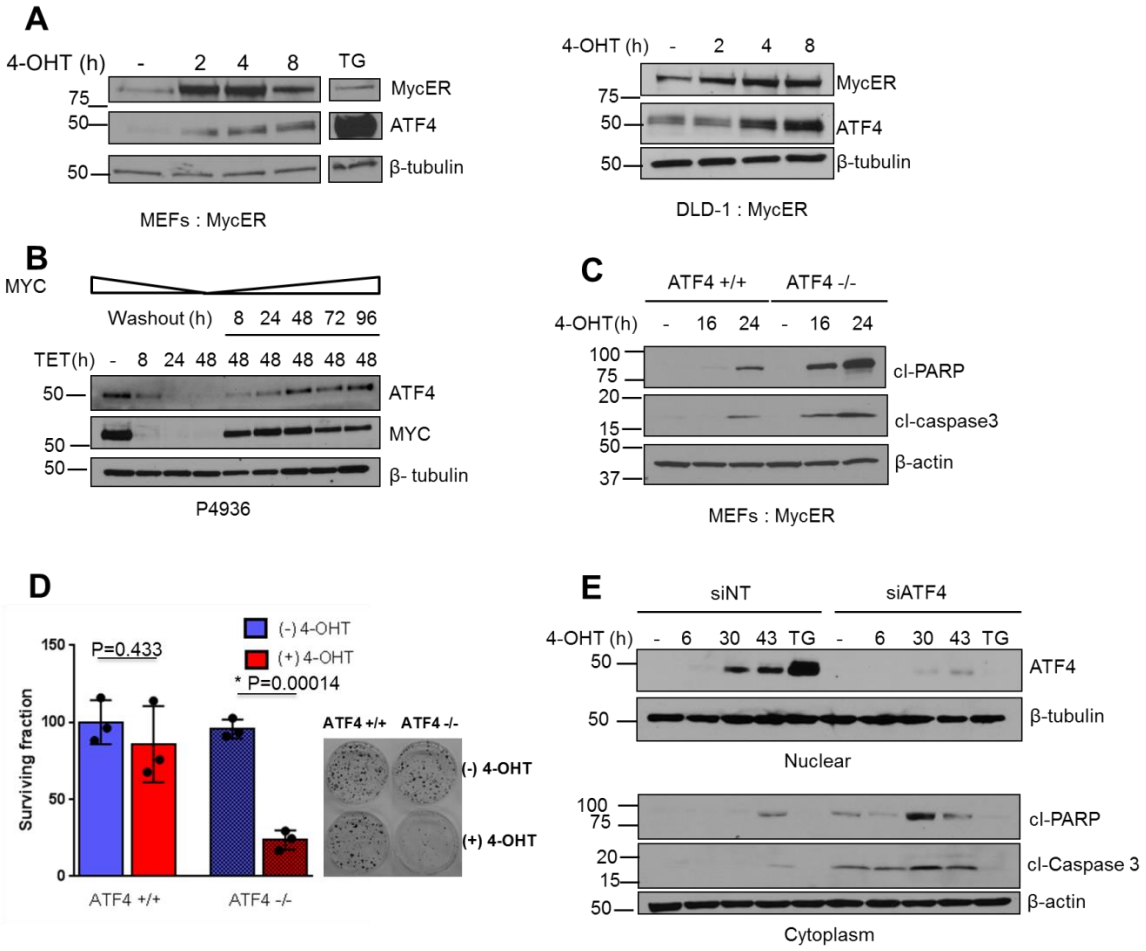

Previous page: Figure 2.1. MYC induced ATF4 inhibits apoptosis and promotes survival. (A). MEFs (left panel) and DLD-1 cells (right panel) expressing MycER were treated with 4-OHT to activate MYC. Indicated proteins were assessed by immunoblotting nuclear lysates. Thapsigargin (0.5μM for 4h) treated cells were used as a positive control for ATF4 induction. (**B).** P4936 cells were treated with tetracycline (0.1ug/ml) to shut off MYC expression or tetracycline was washed off for the indicated times. Nuclear lysates were used for detecting indicated proteins by immunoblotting. **(C).** Immunoblot analysis of whole cell lysates from ATF4 +/+ and ATF4 -/- MEFs treated with 4-OHT for indicated times. **(D).** Clonogenic survival was performed after activating MYC in MEFs, representative plates from 3 biological replicates are shown. Colonies were counted and surviving fraction is shown normalized to no treatment control. Error bars represent mean ± SD, two tailed student t-test. **(E).** DLD-1: MycER cells were transfected with non-targeting siRNA or siRNA targeting ATF4. Cells were treated with 4-OHT and indicated proteins were assessed by immunoblotting.

PERK and GCN2 are required for optimal phosphorylation of eIF2α following MYC induction. Activation of MYC enhances protein synthesis resulting in ER stress[11, 128]. We previously reported that PERK activation within the unfolded protein response (UPR) led to phosphorylation of eIF2α thereby protecting MYC overexpressing cells from proteotoxicity[11]. Although PERK is primarily responsible for phosphorylating eIF2α during MYC activation, residual phosphorylation of eIF2α in PERK knockout cells prompted us to ask whether other ISR kinases phosphorylate eIF2α in the absence of PERK[11]. We focused on the kinase GCN2 since we and others have shown that its activity is upregulated in multiple solid tumors[83, 84]. Interestingly, we noted robust phosphorylation of GCN2 following MYC activation (Figures. 2.2A, 2.2B and 2.2D). Consistent with our previous report[11], phosphorylation of eIF2α was still present upon PERK knockdown albeit at reduced levels compared to control cells (Figure. 2.2B). Notably, eIF2α phosphorylation was markedly reduced in the absence of both kinases, indicating functional compensation between these kinases for phosphorylation of eIF2α upon MYC activation (Figure. 2B).

Consistent with ATF4 loss, knockdown of both PERK and GCN2 enhanced apoptosis following MYC activation (Figure. 2.2B). Silencing PERK or GCN2 also reduced ATF4 protein

levels (Figure. 2.2B), and this effect was more prominent in GCN2 knockdown cells. Similarly, GCN2 knockout transformed MEFs failed to induce ATF4 following MYC activation (Figure. 2.2C). Because GCN2 deficient cells still displayed p-eIF2α, yet ATF4 protein was significantly reduced compared to wild type, we hypothesized that GCN2 may be regulating ATF4 at the transcriptional level. Indeed, induction of MYC resulted in a significant upregulation of ATF4 mRNA only in wild-type cells, though another well-characterized MYC target gene, ornithine decarboxylase (ODC1) was activated independent of GCN2 (Figure. 2.2E, 2.2F). These results suggest that GCN2 is required not only for efficient ATF4 protein expression but also for its transcription in response to MYC activation.

MYC increases ratio of uncharged tRNAs leading to activation of GCN2. Cellular deficiency in any of the 20 amino acids leads to accumulation of uncharged tRNAs which bind to GCN2 resulting in a conformational change to promote its autophosphorylation[131]. Activated GCN2 can then phosphorylate eIF2α, resulting in transient inhibition of general protein synthesis during amino acid deprivation conditions[135]. The robust phosphorylation of GCN2 following MYC activation in cells grown in complete media, replete with essential amino acids, prompted us to investigate the mechanism of GCN2 activation under this cell-intrinsic stress (Figure. 2.2A). MYC has been previously shown to robustly enhance transcription of tRNAs in RNA POL III-dependent manner[136] suggesting that newly synthesized uncharged tRNAs might activate GCN2. To test this hypothesis, we pretreated cells with the highly specific RNA polymerase III inhibitor (ML60218) to suppress tRNA synthesis prior to MYC activation. Inhibition of RNA polymerase III markedly reduced GCN2 phosphorylation, indicating that RNA POL III mediated transcription of tRNAs is required for MYC activation of GCN2 (Figure. 2.2D).

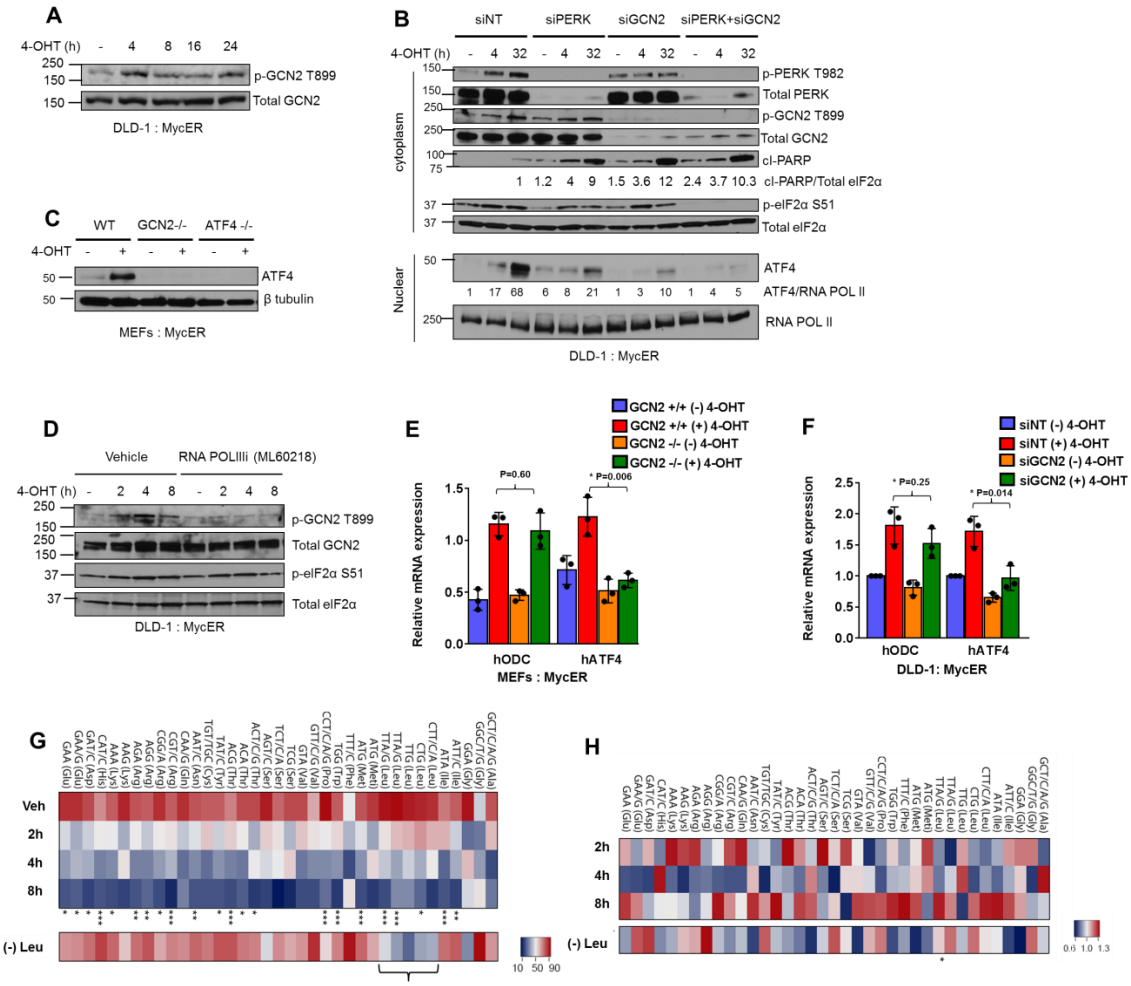
A
4-OHT (h) - 4 8 16 24
250
150
p-GCN2 T899
150
Total GCN2
DLD-1 : MycER
B
siNT
siPERK
siGCN2
siPERK+siGCN2
4-OHT (h) - 4 32 - 4 32 - 4 32 - 4 32
cytoplasm
p-PERK T982
Total PERK
p-GCN2 T899
Total GCN2
cl-PARP
1 1.2 4 9 1.5 3.6 12 2.4 3.7 10.3 cl-PARP/Total eIF2α
p-eIF2α S51
Total eIF2α
Nuclear
ATF4
1 17 68 6 8 21 1 3 10 1 4 5 ATF4/RNA POL II
RNA POL II
DLD-1 : MycER
C
WT
GCN2-/-
ATF4 -/-
4-OHT - + - + - +
ATF4
β tubulin
MEFs : MycER
D
Vehicle
RNA POLIIIi (ML60218)
4-OHT (h) - 2 4 8 - 2 4 8
p-GCN2 T899
Total GCN2
p-eIF2α S51
Total eIF2α
DLD-1 : MycER
E
GCN2 +/+ (-) 4-OHT
GCN2 +/+ (+) 4-OHT
GCN2 -/- (-) 4-OHT
GCN2 -/- (+) 4-OHT
P=0.60
* P=0.006
Relative mRNA expression
hODC
hATF4
MEFs : MycER
F
siNT (-) 4-OHT
siNT (+) 4-OHT
siGCN2 (-) 4-OHT
siGCN2 (+) 4-OHT
* P=0.25
* P=0.014
Relative mRNA expression
hODC
hATF4
DLD-1: MycER
G
Veh
2h
4h
8h
(-) Leu
H
2h
4h
8h
(-) Leu

Previous page: Figure 2.2. The amino acid sensor GCN2 is activated by uncharged tRNAs and is required for optimal activation of ATF4 upon MYC induction. (A). Representative immunoblot showing activation of GCN2 following MYC induction in cytoplasmic lysates. **(B).** DLD-1: MycER cells were transfected with non-targeting siRNA or siRNA against PERK, GCN2 or both. ISR signaling and apoptosis were assessed by immunoblotting after MYC activation. **(C).** Representative immunoblot analysis of nuclear lysates from GCN2 +/+ or GCN2-/- MEFs after 4hr of MYC activation. **(D).** DLD-1: MycER cells were pretreated with DMSO or 50uM RNA POLIII inhibitor (ML60218) for 2hrs prior to MYC activation. Indicated protein levels were measured by immunoblotting from cytoplasmic lysates. **(E).** qRT PCR showing mRNA expression in GCN2 +/+ and GCN2 -/- : MycER MEFs or in DLD-1: MycER cells **(F)** transfected with non-targeting siRNA or siRNA targeting GCN2, normalized to 18s RNA. n=3 independent experiments, error bars represent mean ± SD, two tailed student t-test **(G).** Microarray of aminoacyl–tRNAs of DLD-1: MycER cells after MYC induction at indicated times, four independent experiments, one-way ANOVA, *p<0.05; **, p<0.01; ***, p< 0.001. (-) Leu denotes Leu-deprived cells and the marked tRNAs reading Leu codons are uncharged, n=1. tRNA probes are depicted with their cognate codon and the corresponding amino acid; Meti, initiator $tRNA^{Met}$. Two different probes recognizing two different $tRNA^{Leu}$ isodecoders that pair to the same codon TTA/G Leu codon but differ in their sequence outside the anticodon were used on the arrays. **(H).** Heat map of comparative microarray showing tRNA abundance following MYC activation. Data are depicted relative to the (-) 4-OHT values, four biological replicates, one way-ANOVA, *p<0.05.

RNA polymerase III regulates the transcription of other small structured RNAs including tRNAs[136]. To analyze the levels of aminoacyl-tRNAs following MYC activation more directly, we used tRNA-tailored microarrays that distinguish charged vs uncharged tRNAs. We found a striking and time-dependent increase in the levels of multiple uncharged tRNAs following MYC activation (Figure. 2.2G). There was also a strong increase in the overall abundance of total tRNAs (Figure. 2.2H). As expected, leucine deprivation led to increased uncharging of all leu tRNA isoacceptors, demonstrating the specificity of the assay (Figure. 2.2G). These data indicate that MYC-induced RNA polymerase III dependent transcription of tRNAs leads to accumulation of uncharged tRNAs, thereby activating GCN2.

ATF4 and MYC have common (overlapping) DNA binding sites. Since ATF4 is critical for survival following MYC activation (Figure. 2.1C-E), we next performed chromatin immunoprecipitation (ChIP)-sequencing to map ATF4 bound genes on a genome wide scale

following MYC activation. ChIP-seq was performed in DLD-1, MycER cells with or without MYC activation for 8hrs. We identified 330 unique ATF4 binding sites that had ATF4 ChIP-seq signal significantly enriched (FDR<5%, at least 4-fold) over IgG control (Figure. 2.3A). Approximately 50 % of the biding sites (165 out of 330) were significantly increased following MYC activation (Figure. 2.3B). De-novo motif search revealed that ~90% of identified ATF4 binding sites contained a previously established mouse ATF4 binding motif (GSE35681)[137] (Figure. 2.3B). From the 165 ATF4 binding sites, we identified 79 genes (with Entrez ID) where ATF4 occupied within 5kb from at least one gene transcription start site (TSS). Of this subset, sixteen genes are previously well-characterized ATF4 targets (Figure. 2.3C). Analysis of the 79 gene list for functional and pathway enrichment showed significant overrepresentation of 11 functional categories and 10 pathways (Figure. 2.3D). As expected, one of the pathways was the UPR confirming the well-characterized role of ATF4 in UPR.

Other key functional categories were amino-acid transport, amino acid biosynthesis and tRNA synthetases suggesting the important role of ATF4 in supporting protein synthesis (Figure. 2.3D). We then analyzed the gene list for enrichment of known transcriptional regulators to identify other potential transcriptional co-regulators (Figure. 2.3E). As expected, ATF4 itself was the top significant hit with 16 known targets and a Z-score indicating positive regulation (Z=3.88, based on the majority of targets being upregulated by ATF4). Intriguingly, the only other significant transcriptional co-regulator was MYC with a Z score of at least 1.5, higher than additional factors such as p53, SP1 and Pax3 that also had significant enrichment of targets.

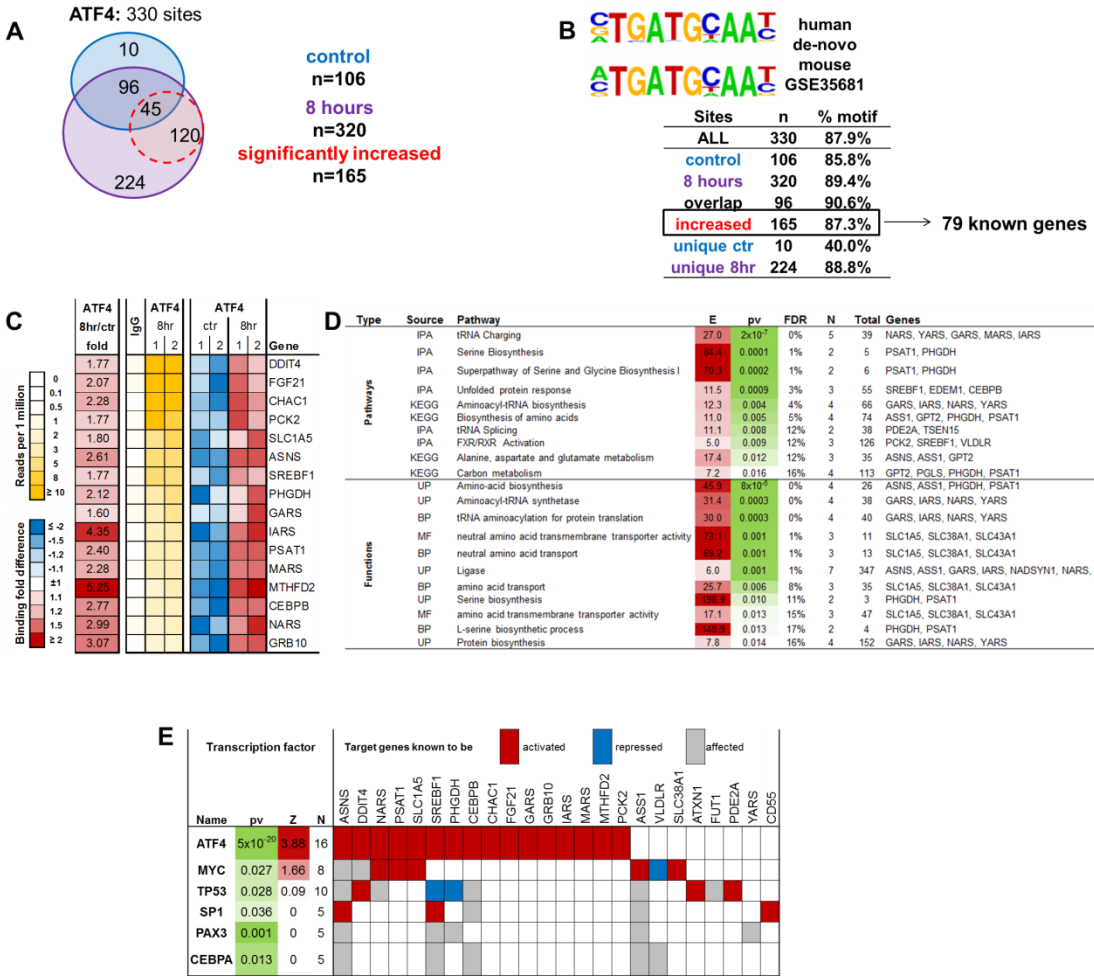

Figure 2.3. ATF4 and MYC bind to common target genes. (A). ATF4 ChIP-seq identified 330 binding sites for ATF4. Binding sites occupied by ATF4 without 4-OHT and with 4-OHT are shown in blue and purple respectively. Binding sites that are significantly increased after 8 hours of MYC activation are shown in red. **(B).** Motif enriched within 330 ATF4 binding sites (human de-novo) and within ATF4 mouse experiment from GSE35681 dataset[23]. Table shows percent of binding sites containing the motif for different site groups. **(C).** Previously reported ATF4 targets occupied by ATF4 at 8hr of MYC induction within 5kb from TSS. **(D).** Functions and pathways significantly enriched among genes bound by ATF4 within 5kb from TSS and upregulated at 8 hours of MYC activation, E=enrichment, FDR=false discovery rate, UP=Uniprot, MF=molecular function, BP=biological process. **(E).** Transcription factors whose known targets were enriched among genes bound by ATF4, Z=z-score for predicted transcription activation state calculated by IPA based on number of targets shown to be activated by the TF.

We then performed ChIP-seq for MYC to map its global binding at 8hr after stimulation with 4-OHT in these adenocarcinoma cells. This experiment identified 3263 peaks at 8hr of MYC induction that were within 5kb from a gene TSS, 33 of which overlapped with ATF4 binding sites (28% of all ATF4 peaks), a significant overlap (2.1 more than expected by chance, $p=2x10^{-5}$ by hypergeometric test) suggesting similar mechanism regulating a significant subset of genes by both MYC and ATF4 (Figure. 2.4A). Among other genes from the enriched pathways and functions (Figure. 2.3D), genes with amino acid transport function (SLC7A11, SLC38A1, SLC43A1) and tRNA charging (IARS, MARS, NARS) were occupied by both ATF4 and MYC (Figure. 2.4B). A ChIP-seq profile at a representative MYC and ATF4 target loci, TBC1D16, (Figure. 2.4C) shows overlapping binding of both MYC and ATF4 (Figure. 3f). We validated the ChIP-seq results by ChIP-qPCR (Figure. 2.4D, 2.4E). The ChIP-seq result suggests that MYC and ATF4 share common target genes, most of which are involved in amino acid transport and tRNA charging process.

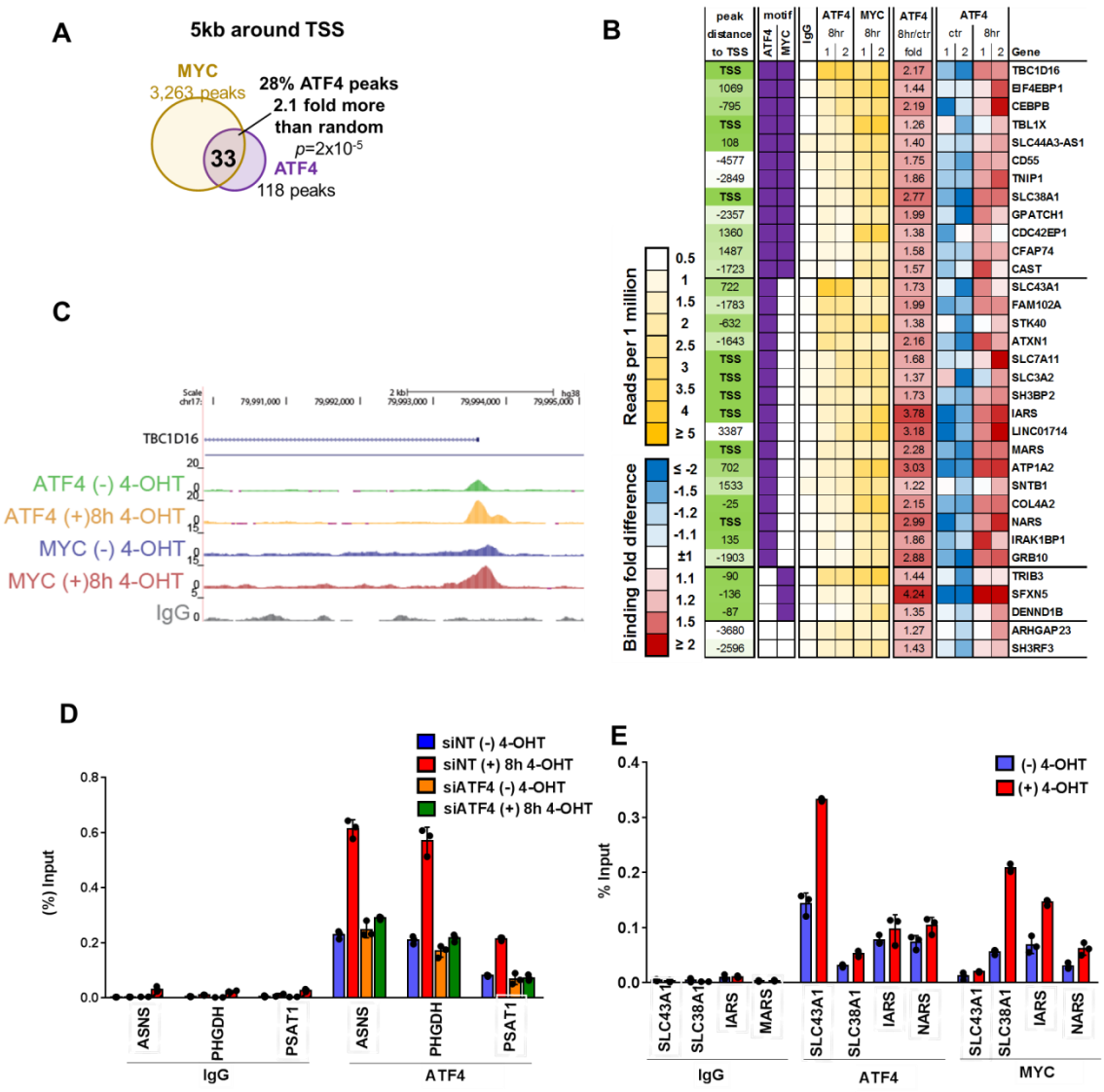

Figure 2.4. ATF4 and MYC ChIP-seq. (A). Overlap of MYC and ATF4 bound genes in 8hr samples: sites co-bound by ATF4 and MYC within 5kb from genes' TSS. **(B).** List of all 33 genes from panel A that were bound by ATF4 and MYC at 8hrs of MYC activation. **(C).** ChIP-seq signal track within TBC1D16 locus showing ATF4 and MYC binding peaks. **(D).** ChIP qPCR validation of ATF4 target genes and **(E)** genes bound by both ATF4 and MYC. Technical replicates, n=3, error bars represent mean ± SD.

ATF4 suppresses mTORC1 dependent signaling to prevent proteotoxicity following MYC activation. Since we identified a strong requirement for ATF4 in survival of MYC overexpressing cells, we sought to determine the mechanism by which ATF4 exerts its pro-survival effects. Given the known role of ATF4 in amino acid metabolism, antioxidant response, and fatty acid synthesis, we attempted to rescue ATF4 deficient cells by supplying metabolites *in trans* in culture media under conditions of MYC activation [40, 48, 138]. ATF4 deficient MEFs require the presence of non-essential amino acids and antioxidants in cell culture media in order to grow. Additional antioxidants or long chain fatty acids were not able to rescue ATF4 deficient cells (Figure 2.5Aand 2.5B). However, supplementation with alpha-ketoglutarate (αKG) delayed apoptosis during earlier time points (16hr) of MYC activation in ATF4 deficient MEFs but was not able to inhibit apoptosis during long-term activation (24hr) (Figure 2.5C). These results suggest that activation of MYC imposes metabolic stress on cells which can be partially rescued by αKG, an intermediary of the TCA cycle. However, since supplementation of metabolites is not sufficient to compensate for loss of ATF4 during activation of MYC, this indicates that there must be additional processes activated by ATF4 to maintain cell viability.

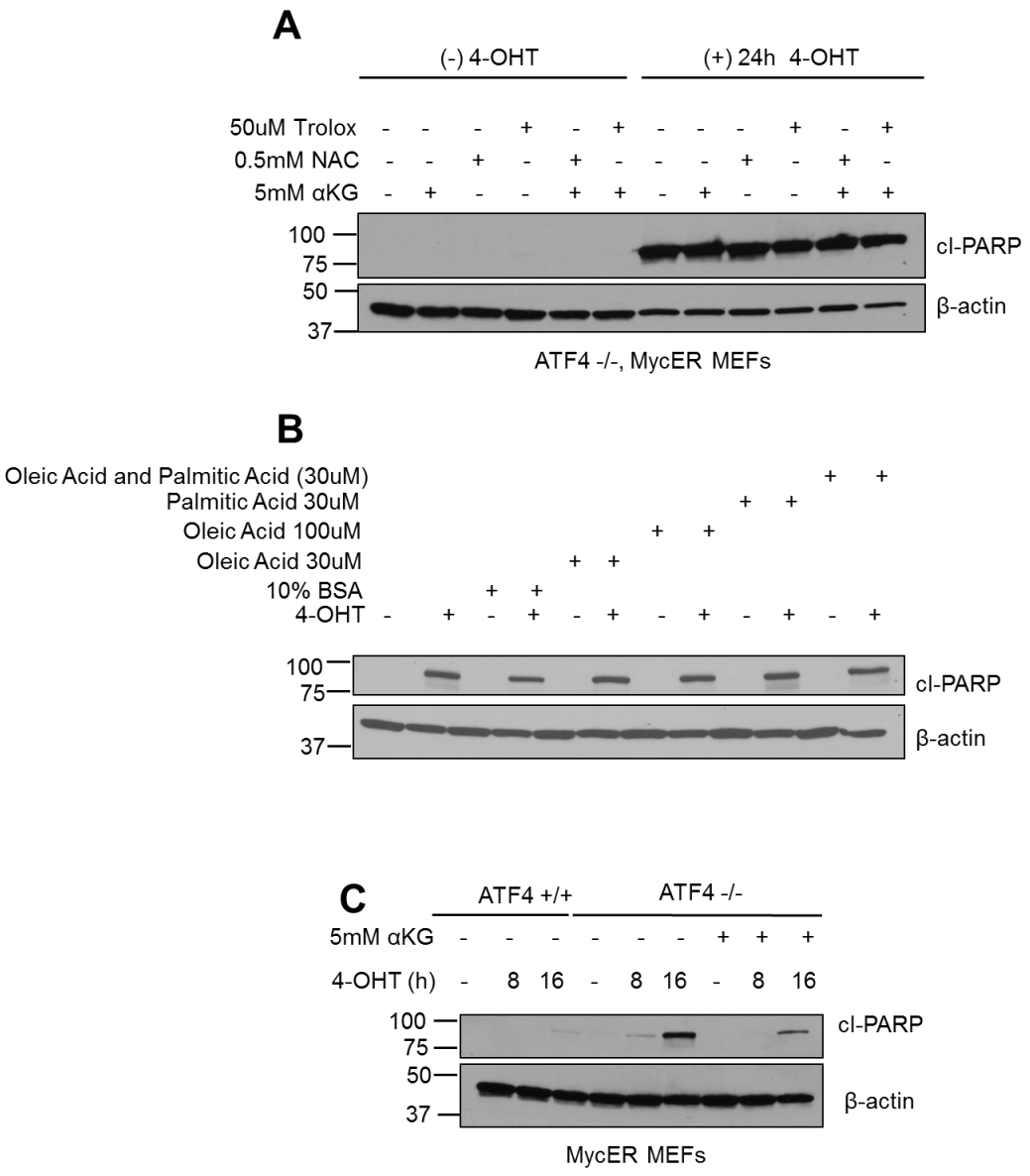

Figure 2.5. Antioxidants, fatty acids or alpha ketoglutarate do not rescue ATF4 deficient cells. (A). Immunoblot of ATF4 deficient MEFs treated with indicated antioxidants, Trolox and N-acetyl-cysteine (NAC) or Dimethyl 2-oxoglutarate (αKG) followed by MYC activation. **(B)**. Immunoblot of ATF4 deficient MEFs treated with indicated fatty acids followed by MYC activation. **(C)**. Representative western blot of MEFs treated with (αKG) at earlier timepoints of MYC activation.

One of the targets in the ChIP-seq analysis that was bound by both MYC and ATF4 was the negative regulator of the major cap-binding protein eIF4E, EIF4E-BP1 (4E-BP1) which is a downstream substrate of mammalian target of rapamycin complex 1 (mTORC1) (Figure 2.6A). mTORC1 integrates oncogenic stimuli into protein synthesis and cell growth signaling [139]. Activated mTORC1 phosphorylates p70S6K and 4E-BP1[140]. Hyperphosphoryaltion of 4E-BP1 by mTORC1 leads to its dissociation from eIF4E, enhancing cap-dependent protein synthesis downstream of eIF4E[141]. We confirmed that both ATF4 and MYC bind to the intron of 4E-BP1 by ChIP-qPCR (Figure 2.6A). Moreover, 4E-BP1 mRNA was reduced in the absence of ATF4 in both DLD-1 and MEFs (Figure 2.6B and 2.6C). We then assessed mTORC1 signaling following MYC activation. We observed MYC activation enhanced levels of phosphorylated 4E-BP1 (Figure 2.6D, 2.6E and 2.6F). Yet, there was a marked reduction in abundance of 4E-BP1 in the absence of ATF4 (Figure 2.6D, 2.6E and 2.6F) indicating that ATF4 is required for MYC-induced 4E-BP1. This also implied that eIF4E is left unchecked in the absence of 4E-BP1 thus driving further cap dependent translation. ATF4 deficient cells also exhibited sustained phosphorylation of p70S6K (Figure 2.6D, 2.6E and 2.6F). We next sought to examine whether mTORC1 suppression in ATF4 deficient cells could reduce cell death during MYC activation. Indeed, inhibition of mTORC1 by rapamycin treatment with MYC induction led to a marked decrease in apoptosis and enhanced clonogenic survival in ATF4 deficient cells (Figure 2.6E, 2.6Fand 2.6G).

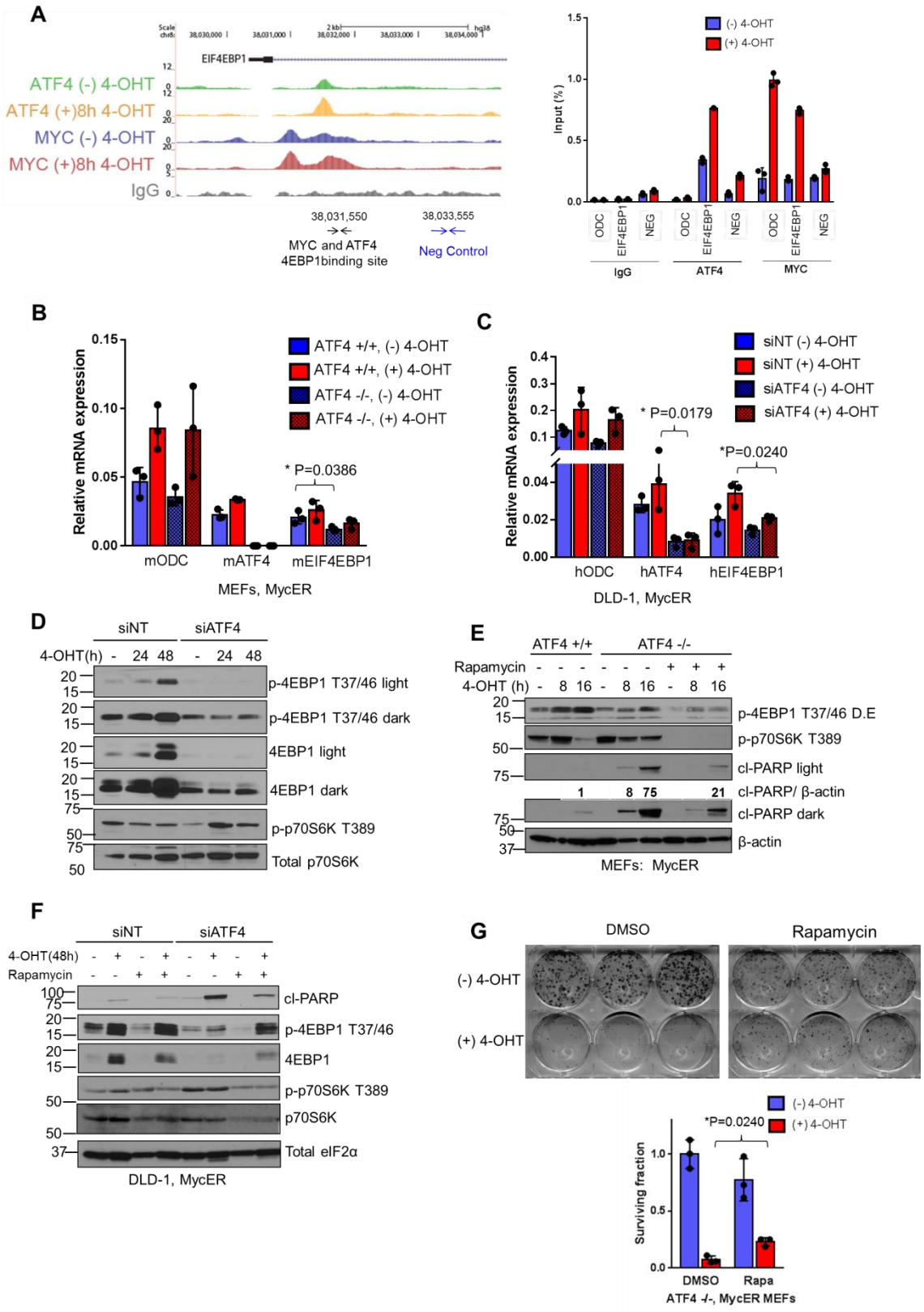
A
EIF4EBP1
ATF4 (-) 4-OHT
ATF4 (+)8h 4-OHT
MYC (-) 4-OHT
MYC (+)8h 4-OHT
IgG
38,031,550
38,033,555
MYC and ATF4 4EBP1binding site
Neg Control
(-) 4-OHT
(+) 4-OHT
Input (%)
ODC
EIF4EBP1
NEG
IgG
ATF4
MYC
B
ATF4 +/+, (-) 4-OHT
ATF4 +/+, (+) 4-OHT
ATF4 -/-, (-) 4-OHT
ATF4 -/-, (+) 4-OHT
Relative mRNA expression
* P=0.0386
mODC
mATF4
mEIF4EBP1
MEFs, MycER
C
siNT (-) 4-OHT
siNT (+) 4-OHT
siATF4 (-) 4-OHT
siATF4 (+) 4-OHT
Relative mRNA expression
* P=0.0179
*P=0.0240
hODC
hATF4
hEIF4EBP1
DLD-1, MycER
D
siNT
siATF4
4-OHT(h) - 24 48 - 24 48
p-4EBP1 T37/46 light
p-4EBP1 T37/46 dark
4EBP1 light
4EBP1 dark
p-p70S6K T389
Total p70S6K
E
ATF4 +/+
ATF4 -/-
Rapamycin - - - - - - + + +
4-OHT (h) - 8 16 - 8 16 - 8 16
p-4EBP1 T37/46 D.E
p-p70S6K T389
cl-PARP light
1 8 75 21
cl-PARP/ β-actin
cl-PARP dark
β-actin
MEFs: MycER
F
siNT
siATF4
4-OHT(48h) - + - + - + - +
Rapamycin - - + + - - + +
cl-PARP
p-4EBP1 T37/46
4EBP1
p-p70S6K T389
p70S6K
Total eIF2α
DLD-1, MycER
G
DMSO
Rapamycin
(-) 4-OHT
(+) 4-OHT
(-) 4-OHT
(+) 4-OHT
*P=0.0240
Surviving fraction
DMSO
Rapa
ATF4 -/-, MycER MEFs

Previous page: Figure 2.6. ATF4 suppresses mTORC1 dependent signaling and inhibition of mTORC1 reduces cell death of ATF4 deficient cells following MYC activation. (A). ATF4 and MYC ChIP followed by qPCR at the EIF4EBP1 locus (above schematic shows locus for primers used). **(B)**. qPCR showing expression of indicated mRNAs in wild type and ATF4 -/-, MycER MEFs normalized to 18s RNA after 8hr of MYC activation. Three independent experiments, error bars represent mean ± SD, two tailed student t-test. **(C)**. qPCR showing expression of mRNAs in control and ATF4 knockdown DLD-1, MycER cells normalized to 18s RNA after 8hr of MYC activation. Three independent experiments, error bars represent mean ± SD, two tailed student t-test. **(D)**. DLD-1: MycER cells were transfected with non-targeting siRNA or one targeting ATF4, and proteins were assessed by immunoblotting after MYC activation. **(E)**. Representative immunoblot of ATF4 -/-, MycER MEFs pretreated with indicated drugs for 2 hours prior to MYC activation. Rapamycin (Rapa) 200nM. **(F)**. Immunoblot of DLD-1 cells pretreated for 2 hours with Rapamycin followed by MYC activation. **(G)**. Clonogenic survival of ATF4 -/-, MycER MEFs after activation of MYC in the absence or presence of Rapamycin (200nM). Graph from there independent experiments, error bars represent mean ± SD, two tailed student t-test.

To further probe the link between ATF4 and the mTORC1 effectors, we knocked down p70S6K and eIF4E two major translational activators downstream of mTORC1 signaling using siRNA in the absence of ATF4 and assessed cell death. Consistent with the increased cell viability achieved by rapamycin treatment, knocking down p70S6K reduced cell death incurred due to ATF4 deficiency when MYC was activated. Additionally, knocking down both p70S6K and eIF4E further reduced cell death in the absence of ATF4 (Figure 2.7A). These data suggest that ATF4 is required for defenses against proteotoxicity in the context of hyperactive MYC-mTORC1 signaling funneled through p70S6K and eIF4E. Indeed, inhibiting protein synthesis with low doses of cycloheximide led to a similar reduction in cell death in ATF4 deficient cells (Figure 2.7B). Furthermore, treatment with a chemical chaperone 4-Phenylbutyric acid (4-PBA) which has been demonstrated to protect against proteotoxicity under other stress contexts [142], also promoted survival of ATF4 deficient cells following MYC activation (Figure 2.7C). However, we did not observe a general increase in rate of translation by ^{35}S-Methionine and Cystine labeling in the absence of ATF4 suggesting that synthesis of specific proteins rather than global translation is deregulated in ATF4 deficient cells and contributes to proteotoxicity (Figure 2.7D). Collectively, these data suggest that inhibiting mTORC1 in ATF4 deficient cells reduces the demand of specific protein synthesis and promotes adaptation to hyperactive MYC-induced proteotoxicity.

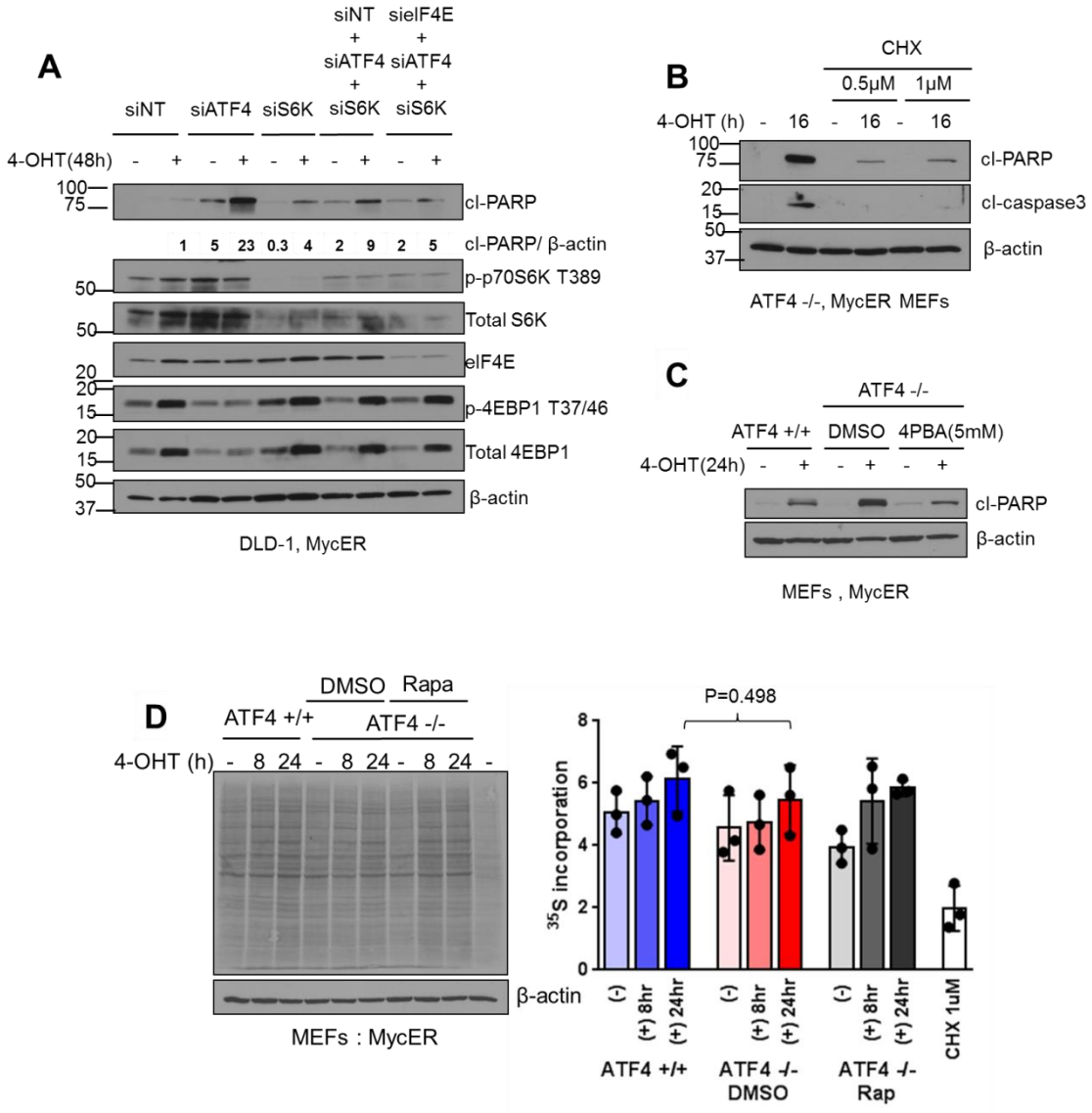

Figure 2.7. Inhibition of protein synthesis rescues ATF4 deficient cells following MYC activation. (A). DLD-1: MycER cells were transfected with non-targeting siRNA or indicated siRNAs, and proteins were assessed by immunoblotting after MYC activation. **(B)**. ATF4-/-, MycER MEFs were pretreated with cyclohexamide (CHX) for indicated times followed by MYC activation. **(C)**. ATF4-/-, MycER MEFs were pretreated with 5mM 4-Phenylbutyric acid (4PBA) for 2hrs followed by MYC activation. **(D)**.^{35}S incorporation in ATF4 -/-, MycER MEFs following MYC activation. Representative autoradiograph is shown. Graph data from three independent experiments, normalized to β-actin. Error bars represent mean ± SD, two tailed student t-test.

Inhibition of both PERK and GCN2 promotes survival of MYC driven lymphoma bearing mice. To test the importance of the GCN2-eIF2α-ATF4 pathway *in vivo*, we used a well characterized mouse model of MYC-driven lymphoma, Eμ-myc mice[117]. These mice harbor MYC coupled to the IgH enhancer and succumb to aggressive B-cell lymphoma between 6-15 weeks of age[117]. *GCN2*$^{-/-}$ mice are viable and fertile, unlike *ATF4*$^{-/-}$ mice which show several pathological abnormalities in utero or shortly after birth[78, 143, 144]. We next generated *Eμ-myc/+; GCN2*$^{+/+}$*, Eμ-myc/+; GCN2*$^{+/-}$ *and Eμ-myc/+; GCN2*$^{-/-}$ mice (Figure 2.8A) To our surprise, loss of GCN2 did not affect tumor initiation or progression and did not significantly affect overall survival of mice (Figure 2.8B). We then assessed ISR signaling in the B cells isolated from each genotype and observed robust phosphorylation of PERK and eIF2α as well as ATF4 in B cell lymphoma compared to normal B cells from littermate controls. Given that ISR signaling was still maintained in the absence of GCN2 indicated that PERK is likely compensating for loss of GCN2 (Figure 2.8C).

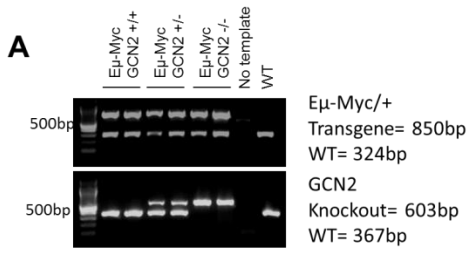

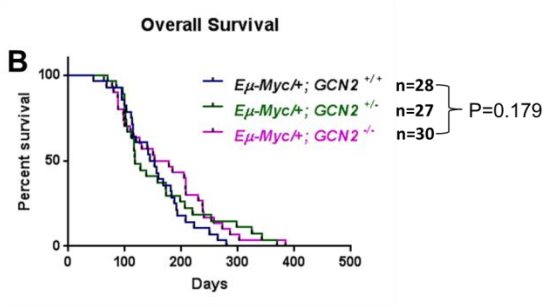

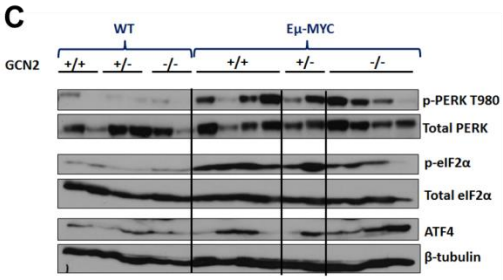

Previous page : Figure 2.8. Loss of GCN2 does not affect MYC driven lymphomagenesis. (A). Representative images of genotyping PCR products of *Eμ-Myc/+; GCN2*$^{+/+}$, *Eμ-Myc/+; GCN2*$^{+/-}$, *Eμ-Myc/+; GCN2*$^{-/-}$ mice. **(B).** Overall survival of *Eμ-Myc/+; GCN2*$^{+/+}$ (n=28), *Eμ-Myc/+; GCN2*$^{+/-}$ (n=27) and *Eμ-Myc/+; GCN2*$^{-/-}$ mice(n=30). **(C).** Representative western blot assessing ISR signaling in B cells isolated from tumor bearing mice or WT litter mates.

To test this notion, we transplanted either *Eμ-myc/+; GCN2*$^{+/+}$ or *Eμ-myc/+; GCN2*$^{-/-}$ lymphomas (Figure 2.9A) into C57BL/6J mice and targeted PERK by using a potent PERK inhibitor, LY-4[145]. LY-4 treatment was well tolerated and did not affect body weight or pancreas weight unlike PERK ablation in adult mice[146] but significantly reduced phosphorylation of PERK (Figure 2.9B, 2.9C and 2.9E). Inhibition of PERK in mice bearing *Eμ-myc/+; GCN2*$^{+/+}$ lymphomas did not affect overall survival (Figure 2.9D). However, Inhibition of PERK significantly increased the survival of mice bearing *Eμ-myc/+; GCN2*$^{-/-}$ lymphoma (Figure 2.9D). Consistent with our *in vitro* data, inhibition of both PERK and GCN2 significantly reduced phosphorylation of eIF2α in the lymphoma cells (Figure 2.9E and 2.9F). Unexpectedly, inhibition of PERK and GCN2 did not reduce ATF4 protein levels, suggesting an eIF2α-independent regulation of ATF4 in the *Eμ-myc* lymphoma model (Figure 2.9E). One possible explanation for the modest increase in survival of these mice is the decreased phosphorylation of eIF2α which can exacerbate ER stress in tumor cells due to unregulated protein synthesis[147]. These *in vivo* results underscore a strict selective pressure for maintenance of robust ATF4 levels in MYC-driven tumors.

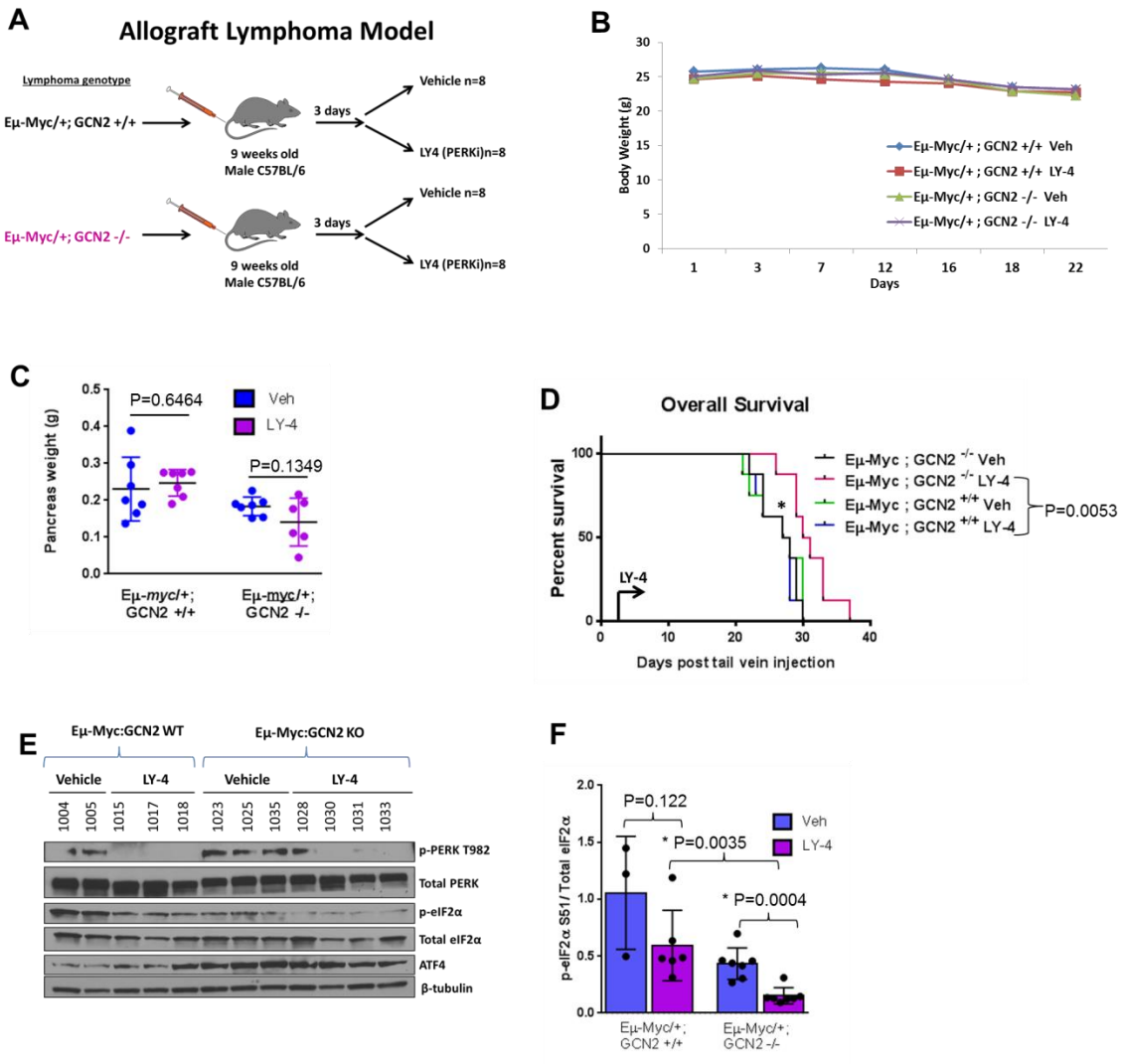

Figure 2.9. Loss of GCN2 combined with inhibition of PERK promotes survival of MYC driven lymphoma bearing mice. (A). Schematic showing the treatment regimen performed in allograft model of lymphomagenesis. 2 million lymphoma cells were injected via tail vein into mice and LY-4 treatment was started three days after tumor injection. **(B)**. Body weight of mice injected with lymphoma cells during LY-4 treatment. **(C)**. Pancreas weight of the mice in panel e. n=7 mice per group, two tailed student t-test. **(D)**. Overall survival of mice treated with either vehicle or LY-4. **(E)**. Representative immunoblot of ISR signaling examined in tumors isolated from the indicated groups by immunoblot. **(F).** Quantification of immunoblots for p-eIF2α, including panel c. n = 3 for GCN2 +/+ : Veh, n = 6 for GCN2 +/+ : LY-4 , n = 7 for GCN2 -/- : Veh and GCN2 -/- : LY-4, two tailed student t-test.

Acute ablation of ATF4 in lymphoma cells significantly enhances tumor-free survival and overall survival. The results with the *Eμ-myc/+; GCN2*$^{-/-}$ mice indicated that maintenance of ATF4 may be important for tumor progression. Therefore, we set out to test the requirement of ATF4 in tumor progression. To make a conditional knockout of ATF4, we utilized the *Rosa26-CreER*$^{T2/+}$ mice[148], which express a ubiquitously expressed tamoxifen inducible Cre recombinase enzyme. *Eμ-myc/+*; *Rosa26-CreER*$^{T2/+}$ were then crossed with ATF4$^{fl/fl}$ mice to generate mice with genotype of *Eμ-myc/+; ATF4*$^{wt/wt}$*; Rosa26-CreER*$^{T2/+}$ and *Eμ-myc/+; ATF4*$^{fl/fl}$*; Rosa26-CreER*$^{T2/+}$ (Figure 2.10A and 2.10B). When these mice developed lymphoma, the lymphoma cells were isolated and allografted by intravenous injection into C57BL/6 syngeneic mice. The recipient mice were then treated either with vehicle or tamoxifen to excise ATF4 specifically in the lymphoma cells (Figure 2.11A). Remarkably, excision of ATF4 significantly delayed lymphoma free survival (Figure 2.11B, left). This effect was not due to tamoxifen treatment because mice with *Eμ-myc/+; ATF4*$^{wt/wt}$*; Rosa26-CreER*$^{T2/+}$ lymphoma showed no significant difference in lymphoma-free survival (Figure 2.11B, right). Importantly, ATF4 excision in lymphoma cells significantly enhanced overall survival of lymphoma bearing mice (Figure 2.11C, left), whereas tamoxifen treatment alone did not promote overall survival of *Eμ-myc/+; ATF4*$^{wt/wt}$*; Rosa26-CreER*$^{T2/+}$ lymphoma bearing mice (Figure 2.11C, right).

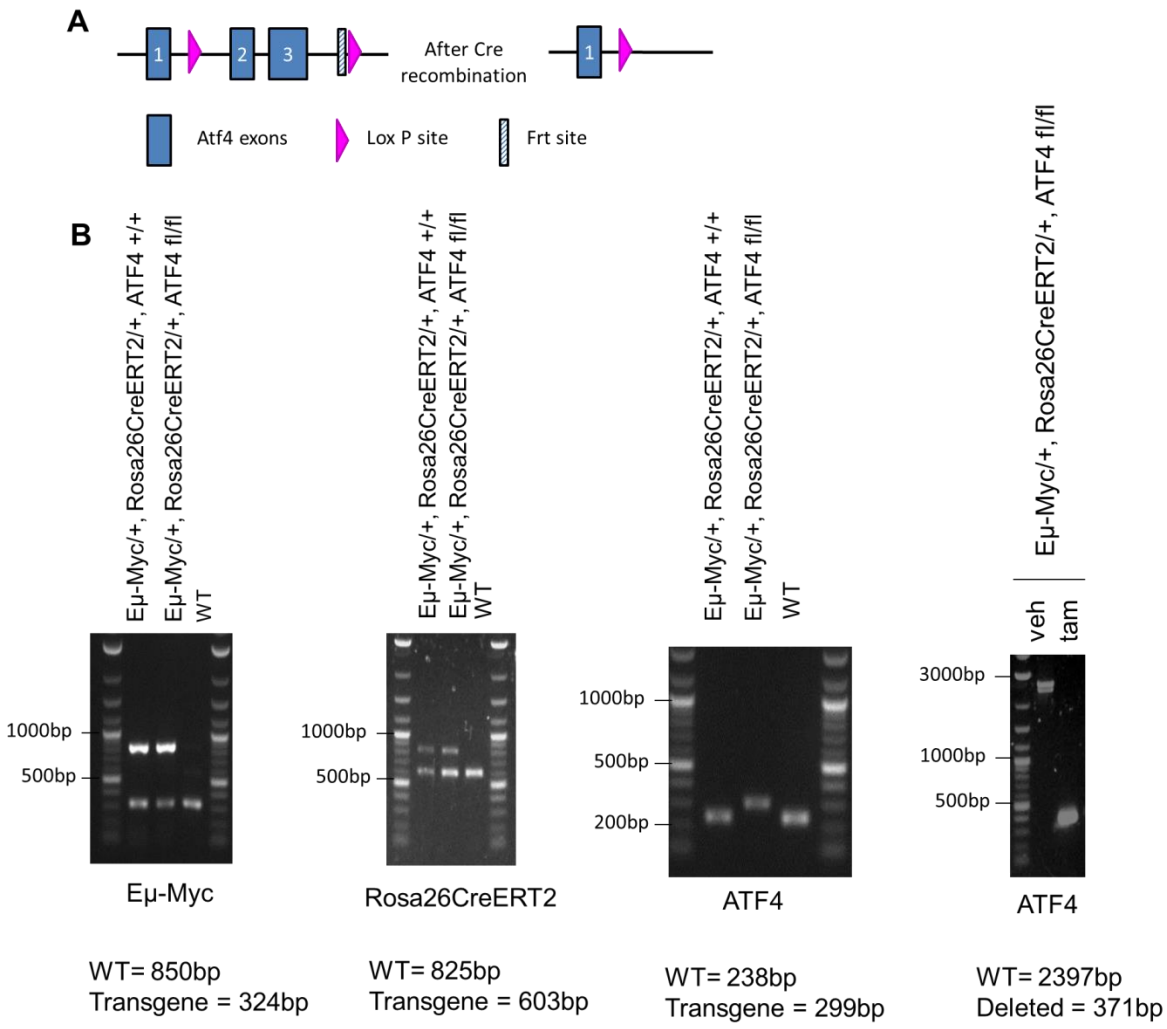

Figure 2.10. Generation of a conditional ATF4 knockout mouse. (A) Schematic showing insertion of LoxP sites in Atf4 locus. Exon 2 and 3, which code for ATF4 protein, are deleted after Cre recombinase mediated excision. **(B)** Gel analysis of PCR products of lymphoma cells used in allograft experiment.

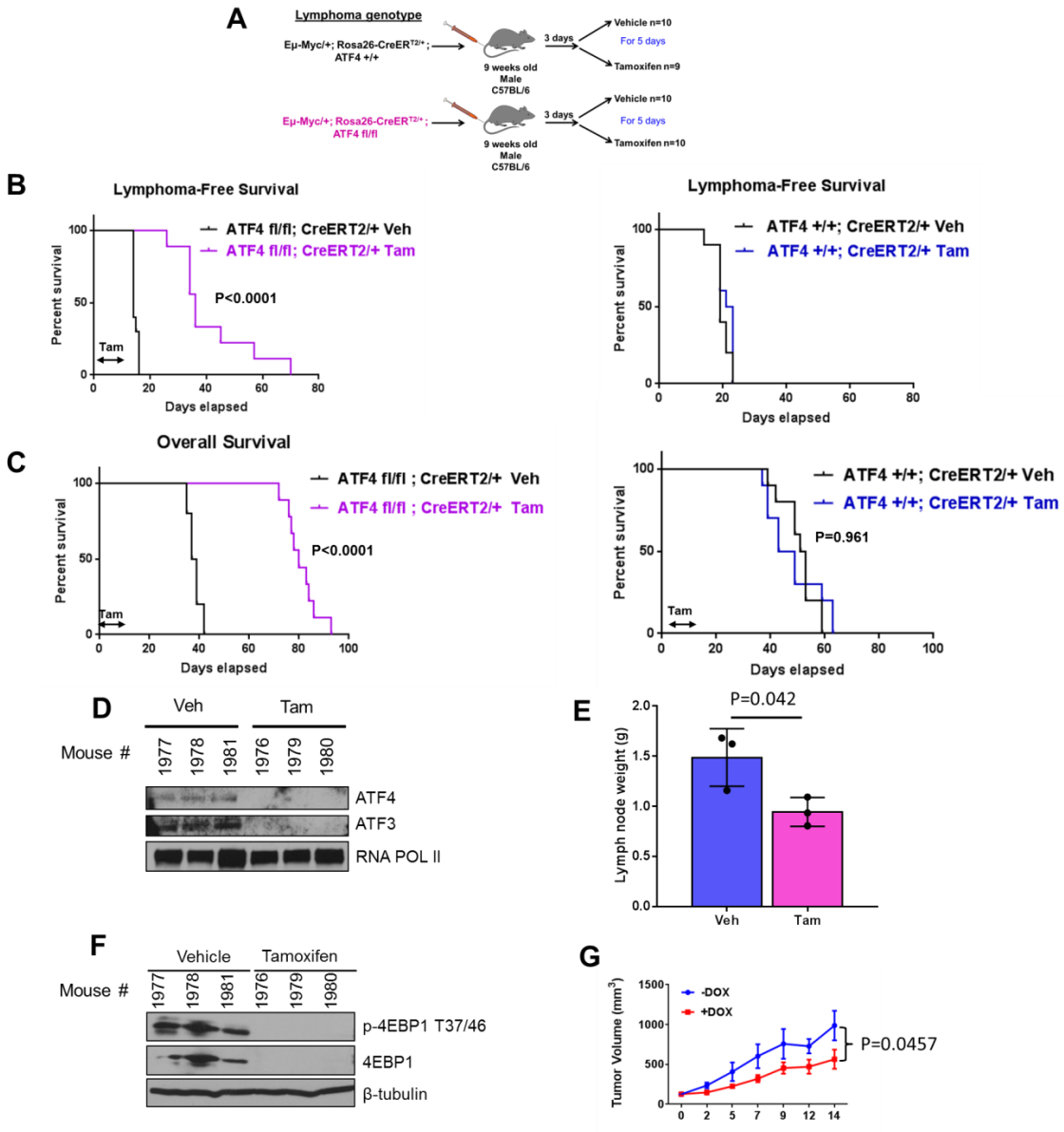
A
Lymphoma genotype
Eμ-Myc/+; Rosa26-CreER$^{T2/+}$; ATF4 +/+
9 weeks old Male C57BL/6
3 days
Vehicle n=10
For 5 days
Tamoxifen n=9
Eμ-Myc/+; Rosa26-CreER$^{T2/+}$; ATF4 fl/fl
9 weeks old Male C57BL/6
3 days
Vehicle n=10
For 5 days
Tamoxifen n=10
B
Lymphoma-Free Survival
ATF4 fl/fl; CreERT2/+ Veh
ATF4 fl/fl; CreERT2/+ Tam
P<0.0001
Tam
Percent survival
Days elapsed
Lymphoma-Free Survival
ATF4 +/+; CreERT2/+ Veh
ATF4 +/+; CreERT2/+ Tam
Percent survival
Days elapsed
C
Overall Survival
ATF4 fl/fl ; CreERT2/+ Veh
ATF4 fl/fl ; CreERT2/+ Tam
P<0.0001
Tam
Percent survival
Days elapsed
ATF4 +/+; CreERT2/+ Veh
ATF4 +/+; CreERT2/+ Tam
P=0.961
Tam
Percent survival
Days elapsed
D
Veh
Tam
Mouse #
1977
1978
1981
1976
1979
1980
ATF4
ATF3
RNA POL II
E
P=0.042
Lymph node weight (g)
Veh
Tam
F
Vehicle
Tamoxifen
Mouse #
1977
1978
1981
1976
1979
1980
p-4EBP1 T37/46
4EBP1
β-tubulin
G
-DOX
+DOX
Tumor Volume (mm^3)
P=0.0457

Previous page: Figure 2.11. Acute ablation of ATF4 significantly delays MYC driven Lymphomagenesis and promotes survival of MYC driven lymphoma bearing mice. (A) Schematic showing allograft lymphoma model, where lymphoma cells are injected via tail vein into 9-weeks-old C57BL/6J mice. Three days after lymphoma engraftment, mice are randomized to receive either vehicle or tamoxifen treatment by oral gavage for 5 days. **(B)**. Kaplan-Meier analysis for lymphoma-free survival of mice bearing Eμ-myc; ATF4 fl/fl; RosaCreERT2/+ lymphoma (left) or Eμ-myc; ATF4 +/+; RosaCreERT2/+ lymphoma (right) treated with either vehicle (veh) or tamoxifen (tam) for 5days. n=9 for Eμ-myc; ATF4 fl/fl; RosaCreERT2/+ lymphoma tamoxifen group, all other groups n=10. **(C)**. Kaplan-Meier analysis for overall survival of mice in panel a. Kaplan-Meier curves were analyzed by log-rank test. **(D)**. Immunoblot of B cells isolated from Eμ-myc; ATF4 fl/fl ; RosaCreERT2/+lymphoma bearing mice a day after the last day of tamoxifen treatment. **(E)**. lymph node weight of mice in panel D, n=3 per group, error bars represent mean ± SD, two tailed student t-test. **(F)**. Immunoblot of lymphoma lysates from mice in panel C. **(G).** DLD-1, MycER, ishATF4 cells were transplanted into 11-weeks-old nude mice and tumor growth curves are shown. One (-) Dox mouse had to be euthanized on day 12 because tumor reached maximum size limit. n=4 (-) Dox and n=4 (+) Dox. Two-way ANOVA, error bars represent mean± SEM.

To more stringently assess the requirement for ATF4 in lymphoma maintenance, we treated a separate cohort of mice as above once lymphoma developed. Treatment with tamoxifen showed efficient ablation of ATF4 and a reduction of ATF3, an ATF4 target gene in the B cells of tamoxifen treated mice (Figure 2.11D). Furthermore, there was a significant reduction in lymph node weight following tamoxifen treatment (Figure 2.11E). Consistent with the protein levels, ATF4 mRNA expression of ATF4 was also significantly reduced following tamoxifen treatment (Figure 2.12A). However, ATF4 expression returned to levels comparable to those of vehicle-treated groups by the endpoint of the experiment in Figure. 5c, suggesting that lymphoma cells that escaped ATF4 excision eventually formed lymphomas (Figure 2.12B).

To further test the requirement for ATF4 in tumor growth in a different tumor type we used the colorectal cancer DLD-1 MycER cells expressing a doxycycline inducible short-hairpin RNA against ATF4. Similar to the lymphoma model, knockdown of ATF4 significantly delayed tumor growth (Figure 2.11G). These results demonstrate the requirement of ATF4 for MYC driven lymphomagenesis and colon tumor growth. Collectively, the *in vivo* data support our hypothesis

that ATF4 is critical for tumor growth driven by hyperactive MYC. Furthermore, these results indicate that targeting ATF4 in the context of activated MYC elicits anti-tumor effects.

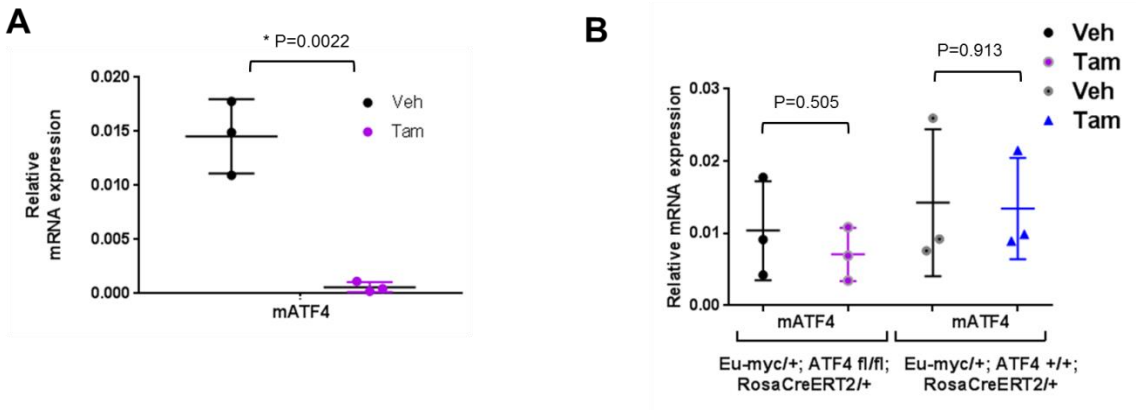

Figure 2.12. ATF4 mRNA expression in lymphoma cells. (A). mRNA expression of ATF4 from Fig 4d, showing a significant reduction of ATF4 mRNA in B cells treated with tamoxifen, n=3, mice per group, two tailed student t-test. **(B)**. mRNA expression of ATF4 at the endpoint mice treated with vehicle or tamoxifen whose survival is shown in Fig 4b and Fig 4c. n=3, mice per group, two tailed student t-test.

Consistent with our *in vitro* data (Figure 2.6D and 2.6E), 4E-BP1 protein levels were ablated in lymphoma cells following depletion of ATF4 (Figure. 2.11F). To investigate the relevance of our findings in human disease, we analyzed the expression of the MYC-ATF4 pathway target 4E-BP1 and tested its correlation with ATF4 activity in different cohorts of patients with colorectal, diffused large B cell lymphoma (DLBCL), as well as breast cancer and sarcomas by mining the TCGA database. Since ATF4 levels are primarily regulated at the translational level, we used a group of 10 well-characterized targets of ATF4 (including ASNS, MTHFD2, CHOP) as a surrogate for ATF4 activation [40, 137]. We found that 4E-BP1 levels displayed a significant positive correlation with ATF4 target genes in colorectal cancer, DLBCL, breast cancer and sarcoma (Figure. 6a). Notably, high expression of 4E-BP1 also correlated with poor prognosis in DLBCL patients (Figure. 6b). These data further support a notion that ATF4-dependent modulation of MYC-driven translational alterations may play a role in progression of MYC-driven lymphomas.

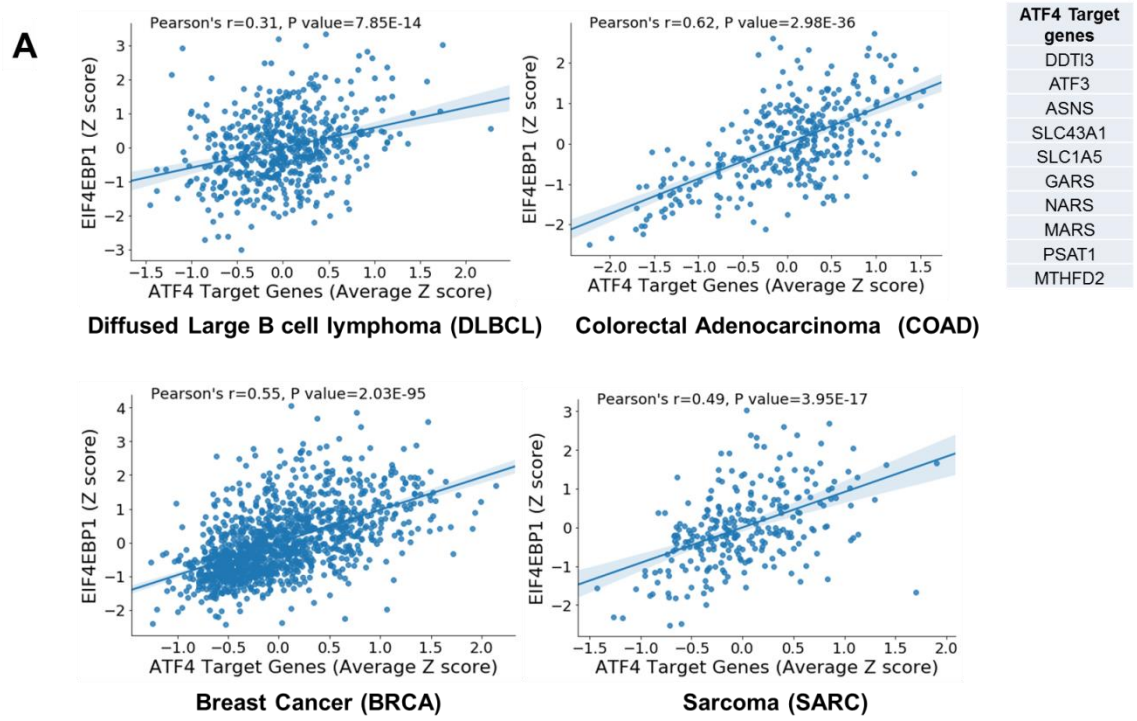

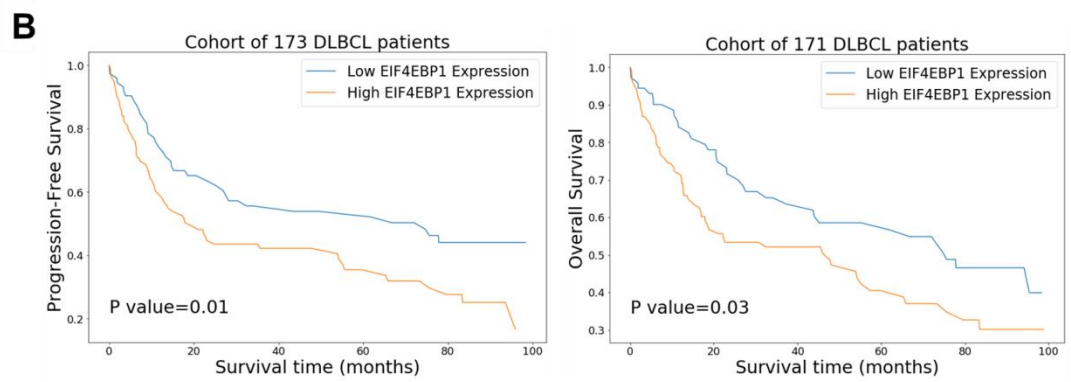

Figure 2.13. EIF4EBP1 positively correlates with ATF4 target gene expression and associates with poor prognosis. (A). Pearson correlation between EIF4EBP1 and ATF4 target gene expression in DLBCL (n=562), COAD (n=329), BRCA (n=1218) and SARC (n=265). Datasets analyzed are listed in the methods section. Previously known ATF4 target gene list used in this analysis is shown in table. **(B)**. Kaplan-Meier plots of progression free survival (left) and overall survival (right) of DLBCL patients with high or low EIF4EBP1 expression.

Discussion

The ISR pathway is critical for survival in response to external stresses found in the tumor microenvironment such as hypoxia and nutrient deprivation [9, 83]. ISR promotes survival by transiently inhibiting general protein synthesis and at the same time enhancing transcription of genes involved in achieving cellular homeostasis. ATF4 is the key downstream effector of the ISR as it regulates the transcriptional response. Even though the role of ATF4 is extensively studied in the context of external stresses faced by tumors, its role in MYC-induced stress is poorly understood. A previous report suggested that ATF4 can contribute to HRAS and SV40-induced transformation [102]. However, the importance of ATF4 as well as the underlying mechanisms of its regulation in the context of other activities of cellular oncogenes remains to be elucidated.

We previously demonstrated PERK is important for promoting survival of MYC overexpression cells. The residual phosphorylation of eIF2α in PERK deficient cells led us to identify that GCN2 is also activated upon MYC induction. Importantly, we discovered that GCN2 is activated in response to MYC via accumulation of excess uncharged tRNAs. Although we have not studied the contribution of the additional kinases, PKR and HRI, targeting both PERK and GCN2 nearly abolished phosphorylation of eIF2α, demonstrating that in at least the tumor cell lines tested, GCN2 and PERK are the two critical kinases responsible for eIF2α phosphorylation. Notably, there was a modest but significant difference in survival of mice bearing aggressive lymphoma when both kinases were inhibited, which could be the result of reduced phospho-eIF2α levels which impacts protein synthesis. Indeed, targeting phosphorylation of eIF2α pharmacologically in patient-derived prostate xenograft models is effective in initiating cytotoxic response which inhibits tumor growth [147]. Our study demonstrates that in the context of MYC driven tumors, additional regulation of protein synthesis besides one exerted by phospho-eIF2α is critical for cancer cell survival.

There is a growing appreciation of regulation of protein synthesis in both physiological and pathological conditions [147, 149]. MYC activation is invariably linked with enhanced protein synthesis which is critical for biomass (e.g., membranes, organelles) build-up, a pre-requisite for

enhanced proliferation and consequently manifestation of MYC's tumorigenic properties [150]. However, increased protein synthesis places heightened demands for cellular import of amino acids, as well as upregulation of levels of tRNAs and tRNA synthetases. The substantial increases in protein synthesis impact multiple cellular organelles, but primarily the endoplasmic reticulum, the site for glycosylation and folding of client proteins destined to be secreted or translocated to the cell membrane [151]. We and others have previously demonstrated that MYC activation initially induces ER stress and expansion of ER capacity to accommodate translation and modification of newly synthesized proteins [11, 128]. While we have shown that phosphorylation of eIF2α can provide initial relief from increased rates of translation, this mechanism may be insufficient for long-term survival due to the presence of a negative feedback loop that promotes dephosphorylation of eIF2α [42]. As a result, inhibiting other components of translation initiation may provide an additional layer of regulation. This work demonstrates that ATF4 is important for survival of MYC overexpressing cells by, on one hand supporting protein synthesis via expression of amino acid transporters and tRNA synthetases while on the other hand, also upregulating the expression of negative regulators of mTORC1 such as 4E-BP1 to prevent "runaway" protein synthesis and subsequent proteotoxicity (Figure 2.14).

4E-BP1 is a negative regulator of eIF4E and thus has been shown to inhibit cap-dependent translation and to promote survival under conditions of nutrient and oxidative stress [152]. Interestingly, higher expression of 4E-BP1 has been noted in human prostate, breast and hepatocellular cancers [153-155]. Furthermore, its high expression is associated with poor prognosis in hepatocellular carcinoma and breast cancer [154, 155]. While ATF4 has been previously shown to regulate 4E-BP1 in the context of extrinsic physiologic stresses [156], its role in upregulating 4E-BP1 in the context of tumorigenesis and particularly MYC-deregulated tumor progression is novel. Since uncontrolled protein synthesis could turn toxic, ATF4 cooperatively with MYC promotes expression of 4E-BP1 which inhibits cap-dependent translation acting as a brake. Because we did not observe a global increase in protein synthesis in response to ATF4 ablation, it is likely that ATF4 negatively regulates the expression of a specific set of gene products, likely those which

are destined to become membrane or secreted proteins and therefore traffic through the ER. In the future, it will be important to identify mRNAs that are selectively translated under the control of the ATF4-4E-BP1 axis.

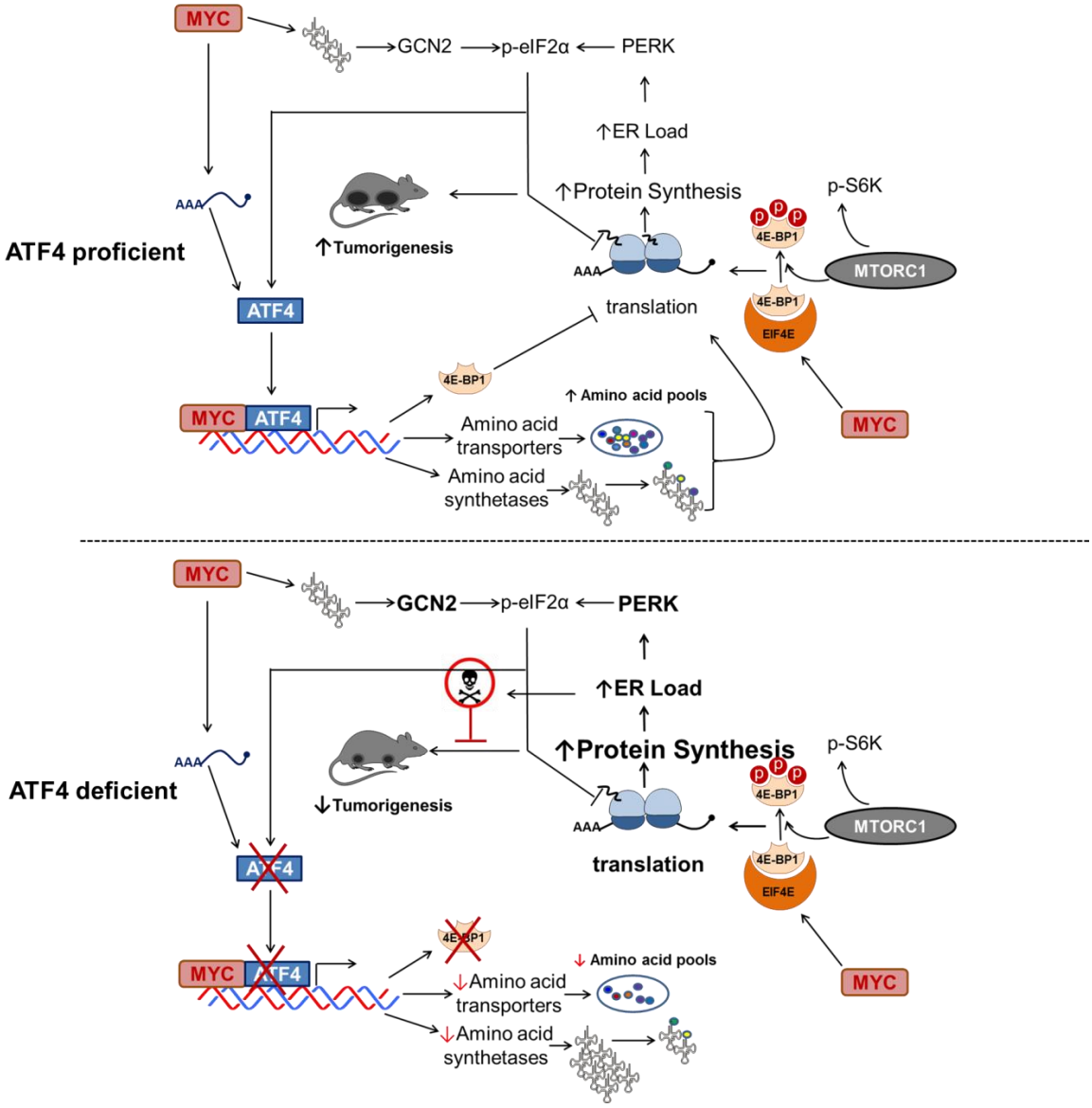

Previous page: Figure 2.14. Model of ATF4 and MYC co-operation during tumorigenesis. MYC activation leads to enhanced accumulation of uncharged tRNAs which activates GCN2. In parallel there is also activation of PERK due to increased protein synthesis. We show that MYC activation leads to ATF4 induction. ATF4 and MYC co-regulate a subset of genes involved in amino acid uptake, tRNA charging as well as 4E-BP1. Upregulation of 4E-BP1 is used to balance protein synthesis by inhibiting eIF4E dependent translation, thus ATF4 acts as a break on enhanced protein synthesis and also supports translation by providing a supply of amino acids and synthetases to charge tRNAs. This promotes survival in MYC high conditions and supports lymphomagenesis. In the absence of ATF4, mTORC1 is uncontrollably active forcing cells to increase protein synthesis in the absence of adequate supply of amino acids or equivalent charged tRNAs. This enhances apoptosis significantly reducing MYC driven lymphomagenesis.

Mechanistically, we demonstrate inhibition of mTORC1 signaling, pharmacologically or by siRNA, partially rescues ATF4 deficient cells from apoptosis following MYC activation. Furthermore, modest inhibition of protein synthesis or addition of chemical chaperone is also able to rescue ATF4 deficient cells. Though the TCA cycle metabolite, αKG, initially rescued ATF4 deficient cells, long term rescue was not achieved because the cells have a defect in translation that cannot be ameliorated by supplementing with metabolites. An interesting follow-up to these studies will be to determine if identified changes in the TCA cycle brought about by ATF4 ablation impose an additional, more long-term constraint in tumor growth to the more immediate stress of proteotoxicity.

Clinically, expression of 4E-BP1 positively correlated with ATF4 gene signature in four different patient datasets. Specifically, in DLBCL patient dataset, higher level of 4E-BP1 correlated with poor outcome. Higher expression of 4E-BP1, a negative regulator of mTORC1, seems paradoxical as mTORC1 is known to drive tumor growth and survival. Our findings provide a novel explanation of why tumors maintain such high levels of 4E-BP1, which is to prevent proteotoxicity.

Our *in vivo* studies demonstrate that ATF4 is critical for tumor cell growth and survival driven by MYC. Thus, acute ablation of ATF4 significantly increased overall survival of lymphoma bearing mice. Therefore, in the context of MYC driven cancers, ATF4 is an attractive target and inhibition of ATF4 can be selectively toxic to tumor cells while sparing normal tissues. Taken

together, the ISR transcription factor ATF4 is necessary for supporting and monitoring protein synthesis thus promotes progression of MYC driven tumorigenesis.

CHAPTER 3: ATF4-MEDIATED METABOLISM DURING MYC ACTIVATION

Introduction

Rapidly growing cells have a higher demand for nutrients to support synthesis of new DNA, proteins, lipids and organelles. In normal differentiated cells, cell growth is tightly coordinated with nutrient availability and growth factor signaling. Cancer cells lose this checkpoint due to mutations in tumor suppressor genes and activation of oncogenes enabling them to grow in the absence of extracellular growth signals[157]. Furthermore, cancer cells have a very different metabolic profile compared to normal cells. For example, cancer cells are characterized by higher levels of glycolytic activity compared to untransformed cells, a phenomenon known as the Warburg effect, where cancer cells shunt glycolytic intermediates from the mitochondrial tricarboxylic acid (TCA) cycle to form lactate and NAD+ in the presence of oxygen[158]. Even though aerobic glycolysis produces less ATP compared to the mitochondrial oxidative phosphorylation, cancer cells rely on this pathway to generate glycolytic intermediates for synthesis of biomass (nucleotides, lipids and amino acids)[159].

MYC stimulates glycolysis by directly activating the transcription of glucose transporters and glycolytic enzymes including hexokinase 1(HK1) and lactate dehydrogenase A (LDHA)[160, 161]. Glutamine metabolism has recently gained attention in the cancer field as cancer cells have been shown to rely on glutamine catabolism for biomass production[162]. Previous work has demonstrated that MYC driven cancers are addicted to glutamine[163]. MYC has been shown to upregulate glutamine catabolism through its regulation of glutamine transporters and enzymes involved in glutaminolysis such as mitochondrial glutaminase 1 (GLS1)[134]. GLS1 converts glutamine to glutamate which is used in the TCA cycle to support antioxidant defense and ATP production for proliferation[164]. Clinically, HCC patients show higher expression of GLS1. GLS1 inhibition has shown promise as anti-cancer therapy in mouse model of hepatocellular carcinoma, renal cell carcinoma as well as xenograft models[118, 165, 166]. Even though MYC is a master regulator of metabolism, it does not reprogram metabolic activity on its own. For example, MYC has been shown to regulate glutamine metabolism and lipid synthesis in cooperation with

MondoA, a glucose responsive transcription factor that activates several metabolic enzymes[167]. It is therefore important to identify other potential regulators that can aid MYC in metabolism.

ATF4 is also known to be a critical factor in regulating cellular metabolism by inducing the expression of genes involved in amino acid import and biosynthesis, one carbon metabolism and lipid biosynthesis[57, 168]. Consequently, ATF4 deficient cells require exogenous supplementation of non-essential amino acids and antioxidants for growth. Furthermore, ATF4 has recently been shown to regulate glycolysis and glutaminolysis in $CD4^+$ T cells to promote anabolic metabolism and redox homeostasis required for T cell function[169]. Other reports have demonstrated that ATF4 and MYCN can cooperatively regulate the glutamine transporter SLC1A5[130]. SLC1A5 expression positively associated with ATF4 and MYCN in high grade neuroblastomas and showed poor prognosis in patients[130]. These studies highlight the importance of ATF4 in metabolism and possible implication in MYCN induced glutamine addiction. However, the role of ATF4 in regulating other aspects of metabolism besides glutaminolysis in the context of MYC has not yet been explored. In this work we demonstrate ATF4 regulates glycolytic, TCA cycle and lipid synthesis metabolites. Furthermore, we show that ATF4 regulates expression of GLUT1 and metabolic enzymes involved in one carbon pathway and alpha-ketoglutarate production.

Results

To better understand the role of ATF4 in MYC induced metabolism, we extracted intracellular metabolites involved in pathways of bioenergetics, stress response and cellular proliferation. Metabolites were assessed by capillary electrophoresis mass spectrometry (CE-MS) based quantitative analysis method. ATF4 depletion led to a significant decrease in metabolites involved in glycolysis pathway, TCA cycle pathway and lipid metabolism (Figure 3.1A). We also saw expected changes in metabolites that ATF4 has been previously reported to regulate such as asparagine and glycine, which were reduced in the absence of ATF4 (Figure 3.1A). This regulation mainly depends on the enzymes involved in the biosynthesis of these amino acids

such as asparagine synthetase (ASNS) and Serine Hydroxymethyltransferase 2 (SHMT2) respectively. Other metabolites that were significantly reduced following MYC activation in the ATF4 knockdown cells included amino acids (β-alanine, alanine and tyrosine), urea cycle metabolites (Arginosuccinic acid and N-Acetylglutamic acid) as well as polyamine metabolites (S-Adenosylmethionine, spermidine and putrescine) (Table 3.1, Table 3.2 and Table 3.3).

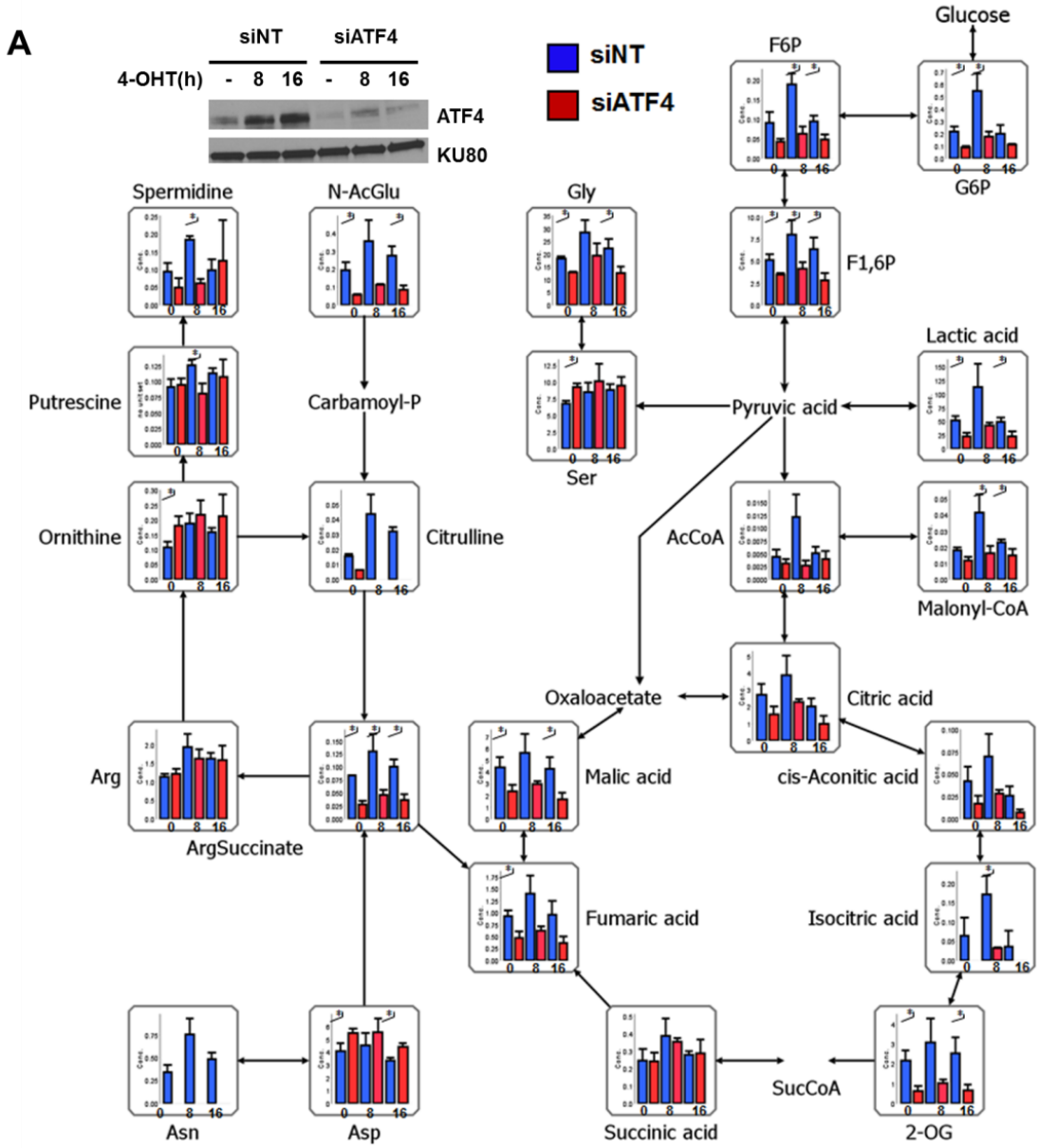

Previous page: Figure 3.1. ATF4 loss impacts intracellular metabolites following MYC activation. (A). Capillary electrophoresis mass spectrometry (CE-MS) based quantitative analysis of metabolites in the indicated pathways shown following c-Myc activation for 8 and 16hrs in siNT (blue bars) and siATF4 (red bars). n=3, two tailed student t-test, *p<0.05. inlet- immunoblot showing knockdown level of ATF4 for the metabolite analysis, representative of three independent experiments.

Table 3.1	siATF4 (-) 4-OHT/ siNT (-)4-OHT	p value
Inosine monophosphate (IMP)	1.76	0.00251
Glucose 6-phosphate	0.41	0.019003
Xylulose 5-phosphate	0.43	0.029252
Glyceraldehyde 3-phosphate	0.71	0.009127
Malonyl CoA	0.65	0.017199
Fructose 1,6-diphosphate	0.68	0.041907
Guanosine monophosphate (GMP)	1.59	0.011055
Adenosine monophosphate (AMP)	1.33	0.046169
Lactic acid	0.43	0.008264
N-Acetylglutamic acid	0.29	0.036103
Malic acid	0.54	0.03583
2-Oxoglutaric acid	0.29	0.018929
Fumaric acid	0.52	0.012097
Glycine	0.71	0.007769
β-alanine	0.46	0.007436
Alanine	0.59	0.000779
Serine	1.36	0.006961
Valine	0.79	0.047944
Isoleucine	0.82	0.02872
Ornithine	1.66	0.035545
Aspartate	1.35	0.036509
Glutamate	0.79	0.042566
Histidine	0.82	0.034256
Phenylalanine	0.77	0.020999
Tyrosine	0.79	0.026778
Tryptophan	0.76	0.023112
Argininosuccinic acid	0.33	0.003683

Table 3.2	siATF4 (+) 8hr 4-OHT/ siNT (+) 8hr 4-OHT	p value
Glucose 6-phosphate	0.32	0.034779
Fructose 6-phosphate	0.33	0.005387
Fructose 1-phosphate	0.23	0.020502
Malonyl CoA	0.39	0.046357
Fructose 1,6-diphosphate	0.51	0.037265
Phosphoribosyl pyrophosphate (PRPP)	0.52	0.011651
Guanosine monophosphate (GMP)	1.46	0.030697
Isocitric acid	0.19	0.040923
Putrescine	0.64	0.022601
β-alanine	0.42	0.024496
Alanine	0.45	0.038817
Spermidine	0.34	0.000169
Argininosuccinic acid	0.36	0.044754
S-Adenosylmethionine	0.65	0.045692

Table 3.3	siATF4 (+) 16hr 4-OHT/ siNT (+) 16hr 4-OHT	p value
Fructose 6-phosphate	0.51	0.020019
Xylulose 5-phosphate	0.24	0.037383
Fructose 1,6-diphosphate	0.44	0.019609
Lactic acid	0.45	0.015347
N-Acetylglutamic acid	0.31	0.013313
2-Hydroxyglutaric acid	0.48	0.035377
Malic acid	0.40	0.026473
2-Oxoglutaric acid	0.26	0.040794
Glycine	0.57	0.026205
β-alanine	0.49	0.003693
Alanine	0.51	0.016702
Aspartate	1.32	0.004645
Tyrosine	0.70	0.034537
Argininosuccinic acid	0.36	0.015739

Highlighted metabolites show an increase in siATF4 cells compared to siNT cells.

Since the first glycolytic metabolite, glucose-6-phosphate, was reduced upon ATF4 knockdown, we hypothesized that perhaps ATF4 regulates glucose uptake. Indeed, 2-Deoxyglucose (2DG) uptake was significantly reduced in the absence of ATF4 in both DLD-1 and MEFs basally as well as following MYC activation (Figure 3.2A).

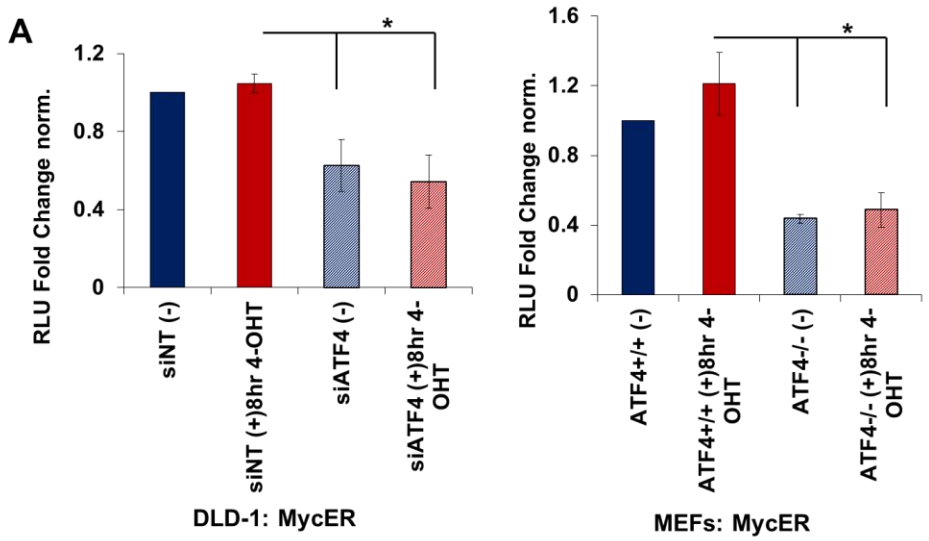

Figure 3.2. ATF4 loss decreases glucose uptake. (**A).** 2DG uptake was measured in control or ATF4 knockdown DLD-1: MycER cells following MYC activation for 8hrs. n=3, student t-test, $p<0.01$ (left) or in MycER MEFs (right) n=2.

ATF4 regulates GLUT1 transcription and but not protein stability

Glucose uptake is facilitated by plasma membrane bound glucose transporters[170]. GLUT1 is a ubiquitously expressed glucose transporter with higher affinity for glucose than other GLUTs[171]. Since we saw a rapid reduction in glycolysis and glucose uptake (Figure 3.1A and Figure 3.2A), we checked the expression of glucose transporter, GLUT1. GLUT1 protein levels were significantly reduced in the absence of ATF4 (Figure 3.3A). To test whether ATF4 regulates the transcription of GLUT1, newly synthesized mRNA were isolated by a nascent RNA isolation method and analyzed by qPCR (Figure 3.3B). ATF4 deficiency resulted in a significant decrease in GLUT1 nascent mRNA levels (Figure 3.3B). We next sought out to address whether ATF4 regulates protein stability of GLUT1. Treatment with Bafilomycin A (inhibits lysosome acidification) or Bortezomib (proteasome inhibitor) resulted in accumulation of GLUT1 in cells transfected with non-targeting siRNA but not in ATF4 knock down cells (Figure 3.3D). Bafilomycin inhibits autophagy, and accordingly led to accumulation of LC3II. Bortezomib treatment led to accumulation of ATF4 as previously reported (Figure 3.3D).[172] Furthermore, cycloheximide mediated chase assay showed a similar rate of decline in GLUT1 protein levels in both siNT or siATF4 cells (Figure 3.3E). Collectively, these data indicate that ATF4 regulates the transcription of GLUT1 but not the protein stability of GLUT1. Furthermore, GLUT1 expression was reduced in prostate cancer, lung cancer and breast cancer cell lines, suggesting the effects of ATF4 on GLUT1 were not cell-type specific (Figure 3.3F). Even though ATF4 regulates transcription of GLUT1, ATF4 did not bind to the promoter of GLUT1 (SLC2A1) suggesting that ATF4 indirectly regulates this gene without DNA binding. One the other hand, multiple MYC peaks were present within SLC2A1 locus (Figure 3.3G). Since we saw strong regulation of ATF4 *in vitro* we also looked at GLUT1 levels in the Eμ-Myc lymphoma cells where ATF4 is ablated with tamoxifen treatment. Loss of ATF4 did not affect GLUT1 levels in the lymphoma cells (Figure 3.3H). This suggests *in vivo* other stresses such as hypoxia can induce GLUT1 independently of ATF4.

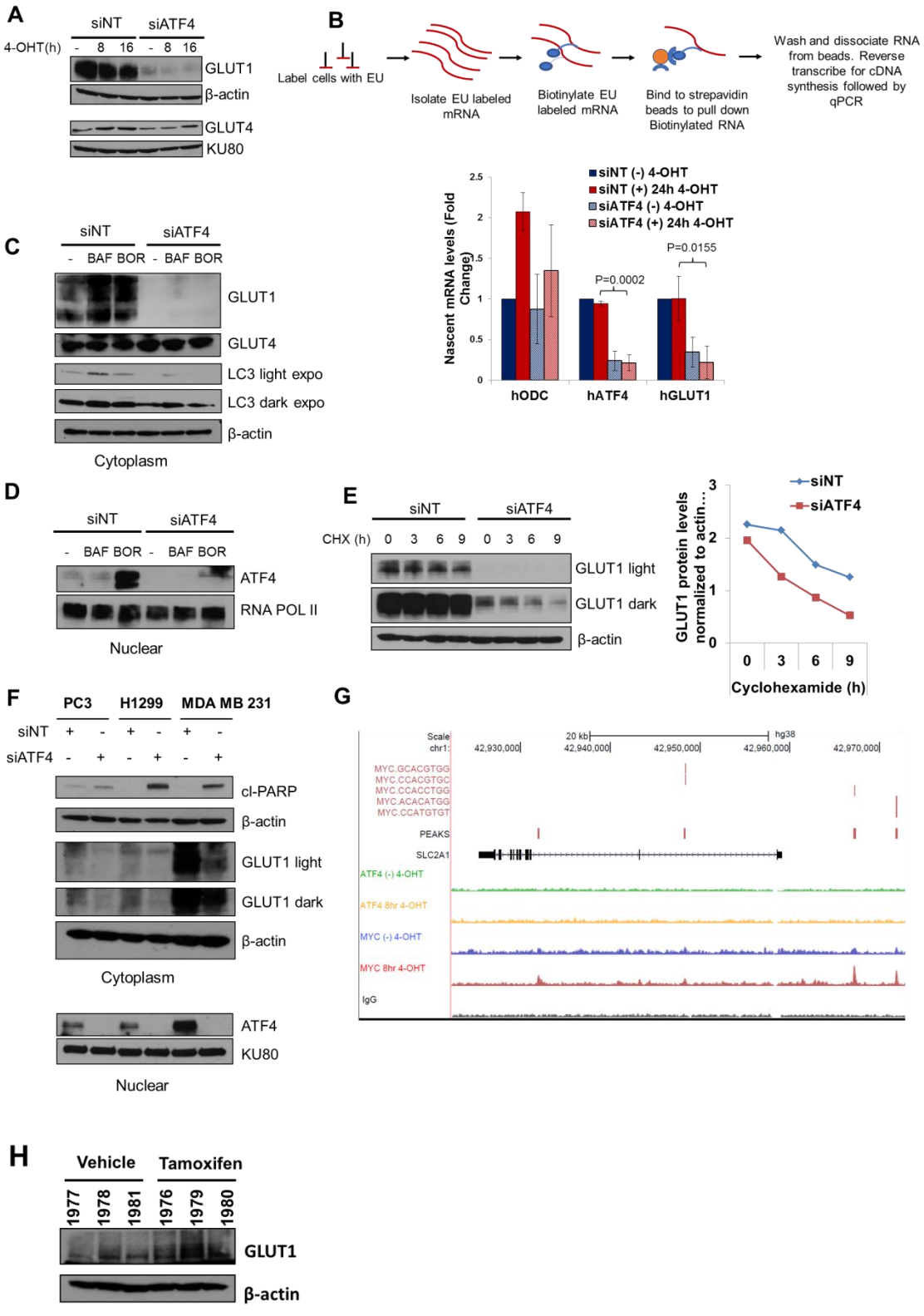
A
siNT
siATF4
4-OHT(h) - 8 16 - 8 16
GLUT1
β-actin
GLUT4
KU80
B
Label cells with EU
Isolate EU labeled mRNA
Biotinylate EU labeled mRNA
Bind to strepavidin beads to pull down Biotinylated RNA
Wash and dissociate RNA from beads. Reverse transcribe for cDNA synthesis followed by qPCR
C
siNT
siATF4
- BAF BOR - BAF BOR
GLUT1
GLUT4
LC3 light expo
LC3 dark expo
β-actin
Cytoplasm
siNT (-) 4-OHT
siNT (+) 24h 4-OHT
siATF4 (-) 4-OHT
siATF4 (+) 24h 4-OHT
Nascent mRNA levels (Fold Change)
P=0.0002
P=0.0155
hODC
hATF4
hGLUT1
D
siNT
siATF4
- BAF BOR - BAF BOR
ATF4
RNA POL II
Nuclear
E
siNT
siATF4
CHX (h) 0 3 6 9 0 3 6 9
GLUT1 light
GLUT1 dark
β-actin
GLUT1 protein levels normalized to actin…
siNT
siATF4
Cyclohexamide (h)
F
PC3
H1299
MDA MB 231
siNT + - + - + -
siATF4 - + - + - +
cl-PARP
β-actin
GLUT1 light
GLUT1 dark
β-actin
Cytoplasm
ATF4
KU80
Nuclear
G
Scale
chr1:
20 kb
hg38
42,930,000
42,940,000
42,950,000
42,960,000
42,970,000
MYC.GCACGTGG
MYC.CCACGTGC
MYC.CCACCTGG
MYC.ACACATGG
MYC.CCATGTGT
PEAKS
SLC2A1
ATF4 (-) 4-OHT
ATF4 8hr 4-OHT
MYC (-) 4-OHT
MYC 8hr 4-OHT
IgG
H
Vehicle
Tamoxifen
1977
1978
1981
1976
1979
1980
GLUT1
β-actin

Previous page: Figure 3.3. ATF4 Regulates transcription but not translation of GLUT1. (**A).** Representative western blot of DLD-1, MycER cells following ATF4 knockdown. Indicated proteins are shown. (**B).** Above schematic shows Click –It Nascent RNA Capture method to capture newly synthesized RNA from total RNA (adapted from Thermofisher). The captured newly synthesized RNA isolated from DLD-1, MycER cells transfected with non-targeting siRNA (siNT) or siRNA against ATF4 (siATF4) was subsequently used for qPCR (below). mRNA expression of ODC, ATF4 and GLUT1 was normalized to 18sRNA and shown as fold change compared to siNT (-) 4-OHT. (**C).** siNT or siATF4, DLD-1, MycER cells were treated with 200nM Bafilomycin (BAF) or 100nM Bortezomib (BOR) for 5hrs. Cytoplasmic lysates were used for western blot to assess indicated proteins. (**D).** Western blot of nuclear lysates of same cells in C. (**E).** siNT or siATF4, DLD-1, MycER cells were treated with 50ug/ml Cyclohexamide (CHX) for indicated times and whole cell lysates were used to look at GLUT1 levels (left). Graph showing GLUT1 levels normalized to β-actin (right). **F.** Immunoblot assessing protein levels of GLUT1 in prostate cancer cell line (PC3), lung cancer cell line (H199) and breast cancer cell line (MDA MB 231). (**G).** ChIP-seq signal track within SLC2A1 locus showing multiple MYC binding peaks. H.

We next tested whether expression of metabolic enzymes was altered in the absence of ATF4. Expression of mitochondrial one carbon metabolism enzymes methylenetetrahydrofolate Dehydrogenase2 (MTHFD2) and SHMT2 were significantly reduced in ATF4 deficient cells (Figure 3.4A, 3.4B). This result is consistent with the ChIP-seq data described in Chapter 2 where ATF4 and MYC peaks were present in both genes. ATF4 deficient cells also had a reduction in expression of amino acid transporters, SLC7A11 and SLC1A5. These transporters are involved in the uptake of glutamine, cysteine, alanine and serine (Figure 3.4A). Metabolite analysis showed a complete absence of asparagine (Figure 3.1A) and accordingly ASNS gene expression was significantly reduced in ATF4 deficient cells (Figure 3.4A).

One TCA cycle metabolite that was significantly reduced in the absence of ATF4 is αKG. In fact, supplementation of αKG partially rescued ATF4 deficient cells at earlier time points of MYC activation (Chapter 2). Therefore, we next silenced ATF4 and assessed the expression of αKG producing enzymes and found that it regulates the expression of glutamic-oxaloacetic transaminase 2 (GOT2), GLS and glutamate pyruvate transaminase 2 (GPT2). Similar to ATF4 knockdown, silencing GCN2 also resulted in reduced expression of SLC7A11, SLC1A5, SHMT2 and MTHFD2 (Figure 3.4D). Together these observations highlight ATF4 as a master regulator of

glycolysis, TCA cycle and amino acid metabolism through its regulation of proteins involved in these pathways.

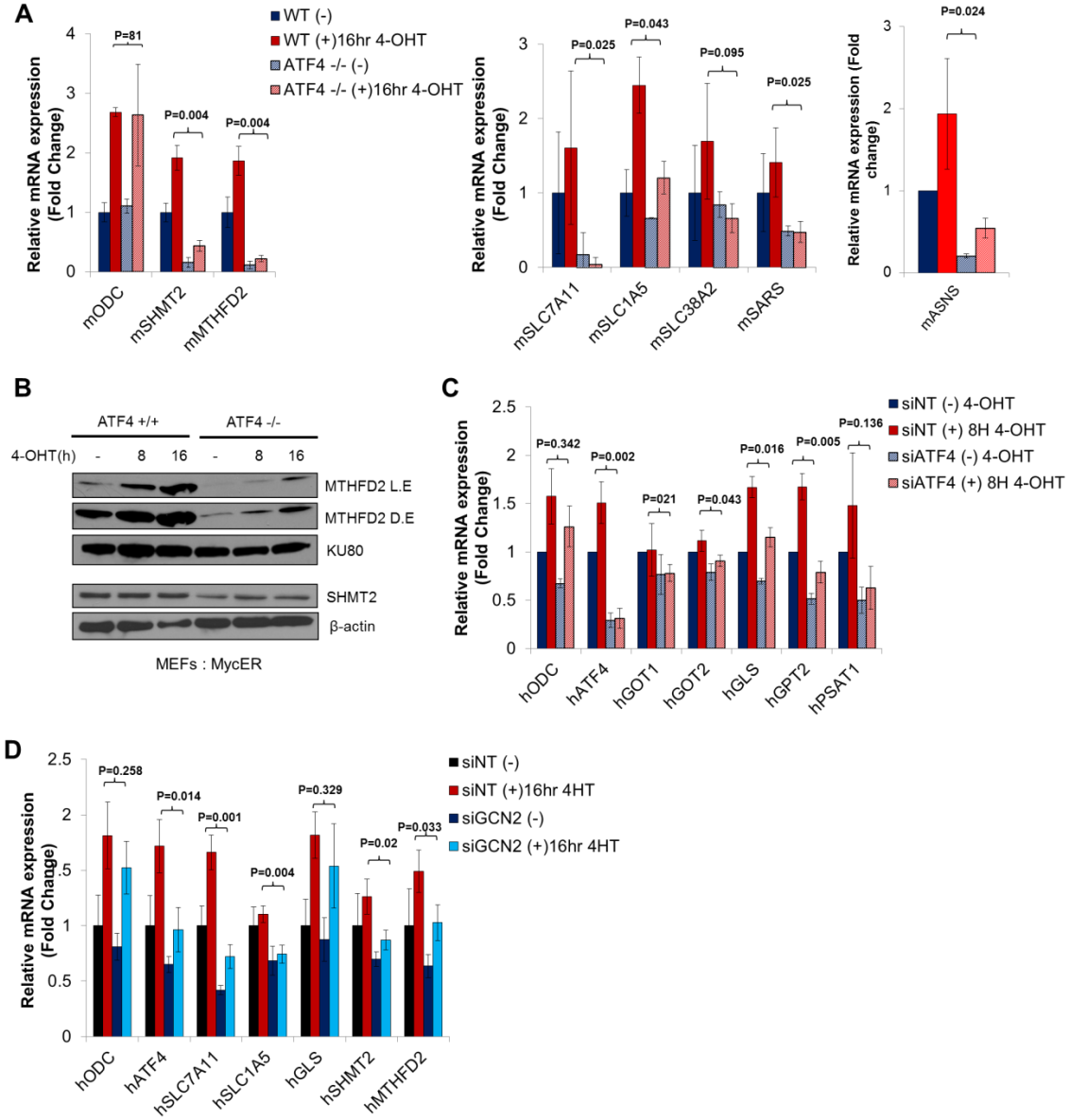

Figure 3.4. ATF4 Regulates expression metabolic genes and amino acid transporters. (**A).** Graph showing expression of enzymes involved in one carbon metabolism (left) and amino acid transporters and seryl-tRNA synthetase (SARS) by qPCR in MEFs: MycER cells. n=3 biological replicates (**B**). Immunoblot of whole cell lysates assessing levels of indicated proteins. (**C).** Graph showing expression of αKG producing enzymes by qPCR in DLD-1; MycER cells that have been transfected with non-targeting siRNA or siATF4, n=3 biological replicates. (**D).** Graph showing expression of indicated genes by qPCR in DLD-1; MycER cells that have been transfected with non-targeting siRNA or siGCN2, n=3 biological replicates.

Discussion

This chapter describes the role of ATF4 in MYC induced metabolism. Analysis of metabolites involved in cellular energy and stress response revealed the critical role ATF4 plays in metabolism. We identified that ATF4 regulates the transcription of GLUT1 in colon, prostate, breast and lung cancer cell lines. ATF4 did not contribute to protein stability of GLUT1 as proteasome or autophagy inhibition did not result in accumulation of GLUT1 protein levels in ATF4 deficient cells. Although ATF4 regulated the transcription of GLUT1, it did not directly bind to GLUT1 locus. However, MYC bound to multiple sites in GLUT1 locus as previously reported[161]. Interestingly in Eμ-Myc lymphoma, loss of ATF4 had no effect on GLUT1 expression. One potential explanation for this result is that other stress response pathways compensate for loss of ATF4 *in vivo.* In the tumor microenvironment cancer cells face additional stresses such as nutrient deprivation and hypoxia. The hypoxia induced transcription factor HIF1α is known to regulate GLUT1 expression and therefore can upregulate GLUT1 in hypoxic regions of the tumor[173]. It is possible that in normoxic parts of the tumor ATF4 may regulate GLUT1 levels. This can be experimentally addressed by injecting lymphoma bearing mice with a hypoxia marker and then staining for ATF4 and GLUT1 to test how they localize in different parts of the tumor in respect to hypoxic regions. This would give a correlative data but conditionally knocking out ATF4 and seeing whether GLUT1 levels change in normoxic regions would indicate the impact of loss of ATF4 on GLUT1 *in vivo.*

We also demonstrate that ATF4 regulates expression of metabolic enzymes involved in amino acid biosynthesis, one carbon metabolism and alpha-ketoglutarate production. Indeed, supplementation of alpha-ketoglutarate is able to partially rescue ATF4 knockout cells from apoptosis during MYC activation. MYC induced intrinsic stress can create metabolic stress in ATF4 deficient cells due to decreased expression of metabolic enzymes. Furthermore, the enhanced protein synthesis driven by MYC can also exacerbate the metabolic stress creating imbalanced proteinstasis. Therefore, ATF4 exerts pro-survival functions by coupling metabolism with balanced translation.

CHAPTER 4: CONCLUSION AND FUTURE DIRECTIONS

This work describes a novel role of the stress response transcription factor ATF4 as a critical regulator of MYC driven tumorigenesis. MYC transcriptionally upregulates ATF4 mRNA expression however its translation *in vitro* is regulated by the ISR kinases PERK and GCN2 through phosphorylation of eIF2α. Genome wide ChIP-seq analysis uncovered that ATF4 and MYC synergistically bind to promoters of genes that regulate protein synthesis and metabolism. Surprisingly, one of the targets of both ATF4 and MYC is the negative regulator of cap-dependent translation, 4E-BP1. MYC has been shown to cooperate with eIF4E in driving tumorigenesis[174]. Here we show that in addition to eIF4E, MYC also upregulates negative regulator of eIF4E, 4E-BP1 in cooperation with ATF4 to balance translation. We also generated a conditional knockout of ATF4 in MYC driven lymphoma to directly test the cooperation of ATF4 with MYC in tumorigenesis. Acute ablation of ATF4 resulted in delayed lymphomagenesis as well as enhanced survival of lymphoma bearing mice. Notably, excision of ATF4 in lymphomas completely reduced 4E-BP1 protein expression. To address the clinical relevance of this work we analyzed expression of 4E-BP1 in four TCGA patient datasets (DLBCL, breast cancer, colon cancer and sarcoma) and found a strong positive correlation between well validated ATF4 target genes and 4E-BP1. Furthermore, higher 4E-BP1 expression associates with poor progression free as well as overall survival.

MYC activates GCN2 through accumulation of uncharged tRNAs

Chapter 2 describes a novel mechanism of how MYC activates the ISR kinase GCN2 through upregulation of tRNA synthesis in RNA POL III dependent manner. By utilizing tRNA microarray, we showed that there is a time dependent accumulation of uncharged tRNAs following MYC induction resulting in activation of GCN2. Furthermore, RNA POL III inhibition abrogates phosphorylation of GCN2 during MYC activation strongly suggesting that newly transcribed tRNAs that are not charged result in activation of GCN2. To further extend the concept that newly transcribed tRNAs activate GCN2 following MYC induction, the tRNA microarray can be carried out in cells where MYC is activated in the presence or absence of RNA

POL III inhibitor. Enhanced protein synthesis utilizes charged tRNAs and can further contribute to accumulation of uncharged tRNAs. Although we haven't experimentally addressed this possibility, it is most likely to occur in MYC driven tumors and aid activation of GCN2. Our results show for the first time that MYC engages an amino acid sensor GCN2.

An interesting finding in this study that requires further investigation is the fact that GCN2 is required for transcriptional induction of ATF4 following MYC activation. GCN2 -/- MEFs as well as DLD-1 cells in which GCN2 is silenced fail to induce ATF4 mRNA following MYC activation. ATF4 is transcriptionally induced during ER stress and amino acid deprivation conditions[59]. It is well established that translational regulation of ATF4 is critical for its protein expression especially during stress conditions[57, 59, 67]. However, both transcriptional and translational regulation of ATF4 contribute to its expression[66]. For example, during UV stress ATF4 mRNA is transcriptionally suppressed ATF4 mRNA is not translated even though there is abundant p-eIF2α present [66]. Similarly, when MYC is induced in the GCN2 deficient cells even though eIF2α is phosphorylated by PERK, ATF4 mRNA levels are not induced which likely results in decreased translation of ATF4 mRNA. In the future, kinase screens can be employed to identify other targets of GCN2 that impact transcription.

ATF4 is critical for MYC induced tumorigenesis

The ability of MYC to enhance protein synthesis is required for its tumorigenic potential. Increased translation rates coupled to cell growth are observed in B cells isolated from Eμ-Myc mice prior to tumor formation suggesting enhanced protein synthesis is involved in MYC induced transformation[116]. However, it was not clear whether increased translation is a consequence of transformation or whether it is required for transformation in MYC driven cancers. To test this, Barna et al used ribosomal haploinsufficient mutants and demonstrated that reducing protein synthesis levels to normal levels suppresses lymphomagenesis in Eμ-Myc mice[126]. This was specific to MYC induced lymphomagenesis and did not affect for example lymphomas that arise

in p53 -/- background suggesting the requirement of increased protein synthesis in the oncogenic potential of MYC[126]. MYC regulates the translational machinery by direct activation of translation initiation factors, translation elongation factors as well as ribosomal proteins[150]. Increased protein synthesis enables macromolecule production and supports cell growth, a key requirement for sustained proliferation. Our work also suggests that ATF4 can support MYC driven protein synthesis through co-regulation of amino acid transporters, amino acid biosynthesis enzymes and tRNA synthetases.

Chapter 3 describes the role of ATF4 in regulating metabolites involved in glycolysis, TCA cycle and lipid metabolism. Supplementation of alpha ketoglutarate rescues ATF4 deficient cells in short-term but not long-term activation of MYC suggesting that loss of ATF4 places metabolic constraints however continued activation of MYC induces another type of stress that cannot be rescued by supplementation of metabolites. Indeed, inhibition of translation with low doses of cyclohexamide rescues ATF4 deficient cells from MYC induced apoptosis suggesting translation stress contributes to cell death. While enhanced protein translation is critical to tumorigenesis, uncontrolled mRNA translation can be detrimental to a cell and must be accompanied with adaptive support pathways that balance translation with ER folding capacity.

My thesis project further extends that MYC not only upregulates the protein synthesis machinery but also cooperates with ATF4 to modulate translation to prevent uncontrolled translation through upregulation of 4E-BP1. This is especially important in the context of the tumor microenvironment cancer cells reside in, which is constantly facing deficit of oxygen and nutrients that can further exacerbate intrinsic stress created by increased protein synthesis. Therefore, having an adaptive mechanism that regulates mRNA translation allows cancer cells to achieve protein homeostasis. The PERK arm of UPR serves as one ‘brake’ to translation through p-eIF2α whereas expression of 4E-BP1 serves as another node of translation regulation. Interestingly, higher expression of 4E-BP1 has been observed in many cancers such as prostate, breast cancer and hepatocellular carcinoma[153-155]. Moreover, high expression of 4E-BP1 is

associated with poor prognosis in hepatocellular carcinoma and breast cancer[153-155]. Elevated expression of 4E-BP1 has also been linked with therapy resistance. Higher protein abundance of 4E-BP1 in luminal epithelial prostate cancer cells promotes resistance to genetic and pharmacologic inhibition of PI3K-AKT-mTOR pathway[175]. These cells exhibited decreased protein synthesis rates and reducing 4E-BP1 abundance made them sensitive to PI3K-AKT-mTOR pathway inhibitors[175]. In another study, high protein levels of 4E-BP1 predicted decreased benefit from tamoxifen treatment in independent breast cancer patient cohorts[154]. Thus, 4E-BP1 can impact treatment outcomes due to its ability to regulate translation.

ATF4 has been shown to regulate other negative regulators of mTORC1 under amino acid and ER stress conditions such as Sestrin 1 (SESN1) and DNA damage inducible transcript 4 (DDIT4)[176, 177]. We also found that ATF4 bound to DDIT4 in our ChIP-seq and ATF4 binding increased with MYC activation (Figure 4.1). In the future, it is important to address the contributions of these negative regulators of mTORC1 in MYC driven cancers. The concept of ATF4 opposing mTORC1 signaling may seem to counterintuitive as mTORC1 activation is one major feature of many cancers. However, sustained activation of mTORC1 during nutrient and oxygen limiting conditions present in the tumor microenvironment creates both metabolic and protein stress. Thus transient expression of negative regulators of mTORC1 mediated by ATF4 can provide selective survival advantage to cancer cells.

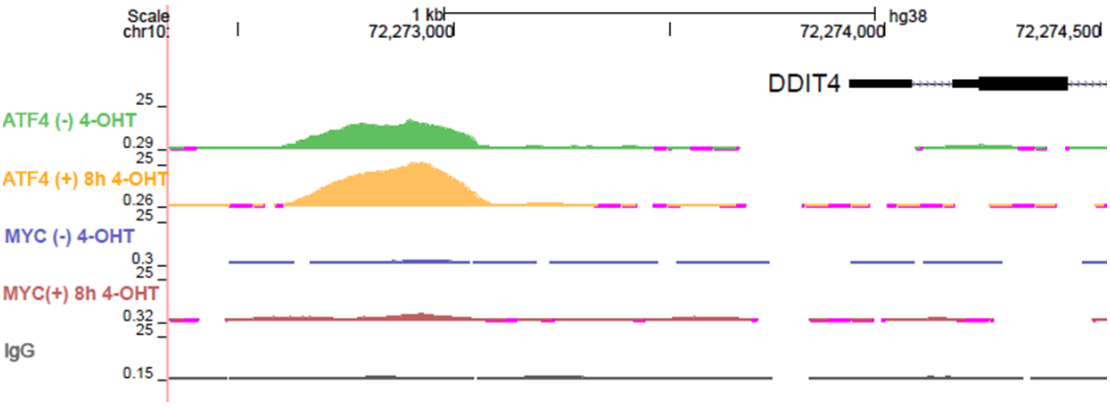

Previous page: Figure 4.1. ChIP-seq track signal at DDIT4 locus. ATF4 peaks are shown following MYC activation.

One intriguing finding in our study is that we did not observe global changes in translation in the absence of ATF4, suggesting that the translation of specific transcripts is modulated in the absence of the ATF4/4E-BP1 axis. Inhibition of protein synthesis with cyclohexamide reduces apoptosis in ATF4 deficient cells implicating proteiotoxicity promotes cell death. More detailed work needs to be carried out to identify selectively translated transcripts in 4E-BP1 dependent manner. High resolution transcriptome scale ribosome profiling method[178] can be employed to identify transcripts that are differentially translated in an ATF4/4E-BP1 dependent manner. This can be carried out in ATF4 deficient cells with and without MYC activation. To validate the identified transcripts are dependent on 4E-BP1, overexpression of 4E-BP1 mutant (that is no longer phosphorylated and inhibited by mTORC1) can be used in ATF4 deficient cells. This mutant can tightly bind to eIF4E and can efficiently inhibit cap-dependent translation[179].

Another possibility is that proteins that are translated in the ER could be altered in an ATF4 dependent manner. The glycosylation process regulates protein stability and impacts ER stress. Since we observed that ATF4 affects glycolysis in cells (Chapter 3) we hypothesized that decreased glucose availability can also impact the glycosylation process in cells. The hexosamine pathway is a glucose metabolism pathway that produces intermediates such as UDP-N-acetylglucosamine (UDP-GlcNAc) which is utilized for glycosylation of proteins[180]. UDP-GlcNAc is used as a substrate by the enzyme O-linked GlcNAc transferase (OGT) which catalyzes the addition of O-GlcNAc to nuclear and cytoplasmic proteins[181]. ATF4 has been reported to be required for O-linked GlcNAcylation during glucose deprivation conditions[182]. Loss of OGT reduces O-linked GlcNAcylation, enhances ER stress and causes cell death in pancreatic β-cells suggesting a link between O-linked GlcNAcylation and ER homeostasis[183]. However,

mechanistically how O-linked GlcNAcylation and ER stress are linked is not yet known. Since O-linked GlcNAcylation has been shown to reduce intracellular calcium levels[183] and ER chaperones require calcium for their activity, it is possible that ER folding capacity is affected by decreased O-linked GlcNAcylation.

Preliminary data indicates that ATF4 can affect O-linked GlcNAcylation (Figure 4.2). Silencing ATF4 led to a remarkable reduction in *O*-GlcNAcylated proteins in DLD-1 cells as well as in Eμ-Myc lymphoma (Figure 4.1A, 4.1B, 4.1C) in which ATF4 was ablated by administration of tamoxifen (Figure 4.1D). Furthermore, there was a reduction in expression of OGT in both ATF4 deficient DLD-1 and Eμ-Myc lymphoma cells (Figure 4.2A). GFPT1, the rate-limiting enzyme in the hexosamine pathway, was also reduced in ATF4 knockdown cells (Figure 4.2A).

The ER is the major folding organelle for all membrane and secreted proteins[2]. We have observed enhanced activation of PERK in ATF4 deficient cells suggesting they have increased ER stress (data not shown). To address whether a decrease in *O*-GlcNAcylated proteins leads to accumulation of newly translated proteins in the ER, newly synthesized proteins can be labeled with ^{35}S and the ER can be fractionated to test whether there is more accumulation of newly synthesized proteins in the ER in the absence of ATF4. We hypothesize that although general protein synthesis is not affected perhaps specific translation of ER destined proteins can be altered.

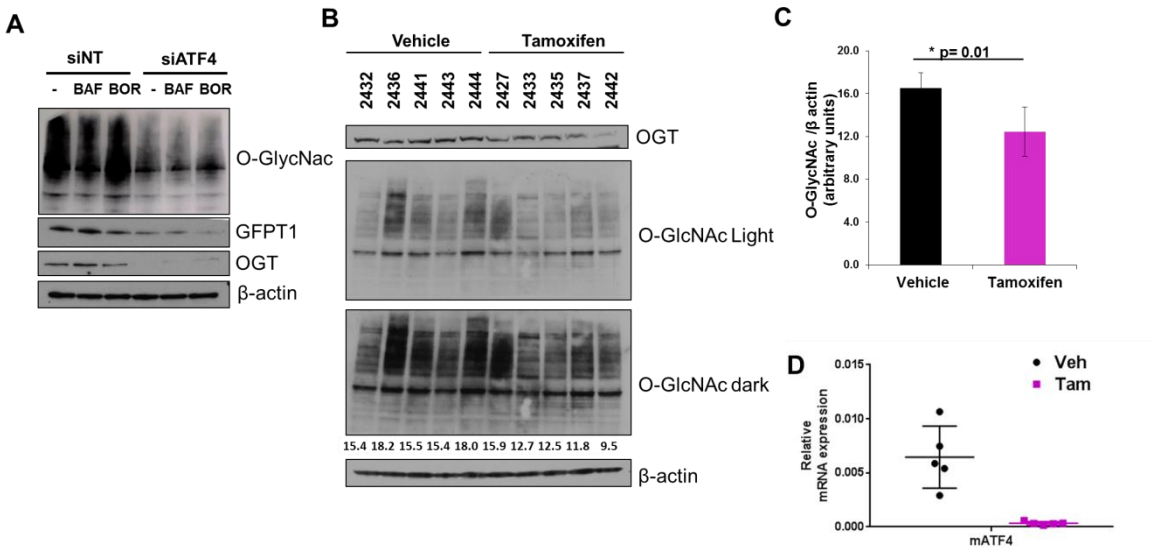

Figure 4.2. Loss of ATF4 reduces *O*-GlcNAcylation of proteins in MYC driven lymphoma. (A). DLD-1, MycER cells were transfected with non-targeting siRNA or one targeting ATF4. Cells were treated with 200nM Bafilomycin (BAF) or 100nM Bortezomib (BOR) for 5hrs. Cytoplasmic lysates were used for western blot to assess indicated proteins. **(B)**. Immunoblot of lymphoma lysates from Eμ-myc; ATF4 fl/fl; RosaCreERT2/+ treated either with Vehicle or tamoxifen following lymphoma development. **(C)**. Quantification of immunoblot in A. **(D)**. mRNA expression of ATF4 assessed by qRT-PCR and normalized to GAPDH.

ATF4 and MYC co-occupy overlapping binding sites

ChIP seq analysis revealed that ATF4 and MYC can co regulate select set of genes including tRNA synthetases, amino acid transporters and the translational regulator 4E-BP1. ATF4 and MYC peaks overlapped in our ChIP-seq raising a very intriguing possibility that these transcription factors could physically interact. ATF4 is a bZIP transcription factor whereas MYC is a bHLH transcription factor but both proteins contain leucine zipper domain which is used for protein-protein interactions. In the future, co immunoprecipitation experiments can be used to test physical interaction between ATF4 and MYC. If they do interact, then truncation mutants can be generated to identify the regions required for interaction and these mutants can be used further to

test whether physical interaction is required for induction of target genes. Furthermore, it would be important to silence ATF4 and perform ChIP-seq to test whether MYC requires ATF4 to bind to select genes that were identified in our ChIP-seq.

The complex regulation of ATF4 expression

This work highlights a requirement for both PERK and GCN2 for MYC induced activation of ATF4. *In vitro* this seems to be dependent on eIF2α phosphorylation. It is important to understand the stresses that activate each kinase are distinct. PERK is activated due to ER stress under MYC-driven protein synthesis whereas GCN2 is activated as a result of increased accumulation of uncharged tRNAs. Therefore, in the absence of one kinase the stress that activates the other kinase is still present therefore one kinase can be activated regardless of the other. However, *in vivo,* we observed that although eIF2α phosphorylation is dependent on these two kinases, ATF4 expression can still occur in the absence of PERK or GCN2 activity. Since there is still some phosphorylation of eIF2α in the absence of both PERK and GCN2, there is a possibility that other ISR kinases can engage in phosphorylating eIF2α. In the future, it would be important to address whether the other ISR kinases, PKR and HRI, are actually active in MYC driven tumors and whether they compensate for loss of PERK and GCN2. Furthermore, multiple stresses present in the tumor microenvironment can put a selective pressure on cancer cells enabling those with ATF4 expression to survive. ATF4 has been previously shown to colocalize to hypoxic regions of tumors and ATF4 deficient cells are also highly sensitive to hypoxia[9].

ATF4 protein can also be stabilized by mutations in β-TrCP, an E3 ubiquitin ligase that targets it for proteasomal degradation. ATF4 itself can be phosphorylated and stabilized in cancer cells. In the future, it will be important to address avenues of increased expression of ATF4 independent of p-eIF2α in the context of MYC driven tumors. PKR and HRI can be deleted using CRISPR in *Eμ-myc/+; GCN2*$^{-/-}$ lymphoma cells which can then be used *in vivo* to test the requirement of ISR kinases for ATF4 expression. Furthermore, PERK can be targeted

pharmacologically in the same tumors as previously described in Chapter 2. These experiments can determine the role of ISR signaling in tumor growth and progression.

Therapeutic implications of targeting the ISR pathway in cancer

Our study also has a significant therapeutic implication for targeting the ISR in the treatment of cancer. Our *in vivo* studies demonstrated that loss of GCN2 or PERK inhibition alone in MYC induced lymphoma does not have any therapeutic benefits. However, combined inhibition of both kinases does have survival advantage for lymphoma bearing mice possibly due to the significant decrease in phosphorylation of eIF2α. In this context, we hypothesize that tumor cells are not able to regulate their translation and experience proteotoxicity affecting their survival. In the future, it would be important to measure protein synthesis rates in the lymphoma cells in the absence of PERK and GCN2. This can be performed by doing ^{35}S incorporation studies in freshly isolated lymphomas. Furthermore, our findings can be extended to other MYC dependent tumors such as triple negative breast cancer and colon cancer. Recently a potent GCN2 inhibitor has been described with *in vivo* anti-tumor activity when combined with L-asparaginase, an enzyme that depletes circulating asparagine[184]. Thus, combination treatments with PERK and GCN2 inhibitors in MYC driven cancers can be used to test the dependency of MYC on these ISR kinases. Other studies have shown strong anti-tumor effects of PERK inhibition as a single agent in pancreatic and melanoma xenograft models[145, 185]. Therefore, the effects of inhibiting ISR kinases can be context dependent. However, our study indicates that in MYC driven lymphoma cells can bypass PERK and GCN2 inhibition by upregulating the downstream effector ATF4 and that ablation of ATF4 can have a dramatic negative impact on lymphoma growth. Hence, it is important to target ATF4 itself. There is currently a compound called ISRIB that inhibits translation of ATF4 by activating eIF2B even in the presence of high levels of p-eIF2α[186]. ISRIB shows potent cytotoxic effect in aggressive metastatic prostate cancer by reversing the effect of p-eIF2α and reducing ATF4 expression[147].

In summary, this study demonstrates that the ISR transcription factor ATF4 is required to overcome MYC induced intrinsic stress and cooperates with MYC in regulation of translation to achieve homeostasis. Importantly, we have uncovered the therapeutic potential of targeting ISR in MYC driven tumors.

CHAPTER 5: MATERIALS & METHODS

Cell culture and reagents. Human colon adenocarcinoma DLD-1 cell lines were purchased from American Type Culture Collection (ATCC) and maintained in DMEM (Invitrogen #21063-029) supplemented with 10% FBS (Sigma) and 1% penicillin-streptomycin (Invitrogen). P493-6 cells were provided by Dirk Eick, German Res. center for Environmental Health, Helmholtz center, Munich and maintained in RPMI-1640 supplemented with 10% FBS and 1% Penicillin-Streptomycin. MYC expression was turned off in P4936 cells by adding 0.1ug/ml Tetracycline. Wild-type and GCN2-knockout, Sv40 immortalized, mouse embryonic fibroblasts were purchased from ATCC. ATF4-knockout Sv40 immortalized MEFs were a kind gift from David Ron (Cambridge Institute for Medical Research (CIMR). Wild-type, ATF4-knockout, GCN2-knockout, Sv40 immortalized, mouse embryonic fibroblasts (MEFs) were maintained in DMEM supplemented with 10% FBS, 1% Penicillin-Streptomycin, 1x non-essential amino acids (Invitrogen) and 55 μM β-mercaptoethanol (Gibco). DLD-1 cells and MEFs were infected with retroviruses expressing MycER. MycER was induced with 250nM or 500nM of 4-hydroxytamoxifen (4-OHT, Sigma-H7904) in MEFs and DLD-1 cells respectively. All cells were determined to be free of mycoplasma and cultured in 5% CO_2 at 37°C. RNA POL III inhibitor ML60218 (577784-91-9), cyclohexamide (C7698), dimethyl-α-ketoglutarate (349631) and rapamycin (R8781) were purchased from Sigma. 4PBA (130380250) was purchased from fisher scientific. siRNAs against ATF4 (L-005125-00), PERK (L-004883-00), GCN2 (L-005314-00), p70S6K (L-003616-00), eIF4E (L-003884-00) and non-targeting siRNA (D-001810-10) control were purchased from Dharmacon. LY-4 was provided by Eli Lilly.

Plasmids and retro viruses. MycER plasmid was provided by Dr. Andrei Thomas-Tikhonenko (The Children's Hospital of Philadelphia). Retrovirus construct and packaging plasmids, pEco-clontech (for mouse cells), pAmpho-clontech (for human cells) and gag pol were co-transfected into 293T cells by lipofectamine 2000 (Invitrogen), according to manufacturer's instructions. Retroviral supernatant was collected 48-72hours post transfection and supplied with 8ug/ml polybrene (28728-55-4 Sigma) to infect target cells. Lentiviral TRIPZ inducible shRNA against

ATF4 plasmid was purchased from Dharmacon (V3THS_302004). Lentivirus was made in 293T cells by co-transfecting lentiviral vector and packaging plasmids. Lentiviral supernatant was collected 48-72 hours post transfection and used to infect target cells.

Immunoblotting and antibodies. Cells were harvested in ice cold PBS and nuclear and cytoplasmic fraction were isolated by BioVision Nuclear Cytoplasm fractionation kit according to manufacturer's instructions (BioVision K266). RIPA buffer supplied with protease inhibitors (Roche 11836153001) and phosphatase inhibitors (p5726, p0044, Sigma) was used for whole lysate isolation. Protein concentrations were determined by DC protein assay (BioRad). Equal protein was loaded and resolved on to sodium dodecyl sulfate polyacrylamide gels and transferred to polyvinylidene fluoride membranes. All antibodies were incubated overnight at 4^0C overnight in 5% TBS (20mM Tris-Base and 150mM NaCl), 0.1% Tween-20. Membranes were washed and incubated with secondary antibodies for 1 hour. Membranes were exposed to autoradiography films after washing with TBS, 0.1% tween. The following antibodies were used for detecting proteins: ATF4 (cat# sc-200x, c-20), MYC (cat# sc-764, N-262), ATF3 (cat# sc-188, C-19) were purchased from Santa Cruz. Rabbit β-tubulin (2146), mouse cl-PARP (mouse specific, #9548, 7C9), rabbit cl-PARP (human specific, cat#9541), rabbit cl-caspase3 (cat# 9661), rabbit GCN2 (cat# 3302), rabbit PERK (cat# 3192, C33E10), rabbit p-PERK T980 (cat# 3179,16F8), rabbit p-4E-BP1 T37/46 (cat# 2855, 236B4), rabbit 4E-BP1 (cat#9452), rabbit eIF4e (cat#9742), rabbit p-p70S6K T389 (cat# 9205), rabbit p70S6K (cat#2708, 49D7), rabbit p-eIF2α S51 (cat# 3597, 119A11) and rabbit eIF2α (cat# 9722) were all purchased from Cell Signaling Technology. Rabbit p-PERK T982 was provided by Eli Lilly. Rabbit p-GCN2 T899 (cat# ab 75836) was purchased from Abcam. Mouse β-actin (cat#A5441, AC-15) was purchased from Sigma. Mouse RNA POL II (cat# 39097) was purchased from Active Motif. O-GlycNAc (cat#sc-59624, RL2) and OGT (cat#sc-74546, F-12) antibodies were purchased from Santa Cruz. Horseradish peroxidase- conjugated secondary antibodies, goat anti mouse (cat#31430) and goat anti rabbit (cat#31460) were purchased from Thermo Scientific.

Clonogenic survival assay. Cells were grown in complete media in 60mm dishes or in 6-well plates. The following day cells were treated with 4-OHT. Media was changed after 24 hours. Colonies that formed after a week were fixed with a solution of 10% methanol and 10% acetic acid and then stained with 0.4% crystal violet in 20% ethanol.

^{35}S Methionine and Cysteine labeling. Cells were plated in 6 well dish. The following day, cells were treated with 4-OHT for indicated times and cells were labeled with 50µCi/ml Met/ Cys Express Mix (PerkinElmer, NEG772014MC) for 1hr in Methionine and cysteine free DMEM (21013024, Invitrogen). Cells were washed with ice cold PBS and cell lysates were harvested for protein. Protein concentration was determined by DC protein assay (BioRad) and equal protein was loaded and resolved on to sodium dodecyl sulfate polyacrylamide gels and transferred on to polyvinylidene fluoride membranes. Membranes were exposed to autoradiography films. ^{35}S incorporation was quantified by Image J software. β-actin was used as a loading control.

Magnetic isolation of mouse B cells. Spleens and lymph nodes were excised from euthanized mice and immediately passed through 70um cell strainer. Normal splenic B cells as well as B cells in lymphoma were isolated by using mouse B cell isolation kit (130-090-862, Miltenyi Biotec) according to manufacturer's instructions.

Quantitative Real Time PCR. RNA was harvested for all qPCR analysis by using Qiagen RNeasy Mini Kit (74104) according to manufacturer's instructions. RNA was reverse transcribed by using AMV reverse transcriptase (Promega, M5108) in the presence of RNase inhibitor (Promega, N2111). qPCR was performed with Power SYBR green PCR master mix (Applied Biosystems, 4367659). QuantStudio 6 Flex Real-Time PCR System (Applied Biosystems) was used for data analysis. Primers used for qPCR are listed in supplementary Table 1.

tRNA charging microarray. About 8 million DLD-1, MycER cells were treated with 500nM 4-OHT for 2h, 4h, 8h or EtOH was used as vehicle. To determine the fraction of charged tRNAs, total RNA was isolated in mild acidic conditions using acidic phenol (pH 4.5) whose low pH preserves the aminoacyl-moiety. Each sample was split into two aliquots and one was oxidized with periodate which oxidizes the free non-aminoacyl groups leaving the changed tRNAs intact. Following subsequent deacylation the amino acid-protected tRNAs hybridize to Cy3-labeled RNA/DNA stem-loop oligonucleotide. The second aliquot was deacylated in 100 mM Tris (pH 9.0) at 37°C for 45 min and hybridized to Atto647-labeled RNA/DNA stem-loop oligonucleotide and designated as total tRNA. Both aliquots were loaded on tRNA microarrays with tRNA probes covering the full-length sequence of cytoplasmic tRNA species as described previously. For tRNA abundance, total RNA was isolated with TriReagent (Sigma Aldrich) which alkaline pH simultaneously deacylates all tRNAs. The tRNAs were subsequently labeled with by ligating Cy3-labeled RNA/DNA stem-loop oligonucleotide. The tRNAs isolated from the sample at the onset of MYC activation (zero-time point) were labeled with Att647-labeled RNA/DNA stem-loop oligonucleotide, loaded on all arrays and all other samples were compared to it. The arrays were normalized to spike-in standards which were present in equimolar rations in both Cy3- and Atto647-labeled aliquots. The arrays processing and quantification was performed with in-house python and R scripts. The data was submitted to the Gene Expression Omnibus (GEO) database and can be accessed using accession number GSE116812.

Chromatin immunoprecipitation. ChIP was performed as previously described[187]. Chromatin fragments were prepared from DLD-1: MycER cells following 8hr of MYC activation (EtOH or 4-OHT treatment). DNA was sonicated using Covaris 200 instrument at settings of Temp 5-9, PP200, DF 10, CB 200, 720sec. 50ug DNA was used for each ChIP. The following antibodies were used to perform ChIP at a concentration of 5ug: ATF4 (cat# sc-200x, lot# G0115, c-20), MYC (cat# sc-764, lo#D0413, N-262). Rabbit IgG (cat# sc-2027x, lot# G2516) was used as a negative control. All antibodies were purchased from Santa Cruz Biotechnology. Protein G

Dynabeads (10003D) were purchased from Invitrogen. Primers used for qPCR are listed in supplementary Table 1.

Library preparation, sequencing and analysis. ChIP DNA from two independent experiments was submitted to Wistar genomics core, (Wistar institute, Philadelphia) for library production using NEBNext Ultra II DNA Library Prep Kit for Illumina #E7645S and NEBNext Multiplex Oligos for Illumina #E7335S according to manufacturer's instructions. The library fragments were assessed on an Agilent Technologies 2100 Bioanalyzer and yielded 150-350bp products. Illumina NextSeq 500 instrument was used for sequencing. Select targets were validated by qPCR and primers used for qPCR are listed.

CHIP-seq data was aligned using bowtie[188] against hg38 version of the human genome and HOMER software was used call significant peaks against IgG control or between corresponding replicate pairs of samples using –style factor option and only uniquely aligned reads with duplicates removed. Significant peaks that passed FDR<5% threshold and at least 4 fold over IgG control were used to identify unique binding sites. Only results significant in comparison for both replicates were considered. De-novo motif analysis was performed using HOMER software[189] among the list of sites with significant ATF4 binding in at least one condition (both replicates). Overlap of binding sites with genes was done using Ensemble 84 transcriptome database. Genes with a binding site within 5kb from TSS were considered. Significance of overlap was tested using hypergeometric test using 23,869 Ensemble genes with Entrez ID as a population size. Gene set enrichment analysis of gene sets was done using QIAGEN's Ingenuity® Pathway Analysis software (IPA®, QIAGEN Redwood City,www.qiagen.com/ingenuity) using "Canonical Pathways" and "Upstream Analysis" options. Pathways with at least 2 member genes that passed FDR<20%, enrichment at least 5 fold threshold and upstream regulators (transcription factors only) that passed $p<0.05$ and had at least 5 target genes were considered. Functional and pathway enrichment analysis was done use DAVID software[190] and FDR<20% categories enriched at least 5 fold were considered. The data

was submitted to the Gene Expression Omnibus (GEO) database and can be accessed using accession number: GSE117240

Animal Studies. All animal experiments were approved by Institutional Animal Care and Use Committee at University of Pennsylvania. All mouse experiments comply with all regulations for ethical conduct of research. The *Eμ-myc/+* (stock no. 002728), *GCN2*$^{-/-}$ (stock no. 008240) and *Rosa26-CreER*$^{T2/+}$ (stock no. 008463) transgenic mice were purchased from The Jackson Laboratory. The athymic nude mice were purchased from Charles River Laboratory (stock no. 490). *ATF4*$^{fl/fl}$ mice under C57BL/6 background were generated by Cyagen Biosciences Inc. Briefly, LoxP sites were inserted flanking exon 2 and 3 of Atf4 locus to create a conditional knockout when crossed with *Rosa26-CreER*$^{T2/+}$. *Eμ-myc/+; GCN2*$^{+/+}$ mice were crossed with *GCN2*$^{-/-}$ to generate *Eμ-myc/+; GCN2*$^{+/+}$, *Eμ-myc/+; GCN2*$^{+/-}$ *and Eμ-myc/+; GCN2*$^{-/-}$ mice. *ATF4*$^{fl/fl}$ mice were crossed with *Rosa26-CreER*$^{T2/+}$ to generate *ATF4*$^{fl/fl}$*; Rosa26-CreER*$^{T2/+}$ which were then crossed with *Eμ-myc/+, ATF4* $^{+/+}$ mice. The following mice were obtained and used for transplantable lymphoma experiments- *Eμ-myc/+; Rosa26-CreER*$^{T2/+}$*; ATF4*$^{wt/wt}$ and *Eμ-myc/+; Rosa26-CreER*$^{T2/+}$*; ATF4*$^{fl/fl}$.

For transplantable lymphoma experiments, mice harboring lymphoma were euthanized according to IACUC guidelines. Lymph nodes were collected immediately on ice and miced and passed through 70um cell strainer in 50% Iscove's media and 50% DMEM supplemented with 10% FBS, 1% Penicillin-Streptomycin and 4mM glutamine. Dead cells were removed by spinning cells in Ficoll-Paque PLUS (GE healthcare, # 17-1440-02), 800g for 10min. Lymphoma cells were washed in PBS and 2 million cells were injected into 9 weeks old male C57BL/6J mice via tail vein. Mice were monitored for lymphoma development by palpation every other day.

For PERK inhibitor (LY-4) experiments, 9 weeks old male mice were injected with 2 million *Eμ-myc/+; GCN2*$^{+/+}$ *or Eμ-myc/+; GCN2*$^{-/-}$ lymphoma cells. After 3 days mice were randomized to receive vehicle (captisol, CYDEX) treatment or LY-4 100mg/kg twice a day by oral gavage three days following lymphoma injection for the duration of the experiment.

For ATF4 excision experiment, 2 million *Eμ-myc/+; Rosa26-CreER$^{T2/+}$; ATF4$^{wt/wt}$* or *Eμ-myc/+; Rosa26-CreER$^{T2/+}$; ATF4$^{fl/fl}$* lymphoma cells were injected via tail vein into 9-weeks old male C57BL/6J mice. Three days following lymphoma injection, mice were randomized to receive vehicle (peanut oil, Sigma) or 4mg/20g Tamoxifen (T5648, Sigma) by oral gavage for 5 consecutive days. Mice were monitored every other day for lymphoma development by palpation. 3 million DLD-1, MycER, ishATF4 cells were injected in the flanks of 11-weeks old male nude mice and MYC was activated by treating mice with 1mg/mouse tamoxifen every other day, three days following tumor injection. Once tumors reached 100 cm^3, 2mg/mouse doxycycline treatment was started for every other day until duration of experiment.

Statistics. GraphPad Prism 7 and Excel 2010 were used for statistical analysis. Error bars indicate mean ± S.D. or mean ± SEM (as indicated in Figure legends) and statistical significance was determined by unpaired, two tailed student's t-test. One-way ANOVA analysis was used to determine statistical differences in the tRNA microarray data. A p value less than 0.05 was considered statistically significant. For mouse survival analysis, Kaplan-Meier curves and log-rank test were generated in GraphPad Prism 7 software. For xenograft experiment, two-way ANOVA was used.

Patient data analysis. The gene expression using RNA-seq and survival information of DLBCL dataset[191] were obtained from The NCI Center for Cancer Genomics (CCG) website, and gene expression information of 3 TCGA datasets was from UCSC Xena[192]. For each dataset, the normalized gene expression of EIF4E-BP1 gene and other 10 ATF4 targeted genes (*DDTI3, ATF3, ASNS, SLC43A1, SLC1A5, GARS, NARS, MARS, PSAT1, MTHFD2*) was standardized to Z-score then the Pearson correlation between EIF4E-BP1 and average ATF4 target genes was estimated. The visualization of linear relationships on Figure.6a was performed using seaborn software (https://zenodo.org/record/883859#.Ww2av0gvzAQ). In addition, patients in DLBCL dataset were divided into two groups according to ATF4/ EIF4E-BP1 gene expression: low

ATF4/EIF4E-BP1 expression (<= median) and high ATF4/EIF4E-BP1 expression (> median). The survival analysis using Kaplan-Meier and log-rank test between high and low ATF4/EIF4E-BP1 expression groups were performed using lifelines software (https://zenodo.org/record/1252342#.Ww2WRUgvzAQ), as shown on Figure. 6b.

Metabolite extraction and Capillary electrophoresis mass spectroscopy analysis. Capillary electrophoresis mass spectrometry (CE-MS) -based targeted quantitative analysis[193-195] was performed on DLD-1 : MycER cells transfected with non-targeting (siNT) siRNA or siRNA against ATF4 (Dharmacon) using Lipofectamine RNAiMax reagent (Invitrogen). 72 hours after transfection, cells were used for experiment according to protocol provided by Human Metabolome Technologies, inc. (Tsuruoka, Japan). Briefly on the day of the experiment, media was changed and MYC was induced for indicated times. Cells were washed twice with 5% mannitol solution, treated with methanol and water containing internal standards (H3304-1002). Extracts were centrifuged at 2,300 ×*g* at 4°C for 5 min. The supernatants were centrifugally filtered at 9,100 ×*g* at 4C for 3 hours to remove proteins. Samples were evaporated centrifugally in evaporator unit at 1,500 rpm and 1,000 Pa pressure for 3 hours. The samples were analyzed by capillary electrophoresis time-of-flight mass spectrometry (CE-TOFMS) at HMT.

Glucose uptake assay. 10,000 cells were plated per well in white walled 96-well plates and MYC was activated the following day with addition of 4-OHT. Glucose Uptake-Glo™ Assay (Promega #J1342) was used according to the manufacturer's instruction and luminesce was read using BioTek Hybrid plate reader.

Table 5.1	**ChIP qPCR Primers**	***Homo sapiens***
hODC	Forward primer	ATCACTTCCAGGTCCCTTGCAC
	Reverse primer	TTCCACCTGGCGTTCAGTACC
hASNS	Forward primer	CCTGTGCGCGCTGGTTGGTCCT
	Reverse primer	CGCTTATACCGACCTGGCTCCT
hPSAT1	Forward primer	GTTTGCATCCCTGCGTGT
	Reverse primer	CCGAGCTTCCTCACCAACT
hPHGDH	Forward primer	CGTAAGGCAGCAAACACGTA
	Reverse primer	CCAGCGATAAACCAAAGGTG
hEIF4EBP-1	Forward primer	CTCCTCCCCTCTCATTGT
	Reverse primer	CAGGATCTGTCGCGTTTTCT
hEIF4EBP-1 neg	Forward primer	ATAGAGTGTCTGCATGGCTGT
	Reverse primer	CCCTCCAGGGACAATCACTTG
hSLC43A1	Forward primer	GAGGAAACCAGCTACCCGAC
	Reverse primer	CAAAGCTCAGCTAACGCTGG
hSLC38A1	Forward primer	GCCCGCTCTTTAACCAAAGC
	Reverse primer	TTCCCCGTTGCTCAATCTCC
hIARS	Forward primer	AATGCGGGATCCAGTGAAGG
	Reverse primer	CAGTGGGCGCAATCATGTC
hNARS	Forward primer	GACGCCGTCTTATGACTCCA
	Reverse primer	GCCCACCTCTCGTAACCAAT

Table 5.2	***Mus musculus***	**qPCR primers**
18sRNA	Forward primer	CAATTACAGGGCCTCGAAAG
	Reverse primer	AAACGGCTACCACATCCAAG
mODC	Forward primer	GACCTTGTGAGGAGCTGGTGAT
	Reverse primer	TGGCAGTCAAACTCGTCCTTAG
mATF4	Forward primer	CCTGAACAGCGAAGTGTTGG
	Reverse primer	TGGAGAACCCATGAGGTTTCAA
mEIF4EBP-1	Forward primer	GGGGACTACAGCACCACTC
	Reverse primer	CTCATCGCTGGTAGGGCTA
mSHMT2	Forward primer	TGGCAAGAGATACTACGGAGG
	Reverse primer	GCAGGTCCAACCCCATGAT
mMTHFD2	Forward primer	AGTGCGAAATGAAGCCGTTG
	Reverse primer	GACTGGCGGGATTGTCACC
mSLC7A11	Forward primer	GGCACCGTCATCGGATCAG
	Reverse primer	CTCCACAGGCAGACCAGAAA
mSLC38A2	Forward primer	TAATCTGAGCAATGCGATTGTGG
	Reverse primer	AGATGGACGGAGTATAGCGAAAA
mSARS	Forward primer	CAGCCCTCATCCGAGAGAC
	Reverse primer	TCTGCCCGAAATCTACATCGT

Table 5.3	***Homo sapiens***	**qPCR primers**
18sRNA	Forward primer	CAATTACAGGGCCTCGAAAG
	Reverse primer	AAACGGCTACCACATCCAAG
hODC	Forward primer	TTGCGGATTGCCACTGATGATTCC
	Reverse primer	ATCAGAGATTGCCTGCACGAA
hATF4	Forward primer	CCCTTCACCTTCTTACAACCT
	Reverse primer	TGCCCAGCTCTAAACTAAAGGA
hEIF4EBP-1	Forward primer	CTATGACCGGAAATTCCTGATGG
	Reverse primer	CCCGCTTATCTTCTGGGCTA
hGOT1	Forward primer	AGCTGTGCTTCTCGTCTTGC
	Reverse primer	AGATTGCACACCTCCTACCC
hGOT2	Forward primer	GACCAAATTGGCATGTTCTGT
	Reverse primer	CGGCCATCTTTTGTCATGTA
hGPT2	Forward primer	GGATCTTCATTCCTGCCAAA
	Reverse primer	ACATGTCTGGAGCCATTTGA
hGLS	Forward primer	AGGGTCTGTTACCTAGCTTGG
	Reverse primer	ACGTTCGCAATCCTGTAGATTT
hSHMT2	Forward primer	CCCTTCTGCAACCTCACGAC
	Reverse primer	TGAGCTTATAGGGCATAGACTCG
hMTHFD2	Forward primer	AGGACGAATGTGTTTGGATCAG
	Reverse primer	GGAATGCCAGTTCGCTTGATTA
hSLC7A11	Forward primer	TCTCCAAAGGAGGTTACCTGC
	Reverse primer	AGACTCCCCTCAGTAAAGTGAC
hPSAT1	Forward primer	CGGTCCTGGAATACAAGGTG
	Reverse primer	AACCAAGCCCATGACGTAGA

Table 5.4	**Genotyping primers**	***Mus musculus***
Eμ-myc	Forward primer	TTAGACGTCAGGTGGCACTT
	Reverse primer	TGAGCAAAAACAGGAAGGCA
	Forward primer-internal positive control	CTAGGCCACAGAATTGAAAGATCT
	Reverse primer-internal positive control	GTAGGTGGAAATTCTAGCATCATCC
GCN2-/-	Forward primer-common	TCTCCCAGCGGAATCCGCACATCG
	Reverse primer-wt	ATCCAGGCGTTGTAGTAGCGCACA
	Reverse primer- knockout	TGCCACTGTCAGAATCTGAAGCAGG
ATF4 fl/fl	Forward primer	CTTGTTTGCGTTGCCTGCGAC
	Reverse primer	AGGAAGCAGCTTGTCCTCGCG
ATF4 fl/fl-excision	Forward primer	GGTTTTACAAGCGGCCGGAC
	Reverse primer	TCCACTCTTGGCCAGACTACG
RosaCreERT2	Forward primer-common	AAAGTCGCTCTGAGTTGTTAT
	Reverse primer-wt	GGAGCGGGAGAAATGGATATG
	Reverse primer- mutant	CCTGATCCTGGCAATTTCG

BIBLIOGRAPHY

1. Healy, S.J., Gorman, A.M., Mousavi-Shafaei, P., Gupta, S. & Samali, A. Targeting the endoplasmic reticulum-stress response as an anticancer strategy. *Eur J Pharmacol* **625**, 234-246 (2009).
2. Braakman, I. & Bulleid, N.J. Protein folding and modification in the mammalian endoplasmic reticulum. *Annu Rev Biochem* **80**, 71-99 (2011).
3. Boyce, M. & Yuan, J. Cellular response to endoplasmic reticulum stress: a matter of life or death. *Cell Death Differ* **13**, 363-373 (2006).
4. Schroder, M. & Kaufman, R.J. The mammalian unfolded protein response. *Annu Rev Biochem* **74**, 739-789 (2005).
5. Rutkowski, D.T. & Kaufman, R.J. A trip to the ER: coping with stress. *Trends Cell Biol* **14**, 20-28 (2004).
6. Friedlander, R., Jarosch, E., Urban, J., Volkwein, C. & Sommer, T. A regulatory link between ER-associated protein degradation and the unfolded-protein response. *Nat Cell Biol* **2**, 379-384 (2000).
7. Schroder, M. Endoplasmic reticulum stress responses. *Cell Mol Life Sci* **65**, 862-894 (2008).
8. Szegezdi, E., Logue, S.E., Gorman, A.M. & Samali, A. Mediators of endoplasmic reticulum stress-induced apoptosis. *EMBO Rep* **7**, 880-885 (2006).
9. Bi, M. *et al.* ER stress-regulated translation increases tolerance to extreme hypoxia and promotes tumor growth. *EMBO J* **24**, 3470-3481 (2005).
10. Ma, Y. & Hendershot, L.M. The role of the unfolded protein response in tumour development: friend or foe? *Nat Rev Cancer* **4**, 966-977 (2004).
11. Hart, L.S. *et al.* ER stress-mediated autophagy promotes Myc-dependent transformation and tumor growth. *J Clin Invest* **122**, 4621-4634 (2012).
12. Bagratuni, T. *et al.* XBP1s levels are implicated in the biology and outcome of myeloma mediating different clinical outcomes to thalidomide-based treatments. *Blood* **116**, 250-253 (2010).
13. Ruggero, D. Translational control in cancer etiology. *Cold Spring Harb Perspect Biol* **5** (2013).
14. Brown, J.M. & Wilson, W.R. Exploiting tumour hypoxia in cancer treatment. *Nat Rev Cancer* **4**, 437-447 (2004).
15. Lee, A.S. Glucose-regulated proteins in cancer: molecular mechanisms and therapeutic potential. *Nat Rev Cancer* **14**, 263-276 (2014).
16. Lee, A.S., Delegeane, A. & Scharff, D. Highly conserved glucose-regulated protein in hamster and chicken cells: preliminary characterization of its cDNA clone. *Proc Natl Acad Sci U S A* **78**, 4922-4925 (1981).
17. Lee, A.S. Coordinated regulation of a set of genes by glucose and calcium ionophores in mammalian cells. *Trends Biochem Sci* **12**, 20-23 (1987).
18. Jamora, C., Dennert, G. & Lee, A.S. Inhibition of tumor progression by suppression of stress protein GRP78/BiP induction in fibrosarcoma B/C10ME. *Proceedings of the National Academy of Sciences* **93**, 7690-7694 (1996).
19. Dong, D. *et al.* Critical role of the stress chaperone GRP78/BiP in tumor proliferation, survival, and tumor angiogenesis in transgene-induced mammary tumor development. *Cancer Res* **68**, 498-505 (2008).

20. Fu, Y. *et al.* Pten null prostate tumorigenesis and AKT activation are blocked by targeted knockout of ER chaperone GRP78/BiP in prostate epithelium. *Proc Natl Acad Sci U S A* **105**, 19444-19449 (2008).
21. Luo, B. & Lee, A.S. The critical roles of endoplasmic reticulum chaperones and unfolded protein response in tumorigenesis and anticancer therapies. *Oncogene* **32**, 805-818 (2013).
22. Hendershot, L.M. The ER function BiP is a master regulator of ER function. *Mt Sinai J Med* **71**, 289-297 (2004).
23. Bertolotti, A., Zhang, Y., Hendershot, L.M., Harding, H.P. & Ron, D. Dynamic interaction of BiP and ER stress transducers in the unfolded-protein response. *Nat Cell Biol* **2**, 326-332 (2000).
24. Wang, P., Li, J., Tao, J. & Sha, B. The luminal domain of the ER stress sensor protein PERK binds misfolded proteins and thereby triggers PERK oligomerization. *J Biol Chem* **293**, 4110-4121 (2018).
25. Karagoz, G.E. *et al.* An unfolded protein-induced conformational switch activates mammalian IRE1. *Elife* **6** (2017).
26. Ye, J. *et al.* ER stress induces cleavage of membrane-bound ATF6 by the same proteases that process SREBPs. *Mol Cell* **6**, 1355-1364 (2000).
27. Adachi, Y. *et al.* ATF6 is a transcription factor specializing in the regulation of quality control proteins in the endoplasmic reticulum. *Cell Struct Funct* **33**, 75-89 (2008).
28. Shuda, M. *et al.* Activation of the ATF6, XBP1 and grp78 genes in human hepatocellular carcinoma: a possible involvement of the ER stress pathway in hepatocarcinogenesis. *J Hepatol* **38**, 605-614 (2003).
29. Chang, K.C., Chen, P.C., Chen, Y.P., Chang, Y. & Su, I.J. Dominant expression of survival signals of endoplasmic reticulum stress response in Hodgkin lymphoma. *Cancer Sci* **102**, 275-281 (2011).
30. Lu, Y., Liang, F.X. & Wang, X. A synthetic biology approach identifies the mammalian UPR RNA ligase RtcB. *Mol Cell* **55**, 758-770 (2014).
31. Maurel, M., Chevet, E., Tavernier, J. & Gerlo, S. Getting RIDD of RNA: IRE1 in cell fate regulation. *Trends Biochem Sci* **39**, 245-254 (2014).
32. Lee, A.H., Iwakoshi, N.N., Anderson, K.C. & Glimcher, L.H. Proteasome inhibitors disrupt the unfolded protein response in myeloma cells. *Proc Natl Acad Sci U S A* **100**, 9946-9951 (2003).
33. Xu, G. *et al.* Expression of XBP1s in bone marrow stromal cells is critical for myeloma cell growth and osteoclast formation. *Blood* **119**, 4205-4214 (2012).
34. Fujimoto, T. *et al.* Upregulation and overexpression of human X-box binding protein 1 (hXBP-1) gene in primary breast cancers. *Breast Cancer* **10**, 301-306 (2003).
35. Tang, C.H. *et al.* Inhibition of ER stress-associated IRE-1/XBP-1 pathway reduces leukemic cell survival. *J Clin Invest* **124**, 2585-2598 (2014).
36. Mimura, N. *et al.* Blockade of XBP1 splicing by inhibition of IRE1alpha is a promising therapeutic option in multiple myeloma. *Blood* **119**, 5772-5781 (2012).
37. Zhao, N. *et al.* Pharmacological targeting of MYC-regulated IRE1/XBP1 pathway suppresses MYC-driven breast cancer. *J Clin Invest* **128**, 1283-1299 (2018).
38. Ma, K., Vattem, K.M. & Wek, R.C. Dimerization and release of molecular chaperone inhibition facilitate activation of eukaryotic initiation factor-2 kinase in response to endoplasmic reticulum stress. *J Biol Chem* **277**, 18728-18735 (2002).

39. Harding, H.P., Zhang, Y., Bertolotti, A., Zeng, H. & Ron, D. Perk is essential for translational regulation and cell survival during the unfolded protein response. *Mol Cell* **5**, 897-904 (2000).
40. Harding, H.P. *et al.* An integrated stress response regulates amino acid metabolism and resistance to oxidative stress. *Mol Cell* **11**, 619-633 (2003).
41. B'Chir, W. *et al.* The eIF2alpha/ATF4 pathway is essential for stress-induced autophagy gene expression. *Nucleic Acids Res* **41**, 7683-7699 (2013).
42. Novoa, I., Zeng, H., Harding, H.P. & Ron, D. Feedback inhibition of the unfolded protein response by GADD34-mediated dephosphorylation of eIF2alpha. *J Cell Biol* **153**, 1011-1022 (2001).
43. Cullinan, S.B. *et al.* Nrf2 is a direct PERK substrate and effector of PERK-dependent cell survival. *Mol Cell Biol* **23**, 7198-7209 (2003).
44. Bu, Y. *et al.* A PERK-miR-211 axis suppresses circadian regulators and protein synthesis to promote cancer cell survival. *Nat Cell Biol* **20**, 104-115 (2018).
45. Gupta, S., McGrath, B. & Cavener, D.R. PERK regulates the proliferation and development of insulin-secreting beta-cell tumors in the endocrine pancreas of mice. *PLoS One* **4**, e8008 (2009).
46. Bobrovnikova-Marjon, E. *et al.* PERK promotes cancer cell proliferation and tumor growth by limiting oxidative DNA damage. *Oncogene* **29**, 3881-3895 (2010).
47. Avivar-Valderas, A. *et al.* PERK integrates autophagy and oxidative stress responses to promote survival during extracellular matrix detachment. *Molecular and Cellular Biology* **31**, 3616-3629 (2011).
48. Dey, S. *et al.* ATF4-dependent induction of heme oxygenase 1 prevents anoikis and promotes metastasis. *J Clin Invest* **125**, 2592-2608 (2015).
49. Chitnis, N.S. *et al.* miR-211 is a prosurvival microRNA that regulates chop expression in a PERK-dependent manner. *Mol Cell* **48**, 353-364 (2012).
50. Wek, R.C., Jiang, H.Y. & Anthony, T.G. Coping with stress: eIF2 kinases and translational control. *Biochem Soc Trans* **34**, 7-11 (2006).
51. Hinnebusch, A.G. The scanning mechanism of eukaryotic translation initiation. *Annu Rev Biochem* **83**, 779-812 (2014).
52. Jackson, R.J., Hellen, C.U. & Pestova, T.V. The mechanism of eukaryotic translation initiation and principles of its regulation. *Nat Rev Mol Cell Biol* **11**, 113-127 (2010).
53. Ameri, K. & Harris, A.L. Activating transcription factor 4. *Int J Biochem Cell Biol* **40**, 14-21 (2008).
54. Liang, G. & Hai, T. Characterization of human activating transcription factor 4, a transcriptional activator that interacts with multiple domains of cAMP-responsive element-binding protein (CREB)-binding protein. *J Biol Chem* **272**, 24088-24095 (1997).
55. Fawcett, T.W., Martindale, J.L., Guyton, K.Z., Hai, T. & Holbrook, N.J. Complexes containing activating transcription factor (ATF)/cAMP-responsive-element-binding protein (CREB) interact with the CCAAT/enhancer-binding protein (C/EBP)-ATF composite site to regulate Gadd153 expression during the stress response. *Biochem J* **339 (Pt 1)**, 135-141 (1999).
56. Hai, T. & Curran, T. Cross-family dimerization of transcription factors Fos/Jun and ATF/CREB alters DNA binding specificity. *Proc Natl Acad Sci U S A* **88**, 3720-3724 (1991).
57. Pakos-Zebrucka, K. *et al.* The integrated stress response. *EMBO Rep* **17**, 1374-1395 (2016).

58. Siu, F., Bain, P.J., LeBlanc-Chaffin, R., Chen, H. & Kilberg, M.S. ATF4 is a mediator of the nutrient-sensing response pathway that activates the human asparagine synthetase gene. *J Biol Chem* **277**, 24120-24127 (2002).
59. Harding, H.P. *et al.* Regulated translation initiation controls stress-induced gene expression in mammalian cells. *Mol Cell* **6**, 1099-1108 (2000).
60. Lu, P.D. *et al.* Cytoprotection by pre-emptive conditional phosphorylation of translation initiation factor 2. *EMBO J* **23**, 169-179 (2004).
61. Mo, H. *et al.* ATF4 regulated by MYC has an important function in anoikis resistance in human osteosarcoma cells. *Mol Med Rep* **17**, 3658-3666 (2018).
62. Babcock, J.T. *et al.* Mammalian target of rapamycin complex 1 (mTORC1) enhances bortezomib-induced death in tuberous sclerosis complex (TSC)-null cells by a c-MYC-dependent induction of the unfolded protein response. *J Biol Chem* **288**, 15687-15698 (2013).
63. Afonyushkin, T. *et al.* Oxidized phospholipids regulate expression of ATF4 and VEGF in endothelial cells via NRF2-dependent mechanism: novel point of convergence between electrophilic and unfolded protein stress pathways. *Arterioscler Thromb Vasc Biol* **30**, 1007-1013 (2010).
64. Igarashi, T. *et al.* Clock and ATF4 transcription system regulates drug resistance in human cancer cell lines. *Oncogene* **26**, 4749-4760 (2007).
65. Sachdeva, M.M. *et al.* Pdx1 (MODY4) regulates pancreatic beta cell susceptibility to ER stress. *Proc Natl Acad Sci U S A* **106**, 19090-19095 (2009).
66. Dey, S. *et al.* Both transcriptional regulation and translational control of ATF4 are central to the integrated stress response. *J Biol Chem* **285**, 33165-33174 (2010).
67. Lu, P.D., Harding, H.P. & Ron, D. Translation reinitiation at alternative open reading frames regulates gene expression in an integrated stress response. *J Cell Biol* **167**, 27-33 (2004).
68. Vattem, K.M. & Wek, R.C. Reinitiation involving upstream ORFs regulates ATF4 mRNA translation in mammalian cells. *Proc Natl Acad Sci U S A* **101**, 11269-11274 (2004).
69. Lee, Y.Y., Cevallos, R.C. & Jan, E. An upstream open reading frame regulates translation of GADD34 during cellular stresses that induce eIF2alpha phosphorylation. *J Biol Chem* **284**, 6661-6673 (2009).
70. Zhou, D. *et al.* Phosphorylation of eIF2 directs ATF5 translational control in response to diverse stress conditions. *J Biol Chem* **283**, 7064-7073 (2008).
71. Lehman, S.L. *et al.* Translational Upregulation of an Individual p21Cip1 Transcript Variant by GCN2 Regulates Cell Proliferation and Survival under Nutrient Stress. *PLoS Genet* **11**, e1005212 (2015).
72. Yang, X. *et al.* ATF4 is a substrate of RSK2 and an essential regulator of osteoblast biology; implication for Coffin-Lowry Syndrome. *Cell* **117**, 387-398 (2004).
73. Lassot, I. *et al.* ATF4 degradation relies on a phosphorylation-dependent interaction with the SCF(betaTrCP) ubiquitin ligase. *Mol Cell Biol* **21**, 2192-2202 (2001).
74. Koditz, J. *et al.* Oxygen-dependent ATF-4 stability is mediated by the PHD3 oxygen sensor. *Blood* **110**, 3610-3617 (2007).
75. Hettmann, T., Barton, K. & Leiden, J.M. Microphthalmia due to p53-mediated apoptosis of anterior lens epithelial cells in mice lacking the CREB-2 transcription factor. *Dev Biol* **222**, 110-123 (2000).

76. Zhao, Y. *et al.* ATF4 plays a pivotal role in the development of functional hematopoietic stem cells in mouse fetal liver. *Blood* **126**, 2383-2391 (2015).
77. Pasini, S., Corona, C., Liu, J., Greene, L.A. & Shelanski, M.L. Specific downregulation of hippocampal ATF4 reveals a necessary role in synaptic plasticity and memory. *Cell Rep* **11**, 183-191 (2015).
78. Masuoka, H.C. & Townes, T.M. Targeted disruption of the activating transcription factor 4 gene results in severe fetal anemia in mice. *Blood* **99**, 736-745 (2002).
79. Tanaka, T. *et al.* Targeted disruption of ATF4 discloses its essential role in the formation of eye lens fibres. *Genes Cells* **3**, 801-810 (1998).
80. Wang, C. *et al.* ATF4 regulates lipid metabolism and thermogenesis. *Cell Res* **20**, 174-184 (2010).
81. Chen, A. *et al.* Inducible enhancement of memory storage and synaptic plasticity in transgenic mice expressing an inhibitor of ATF4 (CREB-2) and C/EBP proteins. *Neuron* **39**, 655-669 (2003).
82. Costa-Mattioli, M. *et al.* eIF2alpha phosphorylation bidirectionally regulates the switch from short- to long-term synaptic plasticity and memory. *Cell* **129**, 195-206 (2007).
83. Ye, J. *et al.* The GCN2-ATF4 pathway is critical for tumour cell survival and proliferation in response to nutrient deprivation. *EMBO J* **29**, 2082-2096 (2010).
84. Wang, Y. *et al.* Amino acid deprivation promotes tumor angiogenesis through the GCN2/ATF4 pathway. *Neoplasia* **15**, 989-997 (2013).
85. Gwinn, D.M. *et al.* Oncogenic KRAS Regulates Amino Acid Homeostasis and Asparagine Biosynthesis via ATF4 and Alters Sensitivity to L-Asparaginase. *Cancer Cell* **33**, 91-107 e106 (2018).
86. Pathria, G. *et al.* Targeting the Warburg effect via LDHA inhibition engages ATF4 signaling for cancer cell survival. *EMBO J* (2018).
87. Gonzalez-Gonzalez, A. *et al.* Activating Transcription Factor 4 Modulates TGFbeta-Induced Aggressiveness in Triple-Negative Breast Cancer via SMAD2/3/4 and mTORC2 Signaling. *Clin Cancer Res* (2018).
88. Chen, D. *et al.* ATF4 promotes angiogenesis and neuronal cell death and confers ferroptosis in a xCT-dependent manner. *Oncogene* **36**, 5593-5608 (2017).
89. Vaupel, P. & Mayer, A. Hypoxia in cancer: significance and impact on clinical outcome. *Cancer Metastasis Rev* **26**, 225-239 (2007).
90. Nordsmark, M., Overgaard, M. & Overgaard, J. Pretreatment oxygenation predicts radiation response in advanced squamous cell carcinoma of the head and neck. *Radiother Oncol* **41**, 31-39 (1996).
91. Keith, B., Johnson, R.S. & Simon, M.C. HIF1alpha and HIF2alpha: sibling rivalry in hypoxic tumour growth and progression. *Nat Rev Cancer* **12**, 9-22 (2012).
92. Koumenis, C. *et al.* Regulation of protein synthesis by hypoxia via activation of the endoplasmic reticulum kinase PERK and phosphorylation of the translation initiation factor eIF2alpha. *Mol Cell Biol* **22**, 7405-7416 (2002).
93. Wouters, B.G. & Koritzinsky, M. Hypoxia signalling through mTOR and the unfolded protein response in cancer. *Nature Reviews Cancer* **8**, 851-864 (2008).
94. Koumenis, C. & Wouters, B.G. "Translating" tumor hypoxia: unfolded protein response (UPR)-dependent and UPR-independent pathways. *Mol Cancer Res* **4**, 423-436 (2006).
95. Fels, D.R. & Koumenis, C. The PERK/eIF2alpha/ATF4 module of the UPR in hypoxia resistance and tumor growth. *Cancer Biol Ther* **5**, 723-728 (2006).

96. Blais, J.D. *et al.* Activating transcription factor 4 is translationally regulated by hypoxic stress. *Molecular and Cellular Biology* **24**, 7469-7482 (2004).
97. Rouschop, K.M. *et al.* The unfolded protein response protects human tumor cells during hypoxia through regulation of the autophagy genes MAP1LC3B and ATG5. *J Clin Invest* **120**, 127-141 (2010).
98. Pike, L.R. *et al.* Transcriptional up-regulation of ULK1 by ATF4 contributes to cancer cell survival. *Biochem J* **449**, 389-400 (2013).
99. Mujcic, H. *et al.* Hypoxic activation of the PERK/eIF2alpha arm of the unfolded protein response promotes metastasis through induction of LAMP3. *Clin Cancer Res* **19**, 6126-6137 (2013).
100. Wek, S.A., Zhu, S. & Wek, R.C. The histidyl-tRNA synthetase-related sequence in the eIF-2 alpha protein kinase GCN2 interacts with tRNA and is required for activation in response to starvation for different amino acids. *Mol Cell Biol* **15**, 4497-4506 (1995).
101. Qiu, H., Dong, J., Hu, C., Francklyn, C.S. & Hinnebusch, A.G. The tRNA-binding moiety in GCN2 contains a dimerization domain that interacts with the kinase domain and is required for tRNA binding and kinase activation. *EMBO J* **20**, 1425-1438 (2001).
102. Horiguchi, M. *et al.* Stress-regulated transcription factor ATF4 promotes neoplastic transformation by suppressing expression of the INK4a/ARF cell senescence factors. *Cancer Res* **72**, 395-401 (2012).
103. Wang, Y. *et al.* The unfolded protein response induces the angiogenic switch in human tumor cells through the PERK/ATF4 pathway. *Cancer Res* **72**, 5396-5406 (2012).
104. Ozcan, U. *et al.* Loss of the tuberous sclerosis complex tumor suppressors triggers the unfolded protein response to regulate insulin signaling and apoptosis. *Mol Cell* **29**, 541-551 (2008).
105. Hills, S.A. & Diffley, J.F. DNA replication and oncogene-induced replicative stress. *Curr Biol* **24**, R435-444 (2014).
106. Galluzzi, L., Kepp, O., Vander Heiden, M.G. & Kroemer, G. Metabolic targets for cancer therapy. *Nat Rev Drug Discov* **12**, 829-846 (2013).
107. Dang, C.V. MYC on the path to cancer. *Cell* **149**, 22-35 (2012).
108. Schaub, F.X. *et al.* Pan-cancer Alterations of the MYC Oncogene and Its Proximal Network across the Cancer Genome Atlas. *Cell Syst* **6**, 282-300 e282 (2018).
109. Beroukhim, R. *et al.* The landscape of somatic copy-number alteration across human cancers. *Nature* **463**, 899-905 (2010).
110. Kluk, M.J. *et al.* Immunohistochemical detection of MYC-driven diffuse large B-cell lymphomas. *PLoS One* **7**, e33813 (2012).
111. Horiuchi, D. *et al.* MYC pathway activation in triple-negative breast cancer is synthetic lethal with CDK inhibition. *J Exp Med* **209**, 679-696 (2012).
112. Lee, K.S. *et al.* c-MYC Copy-Number Gain Is an Independent Prognostic Factor in Patients with Colorectal Cancer. *PLoS One* **10**, e0139727 (2015).
113. Fernandez, P.C. *et al.* Genomic targets of the human c-Myc protein. *Genes Dev* **17**, 1115-1129 (2003).
114. Blackwell, T.K. *et al.* Binding of myc proteins to canonical and noncanonical DNA sequences. *Mol Cell Biol* **13**, 5216-5224 (1993).
115. Evan, G.I. *et al.* Induction of apoptosis in fibroblasts by c-myc protein. *Cell* **69**, 119-128 (1992).

116. Iritani, B.M. & Eisenman, R.N. c-Myc enhances protein synthesis and cell size during B lymphocyte development. *Proc Natl Acad Sci U S A* **96**, 13180-13185 (1999).
117. Adams, J.M. *et al.* The C-Myc Oncogene Driven by Immunoglobulin Enhancers Induces Lymphoid Malignancy in Transgenic Mice. *Nature* **318**, 533-538 (1985).
118. Shroff, E.H. *et al.* MYC oncogene overexpression drives renal cell carcinoma in a mouse model through glutamine metabolism. *Proc Natl Acad Sci U S A* **112**, 6539-6544 (2015).
119. Ellwood-Yen, K. *et al.* Myc-driven murine prostate cancer shares molecular features with human prostate tumors. *Cancer Cell* **4**, 223-238 (2003).
120. Gabay, M., Li, Y. & Felsher, D.W. MYC activation is a hallmark of cancer initiation and maintenance. *Cold Spring Harb Perspect Med* **4** (2014).
121. Pelengaris, S., Khan, M. & Evan, G. c-MYC: more than just a matter of life and death. *Nat Rev Cancer* **2**, 764-776 (2002).
122. Gaidano, G. *et al.* p53 mutations in human lymphoid malignancies: association with Burkitt lymphoma and chronic lymphocytic leukemia. *Proc Natl Acad Sci U S A* **88**, 5413-5417 (1991).
123. Alexander, W.S. *et al.* Oncogene cooperation and B-lymphoid tumorigenesis in Emu-myc transgenic mice. *Haematol Blood Transfus* **32**, 423-427 (1989).
124. Langdon, W.Y., Harris, A.W., Cory, S. & Adams, J.M. The c-myc oncogene perturbs B lymphocyte development in E-mu-myc transgenic mice. *Cell* **47**, 11-18 (1986).
125. Lin, C.J. *et al.* Targeting synthetic lethal interactions between Myc and the eIF4F complex impedes tumorigenesis. *Cell Rep* **1**, 325-333 (2012).
126. Barna, M. *et al.* Suppression of Myc oncogenic activity by ribosomal protein haploinsufficiency. *Nature* **456**, 971-975 (2008).
127. Pourdehnad, M. *et al.* Myc and mTOR converge on a common node in protein synthesis control that confers synthetic lethality in Myc-driven cancers. *Proc Natl Acad Sci U S A* **110**, 11988-11993 (2013).
128. Nagy, P., Varga, A., Pircs, K., Hegedus, K. & Juhasz, G. Myc-driven overgrowth requires unfolded protein response-mediated induction of autophagy and antioxidant responses in Drosophila melanogaster. *PLoS Genet* **9**, e1003664 (2013).
129. Qing, G. *et al.* ATF4 regulates MYC-mediated neuroblastoma cell death upon glutamine deprivation. *Cancer Cell* **22**, 631-644 (2012).
130. Ren, P. *et al.* ATF4 and N-Myc coordinate glutamine metabolism in MYCN-amplified neuroblastoma cells through ASCT2 activation. *J Pathol* **235**, 90-100 (2015).
131. Dong, J., Qiu, H., Garcia-Barrio, M., Anderson, J. & Hinnebusch, A.G. Uncharged tRNA activates GCN2 by displacing the protein kinase moiety from a bipartite tRNA-binding domain. *Mol Cell* **6**, 269-279 (2000).
132. Gardner, B.M., Pincus, D., Gotthardt, K., Gallagher, C.M. & Walter, P. Endoplasmic reticulum stress sensing in the unfolded protein response. *Cold Spring Harb Perspect Biol* **5**, a013169 (2013).
133. Tameire, F., Verginadis, II & Koumenis, C. Cell intrinsic and extrinsic activators of the unfolded protein response in cancer: Mechanisms and targets for therapy. *Semin Cancer Biol* (2015).
134. Stine, Z.E., Walton, Z.E., Altman, B.J., Hsieh, A.L. & Dang, C.V. MYC, Metabolism, and Cancer. *Cancer Discov* **5**, 1024-1039 (2015).

135. Sood, R., Porter, A.C., Olsen, D.A., Cavener, D.R. & Wek, R.C. A mammalian homologue of GCN2 protein kinase important for translational control by phosphorylation of eukaryotic initiation factor-2alpha. *Genetics* **154**, 787-801 (2000).
136. Gomez-Roman, N., Grandori, C., Eisenman, R.N. & White, R.J. Direct activation of RNA polymerase III transcription by c-Myc. *Nature* **421**, 290-294 (2003).
137. Han, J. *et al.* ER-stress-induced transcriptional regulation increases protein synthesis leading to cell death. *Nat Cell Biol* **15**, 481-490 (2013).
138. Chen, H. *et al.* ATF4 regulates SREBP1c expression to control fatty acids synthesis in 3T3-L1 adipocytes differentiation. *Biochim Biophys Acta* **1859**, 1459-1469 (2016).
139. Saxton, R.A. & Sabatini, D.M. mTOR Signaling in Growth, Metabolism, and Disease. *Cell* **168**, 960-976 (2017).
140. Hay, N. & Sonenberg, N. Upstream and downstream of mTOR. *Genes Dev* **18**, 1926-1945 (2004).
141. Pause, A. *et al.* Insulin-dependent stimulation of protein synthesis by phosphorylation of a regulator of 5'-cap function. *Nature* **371**, 762-767 (1994).
142. Ozcan, U. *et al.* Chemical chaperones reduce ER stress and restore glucose homeostasis in a mouse model of type 2 diabetes. *Science* **313**, 1137-1140 (2006).
143. Anthony, T.G. *et al.* Preservation of liver protein synthesis during dietary leucine deprivation occurs at the expense of skeletal muscle mass in mice deleted for eIF2 kinase GCN2. *J Biol Chem* **279**, 36553-36561 (2004).
144. Zhang, P. *et al.* The GCN2 eIF2alpha kinase is required for adaptation to amino acid deprivation in mice. *Mol Cell Biol* **22**, 6681-6688 (2002).
145. Pytel, D. *et al.* PERK Is a Haploinsufficient Tumor Suppressor: Gene Dose Determines Tumor-Suppressive Versus Tumor Promoting Properties of PERK in Melanoma. *PLoS Genet* **12**, e1006518 (2016).
146. Gao, Y. *et al.* PERK is required in the adult pancreas and is essential for maintenance of glucose homeostasis. *Mol Cell Biol* **32**, 5129-5139 (2012).
147. Nguyen, H.G. *et al.* Development of a stress response therapy targeting aggressive prostate cancer. *Sci Transl Med* **10** (2018).
148. Ventura, A. *et al.* Restoration of p53 function leads to tumour regression in vivo. *Nature* **445**, 661-665 (2007).
149. Liakath-Ali, K. *et al.* An evolutionarily conserved ribosome-rescue pathway maintains epidermal homeostasis. *Nature* **556**, 376-380 (2018).
150. Ruggero, D. The role of Myc-induced protein synthesis in cancer. *Cancer Res* **69**, 8839-8843 (2009).
151. Xu, C. & Ng, D.T. Glycosylation-directed quality control of protein folding. *Nat Rev Mol Cell Biol* **16**, 742-752 (2015).
152. Tettweiler, G., Miron, M., Jenkins, M., Sonenberg, N. & Lasko, P.F. Starvation and oxidative stress resistance in Drosophila are mediated through the eIF4E-binding protein, d4E-BP. *Genes Dev* **19**, 1840-1843 (2005).
153. Kremer, C.L. *et al.* Expression of mTOR signaling pathway markers in prostate cancer progression. *Prostate* **66**, 1203-1212 (2006).
154. Karlsson, E. *et al.* The mTOR effectors 4EBP1 and S6K2 are frequently coexpressed, and associated with a poor prognosis and endocrine resistance in breast cancer: a retrospective study including patients from the randomised Stockholm tamoxifen trials. *Breast Cancer Res* **15**, R96 (2013).

155. Cha, Y.L. *et al.* EIF4EBP1 overexpression is associated with poor survival and disease progression in patients with hepatocellular carcinoma. *PLoS One* **10**, e0117493 (2015).
156. Yamaguchi, S. *et al.* ATF4-mediated induction of 4E-BP1 contributes to pancreatic beta cell survival under endoplasmic reticulum stress. *Cell Metab* **7**, 269-276 (2008).
157. Lowe, S.W., Cepero, E. & Evan, G. Intrinsic tumour suppression. *Nature* **432**, 307-315 (2004).
158. Warburg, O. On the origin of cancer cells. *Science* **123**, 309-314 (1956).
159. Vander Heiden, M.G., Cantley, L.C. & Thompson, C.B. Understanding the Warburg effect: the metabolic requirements of cell proliferation. *Science* **324**, 1029-1033 (2009).
160. Lewis, B.C. *et al.* Identification of putative c-Myc-responsive genes: characterization of rcl, a novel growth-related gene. *Mol Cell Biol* **17**, 4967-4978 (1997).
161. Osthus, R.C. *et al.* Deregulation of glucose transporter 1 and glycolytic gene expression by c-Myc. *J Biol Chem* **275**, 21797-21800 (2000).
162. Still, E.R. & Yuneva, M.O. Hopefully devoted to Q: targeting glutamine addiction in cancer. *Br J Cancer* **116**, 1375-1381 (2017).
163. Dejure, F.R. & Eilers, M. MYC and tumor metabolism: chicken and egg. *EMBO J* **36**, 3409-3420 (2017).
164. Gao, P. *et al.* c-Myc suppression of miR-23a/b enhances mitochondrial glutaminase expression and glutamine metabolism. *Nature* **458**, 762-765 (2009).
165. Le, A. *et al.* Glucose-independent glutamine metabolism via TCA cycling for proliferation and survival in B cells. *Cell Metab* **15**, 110-121 (2012).
166. Xiang, Y. *et al.* Targeted inhibition of tumor-specific glutaminase diminishes cell-autonomous tumorigenesis. *J Clin Invest* **125**, 2293-2306 (2015).
167. Carroll, P.A. *et al.* Deregulated Myc requires MondoA/Mlx for metabolic reprogramming and tumorigenesis. *Cancer Cell* **27**, 271-285 (2015).
168. DeNicola, G.M. *et al.* NRF2 regulates serine biosynthesis in non-small cell lung cancer. *Nat Genet* **47**, 1475-1481 (2015).
169. Yang, X. *et al.* ATF4 Regulates CD4(+) T Cell Immune Responses through Metabolic Reprogramming. *Cell Rep* **23**, 1754-1766 (2018).
170. Ancey, P.B., Contat, C. & Meylan, E. Glucose transporters in cancer - from tumor cells to the tumor microenvironment. *FEBS J* (2018).
171. Gorovits, N. & Charron, M.J. What we know about facilitative glucose transporters - Lessons from cultured cells, animal models, and human studies. *Biochem Mol Biol Edu* **31**, 163-172 (2003).
172. Milani, M. *et al.* The role of ATF4 stabilization and autophagy in resistance of breast cancer cells treated with Bortezomib. *Cancer Res* **69**, 4415-4423 (2009).
173. Chen, C., Pore, N., Behrooz, A., Ismail-Beigi, F. & Maity, A. Regulation of glut1 mRNA by hypoxia-inducible factor-1. Interaction between H-ras and hypoxia. *J Biol Chem* **276**, 9519-9525 (2001).
174. Ruggero, D. *et al.* The translation factor eIF-4E promotes tumor formation and cooperates with c-Myc in lymphomagenesis. *Nat Med* **10**, 484-486 (2004).
175. Hsieh, A.C. *et al.* Cell type-specific abundance of 4EBP1 primes prostate cancer sensitivity or resistance to PI3K pathway inhibitors. *Sci Signal* **8**, ra116 (2015).
176. Ye, J. *et al.* GCN2 sustains mTORC1 suppression upon amino acid deprivation by inducing Sestrin2. *Genes Dev* **29**, 2331-2336 (2015).

177. Whitney, M.L., Jefferson, L.S. & Kimball, S.R. ATF4 is necessary and sufficient for ER stress-induced upregulation of REDD1 expression. *Biochem Biophys Res Commun* **379**, 451-455 (2009).
178. McGlincy, N.J. & Ingolia, N.T. Transcriptome-wide measurement of translation by ribosome profiling. *Methods* **126**, 112-129 (2017).
179. Hsieh, A.C. *et al.* The translational landscape of mTOR signalling steers cancer initiation and metastasis. *Nature* **485**, 55-61 (2012).
180. Denzel, M.S. & Antebi, A. Hexosamine pathway and (ER) protein quality control. *Curr Opin Cell Biol* **33**, 14-18 (2015).
181. Groves, J.A., Lee, A., Yildirir, G. & Zachara, N.E. Dynamic O-GlcNAcylation and its roles in the cellular stress response and homeostasis. *Cell Stress Chaperones* **18**, 535-558 (2013).
182. Chaveroux, C. *et al.* Nutrient shortage triggers the hexosamine biosynthetic pathway via the GCN2-ATF4 signalling pathway. *Sci Rep* **6**, 27278 (2016).
183. Alejandro, E.U. *et al.* Disruption of O-linked N-Acetylglucosamine Signaling Induces ER Stress and beta Cell Failure. *Cell Rep* **13**, 2527-2538 (2015).
184. Nakamura, A. *et al.* Inhibition of GCN2 sensitizes ASNS-low cancer cells to asparaginase by disrupting the amino acid response. *Proc Natl Acad Sci U S A* **115**, E7776-E7785 (2018).
185. Axten, J.M. *et al.* Discovery of GSK2656157: An Optimized PERK Inhibitor Selected for Preclinical Development. *ACS Med Chem Lett* **4**, 964-968 (2013).
186. Sidrauski, C., McGeachy, A.M., Ingolia, N.T. & Walter, P. The small molecule ISRIB reverses the effects of eIF2alpha phosphorylation on translation and stress granule assembly. *Elife* **4** (2015).
187. Soufi, A., Donahue, G. & Zaret, K.S. Facilitators and impediments of the pluripotency reprogramming factors' initial engagement with the genome. *Cell* **151**, 994-1004 (2012).
188. Langmead, B., Trapnell, C., Pop, M. & Salzberg, S.L. Ultrafast and memory-efficient alignment of short DNA sequences to the human genome. *Genome Biol* **10**, R25 (2009).
189. Heinz, S. *et al.* Simple combinations of lineage-determining transcription factors prime cis-regulatory elements required for macrophage and B cell identities. *Mol Cell* **38**, 576-589 (2010).
190. Huang da, W., Sherman, B.T. & Lempicki, R.A. Systematic and integrative analysis of large gene lists using DAVID bioinformatics resources. *Nat Protoc* **4**, 44-57 (2009).
191. Schmitz, R. *et al.* Genetics and Pathogenesis of Diffuse Large B-Cell Lymphoma. *N Engl J Med* **378**, 1396-1407 (2018).
192. Goldman, M. *et al.* The UCSC Cancer Genomics Browser: update 2015. *Nucleic Acids Res* **43**, D812-817 (2015).
193. Soga, T. & Heiger, D.N. Amino acid analysis by capillary electrophoresis electrospray ionization mass spectrometry. *Anal Chem* **72**, 1236-1241 (2000).
194. Soga, T. *et al.* Simultaneous determination of anionic intermediates for Bacillus subtilis metabolic pathways by capillary electrophoresis electrospray ionization mass spectrometry. *Anal Chem* **74**, 2233-2239 (2002).
195. Soga, T. *et al.* Quantitative metabolome analysis using capillary electrophoresis mass spectrometry. *J Proteome Res* **2**, 488-494 (2003).